CATENARY STRUCTURES

A FEASIBILITY STUDY OF A STEEL CELLULAR DECK IN CATENARY AS A TRAFFIC CARRIAGEWAY

by

A.J. WILSON, B.E.

A Thesis in partial fulfilment of the requirements
for a Master of Engineering Science Degree
at the University of Sydney

1972

ACKNOWLEDGEMENTS

The author wishes to express his gratitude to the Commissioner for Main Roads, N.S.W., for sponsoring the author for the Master of Engineering Science Degree course, of which this thesis is part, at the University of Sydney.

The work was carried out under the supervision of Mr. R.J. Wheen whose suggestions and advice, particularly on practical aspects, are greatly appreciated. The assistance of Professor B.J. Vickery with the aerodynamic analysis (Chapter 6) is also appreciated.

The efforts of Miss P. O'Rourke and others, who assisted in the typing of the manuscript, preparation of the figures and binding of the thesis, are gratefully acknowledged.

CONTENTS

LIST OF FIGURES

LIST OF TABLES

NOTATION

A	-	area of cable. (cross-sectional)
d	-	sag of cable at midspan from straight line joining support points.
d_o	-	central sag of cable under its own self-weight.
E	-	modulus of elasticity.
f	-	stress in cable.
f_o	-	"prestretch" stress.
f_s	-	stress in cable at service loading condition.
f_u	-	stress in cable at ultimate loading condition.
H	-	horizontal component of tension in cable.
I_p	-	polar moment of inertia of a section.
L	-	span length.
l	-	cable length.
l_u	-	unstretched length of cable.
M	-	equivalent span factor (non-dimensional).
m,n	-	cable deflection factors (non-dimensional).
p	-	loading factor (non-dimensional).
p_s	-	serviceability loading factor.
p_u	-	ultimate loading factor.
R	-	radius of curvature.
s	-	length of any arc of a cable.
T	-	axial tension in cable.
t	-	temperature variation.
V	-	vertical component of tension in cable.
V_F	-	critical flutter velocity.
w	-	loading per unit length of cable.
x,y	-	orthogonal cartesian co-ordinates.
α	-	co-efficient of thermal expansion.
β	-	an angle.
ψ	-	an angle.
ρ	-	weight per unit volume of a material.
ρ_A	-	specific weight of air.
ω	-	angular frequency.

ω_v - fundamental vertical frequency.

ω_T - fundamental torsional frequency.

Δ - prefix to other symbols indicating incremental variation.

The subscripts "c" and "d" are often used to differentiate between cable and deck respectively, in sections dealing with interaction between the two.

CHAPTER 1

INTRODUCTION

1.1 CATENARY STRUCTURES - HISTORICAL INTRODUCTION

The catenary structure is a structure employing long-span suspended cables, and is so-called because the profile of the cable is described mathematically by a catenary.

Suspended ropes or cables have been employed by man as a means of communication and transportation between two points for many centuries. Primitive man no doubt copied monkeys in scrambling along vines between treetops and eventually applied this technique to the bridging of ravines and rivers. Pugsley (2) * and Schneigert (3) trace in some detail the historical development of the catenary structure to the modern sophisticated suspension bridges, aerial ropeways and funicular railways. In recent years, the cable has found another application with the construction of a limited number of large-span cable suspension roof structures. Bresler et al (4) give some examples of this type of roof system.

Another recent application is in the "stress-ribbon" bridge concept (5, 6) which consists simply of tightly tensioned steel cables suspended between two abutments and embedded in a thin concrete slab. The slab serves as the carriageway, but apart from continuity and distribution of local loads, it has no load-bearing function. The stress-ribbon bridge has been proposed for spans of up to 1,500 feet as an economical alternative to the suspension bridge and the cable-stayed bridge. By comparison with the suspension bridge, the stress-ribbon bridge is a much simpler structure. Since the tension members may be distributed over the whole cross-section, conventional secondary supporting elements such as cross-girders, wind bracing, suspension hangers etc. may be dispensed with.

* Numbers in brackets refer to references in the Bibliography.

1.2 THE STEEL CELLULAR DECK IN CATENARY

In conventional girder bridge design, the various structural elements (viz deck, longitudinal stringers, transverse floor beams, main girders etc.) are analysed individually. Each element performs a separate, clearly-defined function and live loading is transferred from one element to the next until finally carried by the main girders. Each member is "stiff" and the design is based mainly on flexural analysis. The floor system does not contribute to the strength or rigidity of the main load-carrying members, nor to the transverse stability of the bridge. In long-span bridges, however, the dead weight may account for up to 80% of the total design forces and moments, resulting in massive and expensive structures.

In order to improve efficiency and minimize the superstructure dead weight, two notable developments have been composite construction and steel plate deck construction. In composite construction the concrete deck is bonded to the main girders by means of shear connectors and acts as an upper flange to the girders in carrying the load across the span.

In steel plate deck construction (commonly known as "orthotropic plate" construction) the deck slab, stringers and floor beams are integrated into a single structural element - the stiffened steel plate deck with relatively closely spaced longitudinal and transverse stiffening ribs using the steel plate deck as a common top flange. This stiffened deck then becomes part of the main girders as their upper flange.

The recent development of the steel box girder is a further step from the steel plate deck construction, where the main girder comprises thin orthotropic plates as top and bottom flanges and sides. An important characteristic of the box girder, when used on long slender bridges, is the high torsional rigidity achieved. The girder acts as a single structural unit with traffic using the top flange plate as the bridge deck.

The concept of a steel cellular deck in catenary is a combination of the stress-ribbon concept and the progression of thought leading to the steel box girder. The non load-carrying concrete deck of the stress-ribbon bridge is replaced by a steel cellular section capable of carrying all or part of its own

dead weight plus live loading. The deck is anchored at the abutments and behaves essentially as a simple tension member. The deck may be prestressed by partially supporting it on high-strength steel tendons. The effect of the prestressing is to reduce the tension in the deck under dead load conditions, thereby increasing its tensile capacity to accommodate higher stresses due to live loading.

The purpose of this thesis is to examine the feasibility of a steel cellular deck section in catenary as a traffic carriageway. The feasibility study is undertaken by developing a method of design and analysis for such a structure. The method is also applicable to the stress-ribbon concept enabling comparison of the two concepts. The basic steps are outlined below:

(i) Design and analysis of long-span cables. (Chapters 2 and 3).

(ii) Assumption that the deck is flexible and that it can therefore be analysed as a cable.

(iii) The prestressed deck - solution of the cable-deck interaction problem. (Chapter 4)

(iv) Allowance for the "stiffness" of the deck. (Chapter 5)

(v) Aerodynamic analysis of the structure. (Chapter 6)

(vi) Consideration of other aspects such as material properties, design loading and fabrication and erection of the structure. (Chapter 7)

1.3 THE LONG-SPAN CABLE

The determination of strains, deformations and stresses in long-span suspension cables under load is complicated by the highly non-linear response of the cable to load. This non-linearity occurs despite the fact that the cable material normally displays linear load-extension characteristics, and is a consequence of the extreme flexibility of the cable as compared with the conventional beam and framed structures. Furthermore the non-linear behaviour is amplified as the ratio of central sag/cable span decreases. The resulting gross deformations of the cable under load must be taken into account in any accurate analysis of cable behaviour.

Early methods of cable analysis were confined to simple loading patterns and involved approximate expressions to make some allowance for the non-linear behaviour, together with the assumption that the cable was inextensible. The analysis gave satisfactory results for cables having reasonably large sag/span ratios (say 0.1). However Pippard and Chitty (7) showed in 1942 that the assumption of inextensibility in a cable could produce serious errors if the sag/span ratio was small.

It is appropriate to note at this point that for the application of the catenary structure proposed herein, serviceability criteria will limit the maximum grade as a traffic carriageway to about 6% and the sag/span ratio to a value in the order of 0.015. Thus it will be necessary to take cable extensibility into account in analysis for this thesis.

Various numerical techniques have been proposed to cater for cable extensibility and more complicated loading systems. Michalos and Birnstiel (8) in 1962 described a numerical trial and error method based on the so-called "string polygon" approach, in which the cable dead weight profile is approximately represented as a number of straight hinged weightless segments, with dead loads concentrated at segment joints. An initial guess is made of the magnitude and direction of the cable tension at the left hand support, and the position of the right hand end of the cable is computed. Further guesses are made until the right hand end of the cable coincides with the known position of the right hand support. Michalos and Birnstiel used ten segments. The method is laborious and errors are introduced by the inexact treatment of the cable weight. Jennings (9) in 1962 used a concept of cable flexibility to give an improved technique for modifying the initial guess of cable tension at the left hand support.

O'Brien and Francis (10) using the same basic technique as Michalos and Birnstiel, considered the cable as composed of a small number of segments sufficient to joint the load application positions. Equilibrium at each load point was established, making accurate allowance for the self-weight catenary in each cable segment. Initial guesses of the magnitude and direction of cable tension at the left hand support were progressively modified until the right hand end of the cable converged to the known position of the right hand support.

Harrison (11) extended Michalos and Birnstiel's method to produce a finite element computer programme in which the cable was represented as a

chain composed of a large number of hinged links, each link having the axial stiffness of a corresponding length of cable and infinite flexural stiffness. Allowance is made for the effect of temperature change and also the influence of finite vertical, horizontal and cable slip stiffnesses at the supports. Distributed loading is represented as a system of closely-spaced concentrated loads. The Newton iteration procedure is applied automatically to produce rapid convergence. As in the preceeding numerical techniques, the unstretched length and sectional area of the cable must be nominated and an initial guess made of the magnitude and direction of the tension in the cable under load.

The initial problem posed in the development of this thesis is to design a cable which will satisfy a serviceability criterion at working loads, and a stress criterion under an ultimate loading. For a particular span, the behaviour of the cable under load is dependent on an initial cable profile as well as on the applied loading. The critical design requirement, then, is the determination of the optimum sag/span ratio (defining the initial cable profile) for which both serviceability and stress criteria will just be satisfied. The numerical methods of analysis described above are not immediately convenient as design tools for this problem.

The object of Chapter 2 is to develop a satisfactory design method for the case of a cable subjected to uniformly distributed loading over the full length of a symmetrical span, (i.e. with cable supports at the same elevation). The theory is extended in Chapter 3 to the general case where the cable supports are at different levels. This leads to a general method of cable analysis somewhat similar to that of O'Brien and Francis (10) where the cable is divided into a small number of segments sufficient to joint the load application positions. The method involves calculation of the unextended length of each cable segment. An initial guess of <u>one angle</u> is modified until the sum of the segment unextended lengths converges to the known unextended length of the complete cable. (The previous methods required an initial guess of the <u>magnitude and direction</u> of tension in a cable segment.)

CHAPTER 2

SIMPLE CABLE ANALYSIS AND DESIGN

2.1 THE INEXTENSIBLE CABLE

The simplest form of catenary structure is a single flexible cable suspended between two points. This chapter is concerned only with the special case of a cable suspended betwen two fixed anchorage points at the same level, as shown in Figure 2.1. Analysis of the behaviour of such a structure under load, must commence with a determination of the profile adopted by the cable under its own weight, and determination of the tension in the cable at any point along its length.

Initially it will be assumed that the cable is inextensible, perfectly flexible and of constant cross-sectional area. By "perfectly flexible" it is meant that the cable is incapable of carrying any load other than by means of tension directed along its length.

Notation:	Span length	=	L
	Cable length	=	l
	Cable weight	=	w per lineal foot
	Cable area	=	A
	Sag at mid-span	=	d
	T	=	axial tension
	H	=	horizontal component of T
	V	=	vertical component of T

2.1.1 THE CATENARY CURVE

If the cable weight (w) is distributed uniformly along the cable itself, the resulting cable profile will be defined by the common catenary, as indicated below.

Considering in Figure 2.1, the portion of the cable CB where B may be any point along the cable with co-ordinates (x, y) with respect to C as origin. The length of the cable segment CB is s and the cable slope at B is ψ.

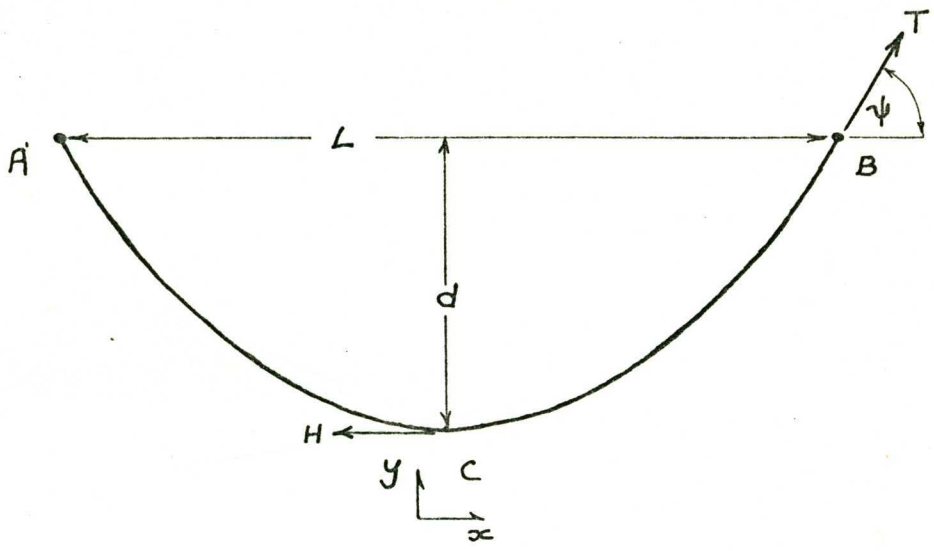

Fig 2.1. SIMPLE CABLE PROFILE

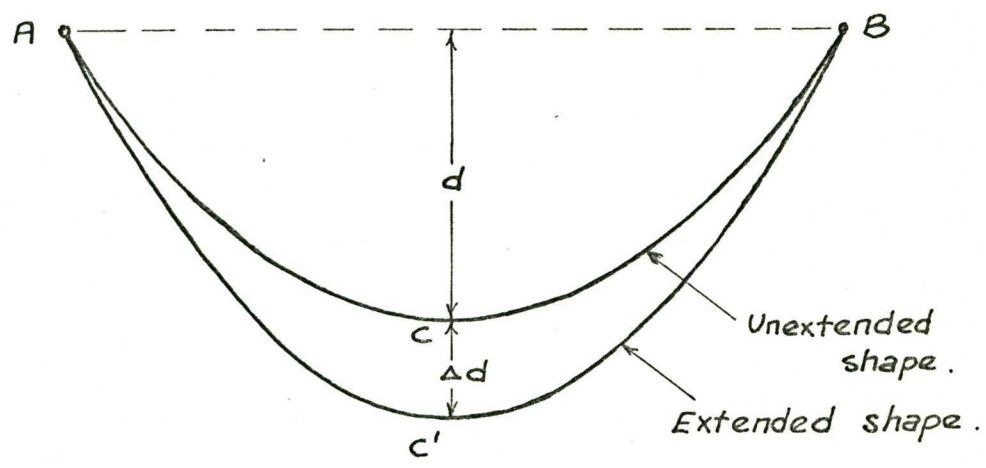

Fig 2.2. CABLE PROFILE UNDER LOADING.

For portion CB, resolving forces horizontally and vertically:

Then $T \cos \psi = H$

and $T \sin \psi = w s$

From statics, the horizontal tension at any point in the cable must be constant. Putting $H = k w$

Then $s = k \tan \psi$

The equivalent Cartesian form is $s = k \frac{dy}{dx}$

Differentiating, $k \frac{d^2 y}{dx^2} = \frac{ds}{dx} = \left\{ 1 + \left(\frac{dy}{dx}\right)^2 \right\}^{\frac{1}{2}}$

Integrating, $k \sinh^{-1} \left(\frac{dy}{dx}\right) = x + m$

Boundary conditions, at C $x = 0$, $\frac{dy}{dx} = 0$

therefore $m = 0$

Thus $\frac{dy}{dx} = \sinh \left(\frac{x}{k}\right)$

Integrating, $y = k \cosh \left(\frac{x}{k}\right) + n$

Boundary conditions, at C $x = 0$, $y = 0$

therefore $n = -k$

Thus $y = k \left\{ \cosh \left(\frac{x}{k}\right) - 1 \right\}$ - (2.1)

This gives the shape adopted by the cable. When required, the length of any arc of the cable is given by

$$s = k \sinh \left(\frac{x}{k}\right)$$

The cable tension is obtained as follows:

$$T^2 = H^2 + V^2$$

$$= w^2 (k^2 + s^2)$$

from which

$$T = w (y + k)$$ - (2.2)

The above derivations are dependent on the value of the catenary parameter k. For a cable hanging symmetrically between two fixed points at the same level, the value of k can be readily determined, provided the cable slope at the fixed points, the central dip d of the cable or the cable length l is stipulated.

2.1.2 THE PARABOLIC CURVE

If the cable weight (w) is distributed uniformly across the length of the span instead of uniformly along the length of the cable, the resulting cable profile will be defined by a parabola.

Considering again the cable segment CB in Figure 2.1, where the coordinates of B are (x,y) with respect to C as origin.

Resolving forces horizontally and vertically:

$$\text{Then} \quad T \cos\psi = H$$

$$\text{and} \quad T \sin\psi = V = wx$$

$$\text{Thus} \quad \tan\psi = \frac{dy}{dx} = \frac{w.x}{H} \qquad -(2.3)$$

$$\text{whence by integration} \quad y = \left\{\tfrac{1}{2} \cdot \frac{w}{H} \cdot x^2\right\} + R$$

Boundary conditions, at C $\quad x = 0, \quad y = 0$

$$\text{Thus} \quad R = 0$$

$$\text{Therefore} \quad y = \frac{w}{2H} \cdot x^2 \qquad -(2.4)$$

which is the equation of the cable profile and constitutes a parabola with its vertex at C.

Boundary conditions, at $x = \frac{L}{2}, \quad y = d$

$$\text{Thus} \quad H = \frac{w L^2}{8d} \qquad -(2.5)$$

$$\text{and} \quad y = \frac{4d}{L^2} \cdot x^2 \qquad -(2.6)$$

To obtain the cable tension

$$T = H\frac{ds}{dx} = H\left\{1 + \left(\frac{dy}{dx}\right)^2\right\}^{\frac{1}{2}}$$

$$= H\left\{1 + \left(\frac{wx}{H}\right)^2\right\}^{\frac{1}{2}}$$

$$= H\left\{1 + \frac{64d^2x^2}{L^4}\right\}^{\frac{1}{2}} \qquad -(2.7)$$

To obtain the cable length

$$\frac{ds}{dx} = \left\{1 + \left(\frac{dy}{dx}\right)^2\right\}^{\frac{1}{2}}$$

Integrating $$1 = 2\int_0^{L/2}\left(1 + \frac{64\,d^2x^2}{L^4}\right)^{\frac{1}{2}} dx$$

$$= \frac{L}{2}\left(1 + \frac{16\,d^2}{L^2}\right) + \frac{L^2}{8d}\log_e\left\{\frac{4d}{L} + \left(1 + \frac{16\,d^2}{L^2}\right)^{\frac{1}{2}}\right\}$$

or alternatively $$1 = L\left\{1 + \frac{8}{3}\left(\frac{d}{L}\right)^2 - \frac{32}{5}\left(\frac{d}{L}\right)^4 + \ldots\right\} \qquad -(2.8)$$

Shaw (12) states that equation (2.8) should be used for values of $\frac{d}{L}$ in the order of 0.1, while for smaller values of $\frac{d}{L}$ the term involving $\left(\frac{d}{L}\right)^4$ becomes negligible and it is sufficient to take

$$1 = L\left\{1 + \frac{8}{3}\left(\frac{d}{L}\right)^2\right\} \qquad -(2.9)$$

For application of the catenary structure as a traffic carriageway, a ruling maximum gradient of about 6% will dictate the maximum profile slope with regard to serviceability. Maximum profile slope will occur at the anchorage points. From equations (2.3) and (2.5), at $x = \frac{L}{2}$

$$\left(\frac{dy}{dx}\right)_{max} = \frac{4d}{L} \qquad -(2.10)$$

Thus for a slope of 6%, $\frac{d}{L} = 0.015$.

Equation (2.9) can therefore be adopted for calculation of the cable length.

The assumption of linear distribution of load across the span rather than along the cable is strictly only an approximation. It is of interest to check

the accuracy of this assumption, at a profile slope of 6% by calculating the length of cable per unit length of span.

$$\frac{ds}{dx} = \left(1 + \left(\frac{dy}{dx}\right)^2\right)^{\frac{1}{2}}$$

For $\frac{dy}{dx} = 0.06$ then $\frac{ds}{dx} = \left(1 + (0.06)^2\right)^{\frac{1}{2}} = 1.0018$

Thus for a maximum gradient of 6% under working load, a variation of up to 0.2% in the distribution of loading across the span will occur. This is not significant for practical purposes.

Pugsley (2) and Schneigert (3) have calculated cable shapes using both catenary and parabolic formulae, and have concluded along with Steinman (1) that for very small values of $\frac{d}{L}$ (as will be herein considered) the variation between the two curves is insignificant.

The parabolic shape will therefore be adopted for all future calculations and analysis because of its greater simplicity and familiarity.

2.2 EXTENSIONS AND DEFORMATIONS OF THE CABLE UNDER LOAD

The preceding analysis has been based on the assumption that the cable is inextensible. If the cable is now allowed to extend under its own weight, or for that matter under any uniformly distributed loading to a new equilibrium position, as shown in Figure 2.2, it will retain its parabolic profile but with an increased dip at centre span due to the increase in cable length.

From equation (2.6), if the initial unextended shape of the cable is

$$y = \frac{4d}{L^2} \cdot x^2$$

For an increase in dip Δd, retaining the origin at C, extended shape is

$$y_e = \left\{\frac{4(d + \Delta d)}{L^2} \cdot x^2\right\} - \Delta d$$

From equation (2.9) $l = L\left(1 + \frac{8}{3}\left(\frac{d}{L}\right)^2\right)$

$$l_e = L\left(1 + \frac{8}{3}\left(\frac{d + \Delta d}{L}\right)^2\right)$$

Increase in length $\Delta l = l_e - l = \frac{8L}{3}\left\{\left(\frac{d + \Delta d}{L}\right)^2 - \left(\frac{d}{L}\right)^2\right\}$

Thus $$\Delta 1 = \frac{8\,\Delta d}{3L}\,(2d + \Delta d) \qquad -(2.11)$$

If 1 is due to the elasticity in the cable,

then $$\Delta 1 = \int_o^{le} \frac{T_e\, ds}{AE}$$

$$= \frac{2H_e}{AE} \int_o^{L/2} 1 + \left(\frac{dy_e}{dx}\right)^2 dx$$

$$= \frac{2H_e}{AE} \int_o^{L/2} \left(1 + \left[\frac{8(d+\Delta d)}{L^2} \cdot x\right]^2\right) dx$$

$$= \frac{2H_e}{AE} \left[x + \frac{64(d+\Delta d)^2}{L^4} \times \frac{x^3}{}\right]_o^{L/2}$$

$$= \frac{H_e L}{AE} \left(1 + \frac{16}{3}\left(\frac{d+\Delta d}{L}\right)^2\right)$$

For very small values of $\frac{d}{L}$ (as herein considered) and assuming Δd is of the same order of magnitude as d

then $$\left\{1 + \frac{16}{3}\left(\frac{d+\Delta d}{L}\right)^2\right\} \doteqdot 1$$

Thus $$\Delta 1 \doteqdot \frac{H_e L}{AE} \qquad -(2.12)$$

As indicated earlier, for a traffic carriageway, maximum slope under load should be about 6% for serviceability.

Thus for $\frac{d+\Delta d}{L} = 0.015$, $\frac{16}{3}\left(\frac{d+\Delta d}{L}\right)^2 \doteqdot 0.001$

In this case, the approximation to equation (2.12) is justified.

Combining equations (2.11) and (2.12)

$$\frac{8\,\Delta d}{3L}\,(2d + \Delta d) = \frac{H_e L}{AE} = \frac{w L^3}{8AE\,(d + \Delta d)}$$

Thus $$\Delta d\,(d + \Delta d)(2d + \Delta d) = \frac{3\,w\,L^4}{64\,AE}$$

Putting $\Delta d = n.d$

Then $$n(n + a)(n + 2) = \frac{3\,w\,L}{64\,AE}\left(\frac{L}{3}\right)^3 \qquad -(2.13)$$

The solution of equation (2.13) yields the cable profile $\{(n+1)\frac{d}{L}\}$ under any total uniformly distributed loading (w), for any specified unextended cable profile $(\frac{d}{L})$. However, in this form, it is not convenient for calculation of cable movement under variable loading increments.

Figure 2.3 shows a plot of the general function $y = n(n+1)(n+2)$. For $y = \frac{3wL}{64AE}(\frac{L}{d})^3 > 0.385$ there is a unique solution for n. In this region the slope of the curve is becoming increasingly steeper with increasing y, or for given initial conditions, with increasing load w. Large variations in w produce relatively small cable deflections. For $0.385 \geqslant \frac{3wL}{64AE}(\frac{L}{d})^3 \geqslant -0.385$, there are theoretically three solutions for n. This is the shaded zone shown in Figure 2.3. Examination of the stress in the cable with varying n, is of assistance in understanding the physical significance of the three solutions.

(a) $n > o$: Cable in tension, decreasing as n approaches o.

(b) $n = o$: Zero stress in cable.

(c) $o > n > -1$: Cable in compression, increasing to a maximum value as n approaches -1.

(d) $-1 > n > -2$: Cable in compression, decreasing as n decreases from -1 to -2.

(e) $n = -2$: Zero stress in cable.

(f) $n < -2$: Cable in tension, increasing as n decreases from -2.

Theoretically the cable is capable of "snap through" in this zone. However this will only occur from a higher to a lower energy level. Evaluation of the potential energy and axial strain energy of the cable within this zone indicates that the lowest energy level always corresponds to the solution for the cable in tension, i.e. $n > o$ and $n < -2$. Thus the possibility of snap through arises only when the cable is subjected to a small upward total loading, i.e. $0 > \frac{3wL}{64AE}(\frac{L}{d})^3 > -0.385$. In a practical situation, this condition would not normally occur. Further, for a large unextended profile ratio $(\frac{d}{L})$ snap through would involve a large physical movement of the cable. It may warrant consideration in a situation such as a cable-supported roof structure.

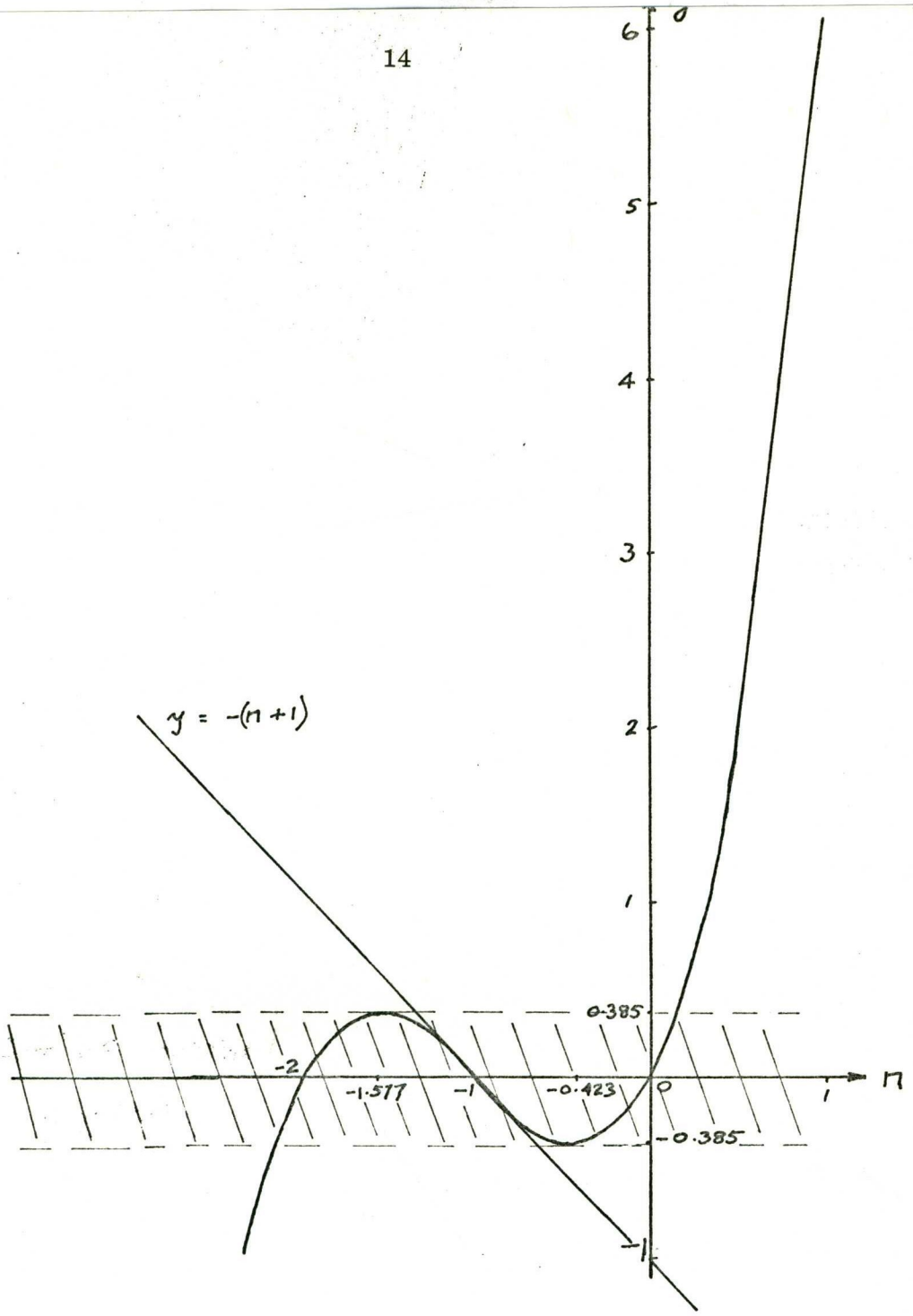

Fig 2.3. PLOT OF $y = n(n+1)(n+2)$

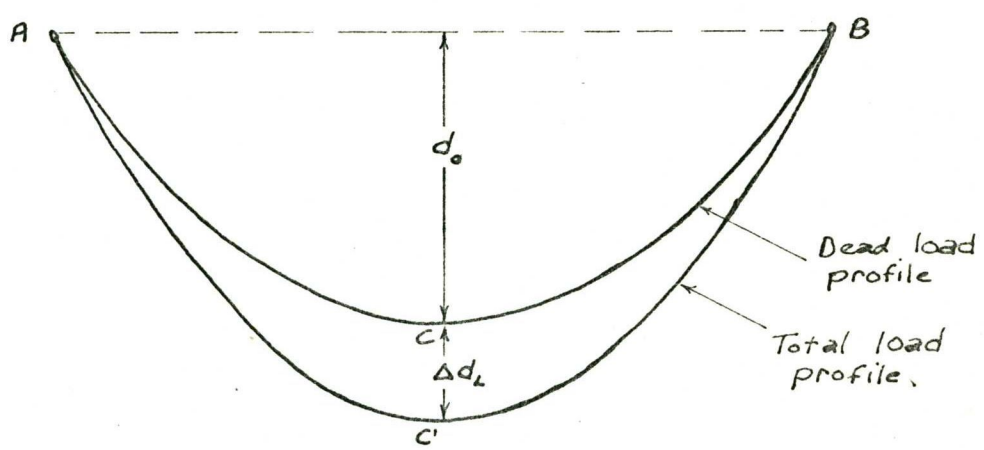

Fig 2.4 CABLE EXTENSION UNDER LIVE LOADING.

2.3 CABLE EXTENSION AND DEFORMATION UNDER VARIABLE LOADING

The foregoing analysis can be extended to account for cable movements under loading increments. The most important example of this is the cable movement from its extended position under its own dead weight (w_d) on application of any increment of live loading (w_l), as shown in Figure 2.4. The self-weight profile will be indicated by the subscript "o".

From equation (2.6), with the origin at C:

Equilibrium shape under dead load (w_d) is $y_o = \frac{4 d_o}{L^2} \cdot x^2$

Extended shape under total load $w_t = w_d + w_l$ is

$$y_t = \frac{4 (d_o + \Delta d_e)}{L^2} \cdot x^2 \quad -\Delta d_e$$

From equation (2.9) $l_e = L \left\{ 1 + \frac{8}{3} \left(\frac{d_o}{L} \right)^2 \right\}$

$$l_t = L \left\{ 1 + \frac{8}{3} \left(\frac{d_o + \Delta d_e}{L} \right)^2 \right\}$$

Thus extension under live loading $\Delta l_e = l_t - l_o$

$$= \frac{8 \Delta d_e}{3L} (2 d_o + \Delta d_e) \qquad -(2.14)$$

This is an alternative form of equation (2.11).

If Δl_e is due to the elasticity in the cable, then

$$\Delta l_e = \int_o^l \frac{\Delta T \quad ds}{AE}$$

$$= \frac{2 H_t}{AE} \left\{ \frac{L}{2} + \frac{8 (d_o + \Delta d_e)^2}{3L} \right\} - \frac{2 H_o}{AE} \left\{ \frac{L}{2} + \frac{8 d_o^2}{3L} \right\}$$

$$= \frac{L}{AE} \left\{ \frac{(w_d + w_L) L^2}{8 (d_o + \Delta d_e)} \right\} \left\{ 1 + \frac{16}{3} \left(\frac{d_o + \Delta d_e}{L} \right)^2 \right\}$$

$$- \frac{L}{AE} \left\{ \frac{(w_d) L^2}{8 d_o} \right\} \left\{ 1 + \frac{16}{3} \left(\frac{d_o}{L} \right)^2 \right\}$$

For very small $\left(\frac{d_o}{L} \right)$ then $\left(\frac{d_o}{L} \right)^2 \rightarrow 0$

and $$\Delta l_e = \frac{L^3}{8 AE} \left\{ \frac{(w_d + w_L)}{(d_o + \Delta d_e)} - \frac{w_d}{d_o} \right\} \qquad -(2.15)$$

Combining equations (2.14) and (2.15)

then $$\frac{8\ \Delta d_e}{3L}\ (2 d_o + \Delta d_e) = \frac{L^3}{8AE}\left\{\frac{(w_d + w_L)}{(d_o + \Delta d_e)} - \frac{w_d}{d_o}\right\}$$

Putting $\Delta d_e = m \cdot d_o$ and $w_L = p \cdot w_d$

then $$\frac{8m}{3L}\ (2 + m) = \frac{1}{8AE}\ \left(\frac{L}{d_o}\right)^3\ \left\{w_d\ \frac{(p+1)}{(m+1)} - w_d\right\}$$

thus $$m(m+1)(m+2) = \frac{3 w_d L}{64 AE}\ \left(\frac{L}{d_o}\right)^3\ (p - m) \qquad - (2.16)$$

Equation (2.16) is of the same form as equation (2.13) with an additional term on the right hand side to account for the change in loading. It is much more general in application than equation (2.13). For any given uniform loading (w) and cable profile under this loading $\left(\frac{d_o}{L}\right)$, any increment of loading (p.w) will yield a cable profile defined by

$$\frac{(m+1)\ d_o}{L}$$

If the given loading system is specified as the weight of the cable (w_c) and the cross-sectional area of the cable is A_c, then $\frac{w_c}{A_c} = \rho_c$ the weight per unit volume of material comprising the cable. In this case, equation (2.16) reduces to:

$$m(m+1)(m+2) = \frac{3 \rho_c L}{64 E_c}\ \left(\frac{L}{d_o}\right)^3\ (p - m) \qquad - (2.17)$$

Thus with the cable material properties specified, equation (2.17) defines the relationship between loading and cable profile (p vs m). A series of graphs have been included in Appendix A showing p vs $(m+1)\frac{d_o}{L}$ for steel having ρ = 490 p.c.f. and E = 30,000 Ksi over a range of $\left(\frac{d_o}{L}\right)$ from 0.0015 to 0.025 and for span length L between 400 feet and 2,000 feet.

The non-dimensional load factor $p = \frac{w_L}{w_d}$ is particularly useful in cable design. For any given initial profile $\left(\frac{d_o}{L}\right)$ and serviceability criterion such as a maximum value of $(m+1)\frac{d_o}{L}$ the corresponding value of p can be obtained. Knowing absolute design values of live loading and dead load other than self-weight, the required cable weight and hence the cable area can then be ascertained.

Referring again to Figure 2.3, equation (2.17) is essentially the solution

of two functions $y = m\,(m + 1)\,(m + 2)$ and $y = K\,(p - m)$

For $K = \frac{3\,\rho_c\,L}{64\,E_c}\left(\frac{L}{d_o}\right)^3 > 1$ there will be a unique solution for m.

For $K < 1$ there will be a limited zone where three solutions are possible, depending on the value of p. Comments in Section 2.2 concerning the three solutions are applicable here.

The unextended cable profile can be obtained from equation (2.17) by substituting $p = -1$. Equation (2.17) then reduces to:

$$m\,(m + 2) = -\frac{3\,\rho_c\,L}{64\,E_c}\left(\frac{L}{d_o}\right)^3$$

Thus $$(m + 1)^2 = 1 - \frac{3\,\rho_c\,L}{64\,E_c}\left(\frac{L}{d_o}\right)^3$$

When $\frac{3\,\rho_c\,L}{64\,E_c}\left(\frac{L}{d_o}\right)^3 > 1$, $(m + 1)$ is equal to the square root of a negative number, and the unextended cable profile $\frac{(m + 1)\,d_o}{L}$ is meaningless. This situation represents the case of a cable whose unextended length is less than the span length L. The unextended length can still be computed using equation (2.9) in the following form:

$$l = L\left[1 + \frac{8}{3}\left(\frac{d_o}{L}\right)\right](m + 1)^2$$

For such a cable, equation (2.17) will always have a unique solution.

In addition to serviceability criteria it is necessary to consider stress criteria. From equation (2.5), for any general cable profile $\left(\frac{d}{L}\right)$ and loading (w),

Horizontal tension $$H = \frac{w\,L^2}{8d}$$

Stress in cable $$f_c \doteqdot \frac{H}{A_c} = \frac{w\,L^2}{8\,A_c\,d}$$

For the cable profile $\frac{(m + 1)\,d_o}{L}$ under loading $(p + 1)\,w_c$,

$$\text{then } f_c = \frac{w_c}{8\,A_c} \cdot \frac{L^2}{d_o} \cdot \frac{(1 + p)}{(1 + m)}$$

$$= \frac{\rho_c\,L}{8}\left(\frac{L}{d_o}\right)\frac{(1 + p)}{(1 + m)} \qquad - (2.18)$$

Using in equation (2.18) values of m and p obtained from the solution of equation (2.17), the resultant stress in the cable can be calculated. A series of graphs showing p vs f have been included in Appendix A to complement those of p vs $(m+1)\ \frac{d_o}{L}$ for the steel having ρ = 490 p.c.f. and E = 30,000 Ksi over the same range of $(\frac{d_o}{L})$ and span length L.

For the cable whose unextended length is less than the span length L, substitution of m = -1 into equation (2.17) will correspond to the situation where the cable is straight and stretches just across the span. For m = -1, p also takes the value -1, and the "prestretch" stress required to fit the cable into the span cannot be computed directly by substitution into equation (2.18). However, the ratio $(\frac{1+p}{1+m})$ does have a finite value for this special case, and can be obtained by rearranging equation (2.17) as

$$m(m+2) = \frac{3\rho_c L}{64 E_c} \cdot (\frac{L}{d_o})^3 \cdot \left\{ \frac{p+1}{m+1} - 1 \right\}$$

$$\text{Thus } \frac{p+1}{m+1} = \left\{ \frac{64 E_c}{3\rho_c L} (\frac{d_o}{L})^3 \cdot m(m+2) \right\} + 1$$

Putting m = -1 and substituting this expression in equation (2.18) gives

$$\text{"Prestretch" stress } f_o = \frac{\rho_c L}{8} (\frac{L}{d_o}) \left\{ 1 - \frac{64 E_c}{3\rho_c L} (\frac{d_o}{L})^3 \right\} \quad - (2.19)$$

2.4 EFFECT OF TEMPERATURE ON CABLE BEHAVIOUR

Cable extensions and deformations as a result of variations in temperature, will occur independently of the external loading. Analysis of this effect must be based on the unextended length of the cable and is similar to that in Section 2.2 where a change in cable length under constant external loading was considered.

For an unextended cable profile of $(\frac{d}{L})$, from equation (2.11).

Change in length $\Delta l = \frac{8 \Delta d}{3L} (2d + \Delta d)$

If Δl is due to the thermal expansion of the cable,

then $\Delta l = l \alpha t$

where α = co-efficient of thermal expansion

t = temperature variation

then $\Delta l = \alpha t L \left\{ 1 + \frac{8}{3} \left(\frac{d}{L}\right)^2 \right\}$ - (2.20)

Combining equations (2.11) and (2.20), and assuming (as was done previously) for small $\left(\frac{d}{L}\right)$ that $\left\{ 1 + \frac{8}{3} \cdot \left(\frac{d}{L}\right)^2 \right\} \doteqdot 1$

then $\frac{8 \Delta d}{3L} (2d + \Delta d) = \alpha t L$

Putting $\Delta d = k \cdot d$

then $k(2 + k) = \frac{3 \alpha t}{8} \cdot \left(\frac{L}{d}\right)^2$

giving $(k+1)^2 = \left\{ 1 + \frac{3 \alpha t}{8} \cdot \left(\frac{L}{d}\right)^2 \right\}$ - (2.21)

The new unextended cable profile is $(k+1)\frac{d}{L}$

The response of the cable to any loading can then be determined using equation (2.13).

2.5 SUMMARY OF ANALYSIS

(i) Under a uniformly distributed loading, a cable between two fixed supports at the same level (as in Figure 2.1) assumes a parabolic profile defined by:

$$y = \frac{4d}{L^2} \cdot x^2 \qquad \text{- (2.6)}$$

(ii) The horizontal component of cable tension is given by:

$$H = \frac{w L^2}{8 d} \qquad \text{- (2.5)}$$

(iii) The cable length can be expressed as:

$$l = L \left\{ 1 + \frac{8}{3} \left(\frac{d}{L}\right)^2 \right\} \qquad \text{- (2.9)}$$

(iv) The cable slope at each extremity is:

$$\frac{dy}{dx} = \frac{4d}{L}$$

(v) A cable of unextended length l and unextended profile $\left(\frac{d}{L}\right)$ will extend under any total loading (w) to take up a profile defined by $\frac{(n+1)d}{L}$ where n is obtained from:

$$n(n+1)(n+2) = \frac{3 w L}{64 AE} \left(\frac{L}{d}\right)^3 \qquad \text{- (2.13)}$$

(vi) For any given loading system (w), and cable profile under this loading $(\frac{d_o}{L})$, any increment of loading (p.w) will yield a cable profile defined by $\frac{(m + 1)\ d_o}{L}$ where m is obtained from:

$$m\,(m + 1)\,(m + 2) = \frac{3\ w\ L}{64\ AE}\ (\frac{L}{d_o})^3\ (p - m) \qquad - (2.16)$$

(vii) The stress in the cable under these conditions is given by:

$$f_c = \frac{w\ L}{8\ A_c}\ (\frac{L}{d_o})\ \frac{(1 + p)}{(1 + m)} \qquad - (2.18)$$

(viii) For a cable having an unextended profile $(\frac{d}{L})$, any variation in temperature (t) will yield a new unextended profile defined by $(k + 1)\ \frac{d}{L}$ where k is obtained from:

$$(k + 1)^2 = 1 + \frac{3\ \alpha\ t}{8}\ (\frac{L}{d})^2 \qquad - (2.21)$$

2.6 REMARKS ON CABLE BEHAVIOUR UNDER LOAD

Because the cable in catenary is for all practical purposes defined by a simple parabola under the type of loading considered so far, the bending moment at any point along the cable is equal to zero, and the cable experiences axial stresses only.

From the formulae summarized in Section 2.5 it can be seen that, for any specified cable material properties, the cable behaviour is dependent on three factors - span length (L), sag/span ratio $(\frac{d}{L})$, and loading (p) - as compared with dependence on only span length and loading for normal flexural analysis of structural members.

Figures 2.5 - 2.11 have been compiled from the graphs in Appendix A, to demonstrate the effect of these three factors.

Figure 2.5 shows the response of the deflection increment $(\frac{\Delta\ d}{L})$ with variation of $(\frac{d_o}{L})$ the initial cable dead-load profile, for a span of 800 feet and constant load factor p = 6. $(\frac{d_o}{L}$ is plotted to a logarithmic scale.) The non-linear nature of this response is apparent.

For the same conditions, Figure 2.6 shows the stress response as $(\frac{d_o}{L})$ is varied. The curve (f_o) represents the initial stress in the cable under dead load only (i.e. p = 0), and is linearly proportional to $(\frac{L}{d_o})$. The curve (f_t) represents the final stress in the cable under the live loading (i.e.

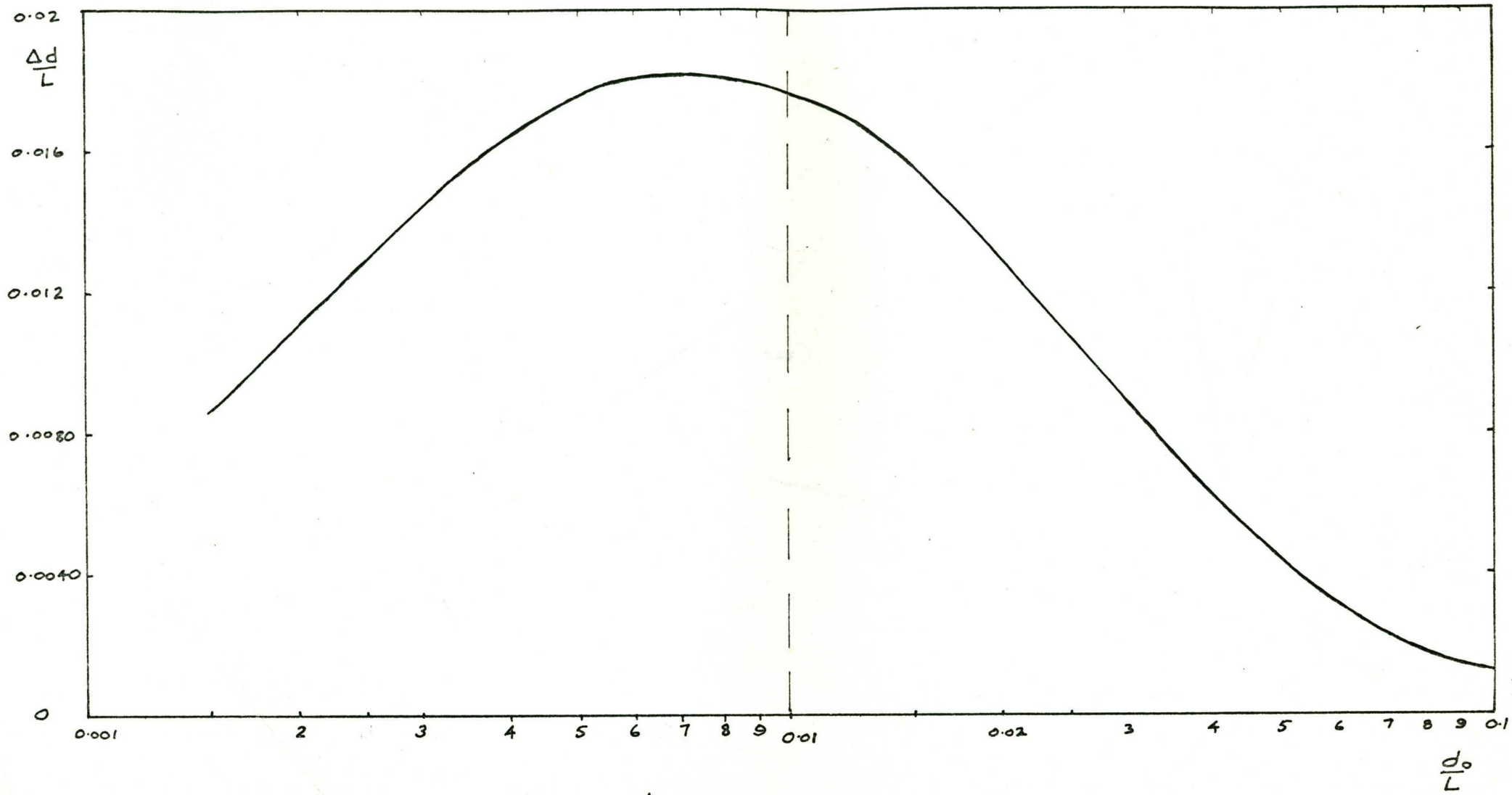

Fig 2.5 $\frac{\Delta d}{L}$ vs $\frac{d_0}{L}$ for $L = 800$ ft and $p = 6$

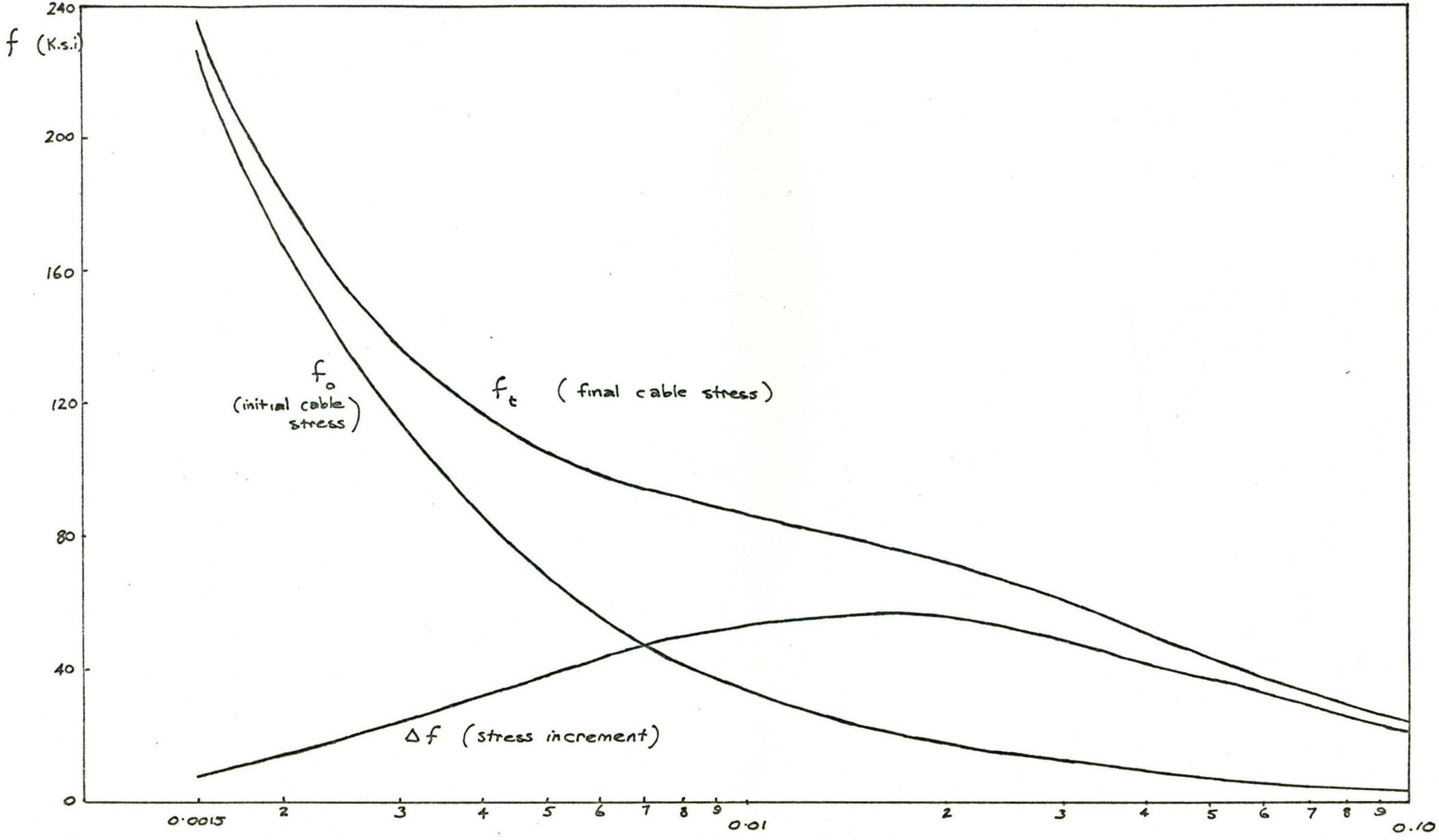

Fig 2.6 f vs $\frac{d_o}{L}$ for L = 800 ft and p = 6

Fig 2.7.

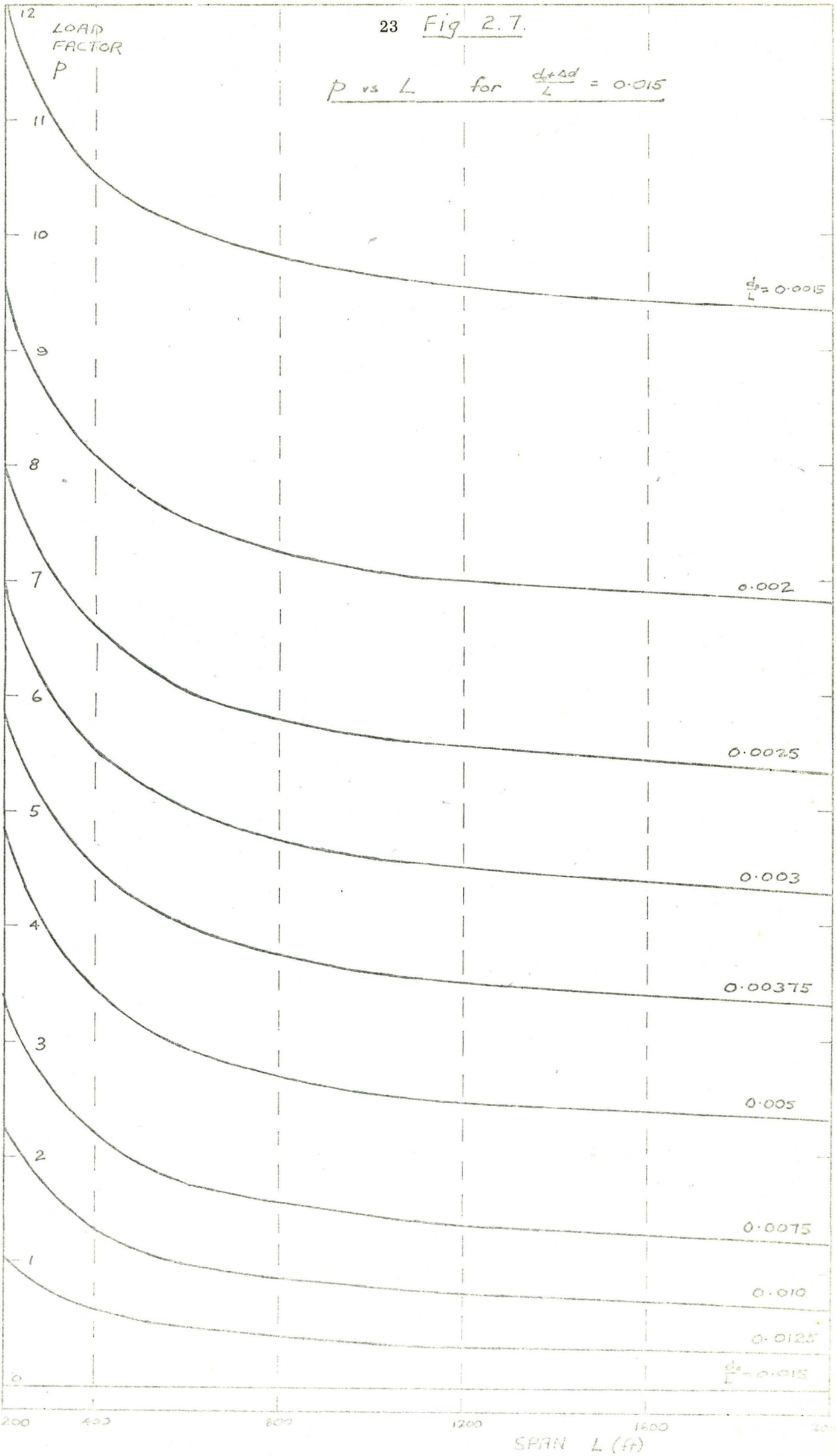
LOAD FACTOR p
p vs L for $\frac{d_0+\Delta d}{L} = 0.015$
12
11
10
9
8
7
6
5
4
3
2
1
0
$\frac{d_0}{L} = 0.0015$
0.002
0.0025
0.003
0.00375
0.005
0.0075
0.010
0.0125
$\frac{d_0}{L} = 0.015$
200
400
800
1200
1600
SPAN L (ft)

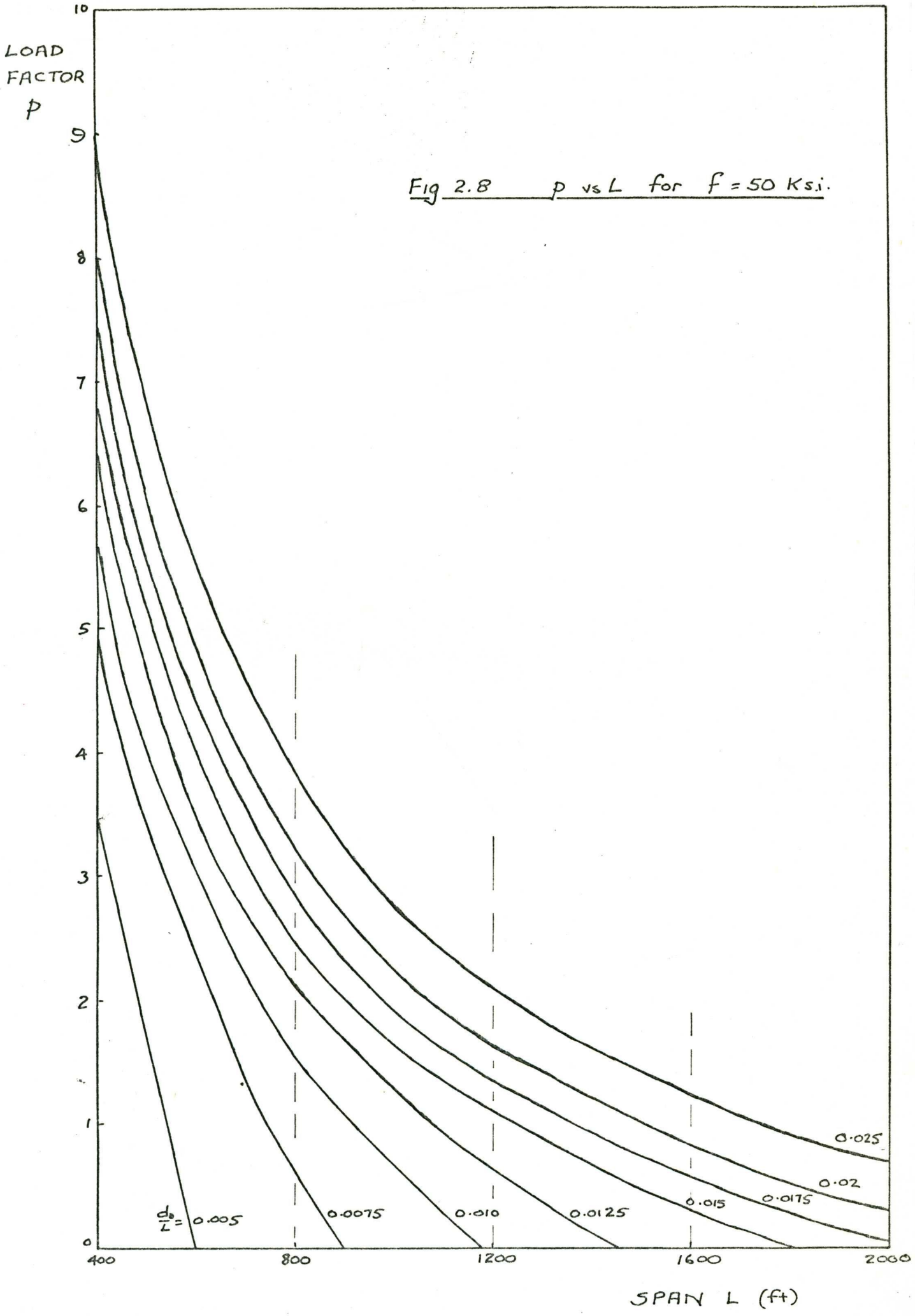

Fig 2.8 p vs L for f = 50 Ksi.

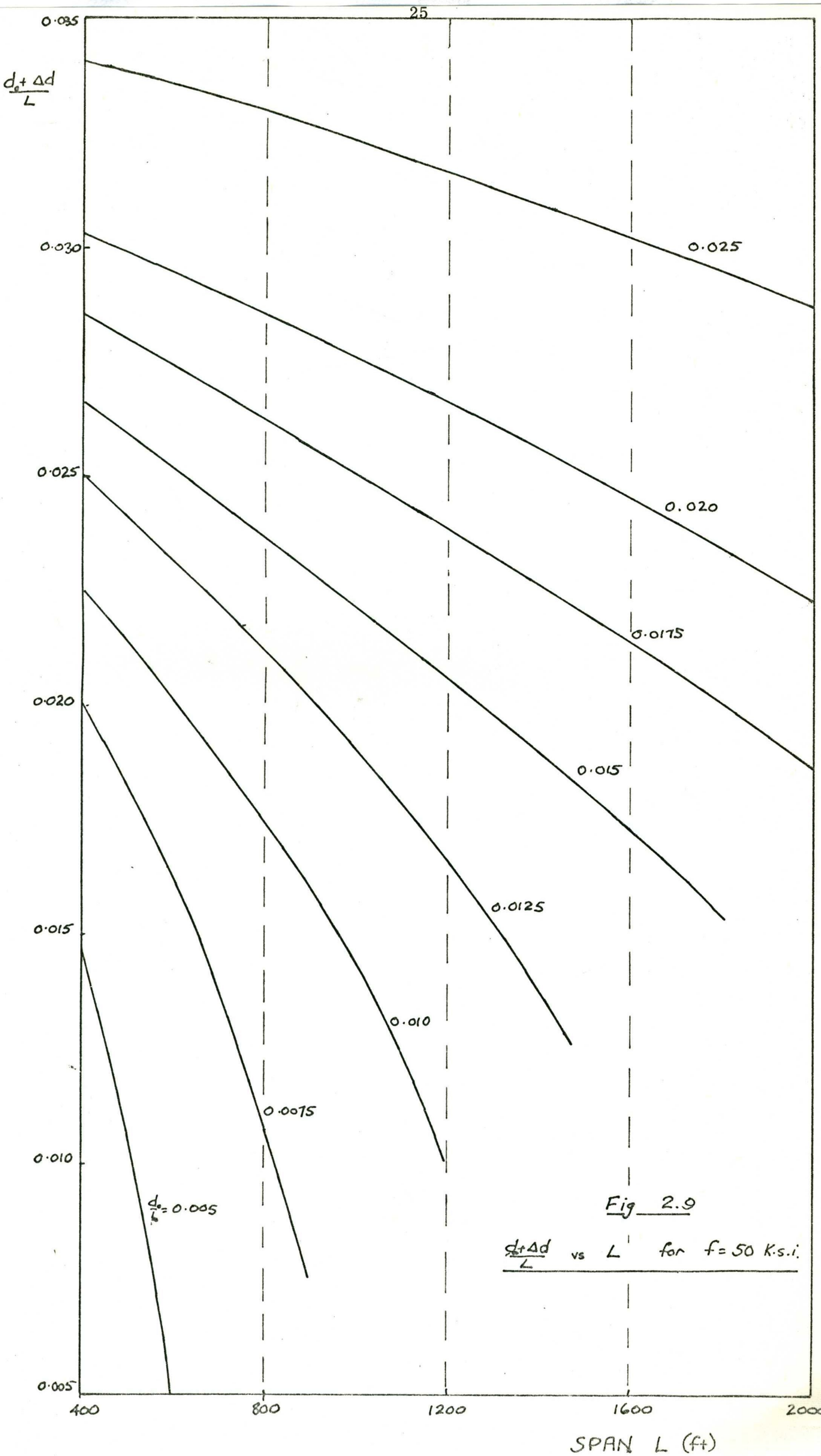

Fig 2.9

$\frac{d_e + \Delta d}{L}$ vs L for f = 50 K.s.i.

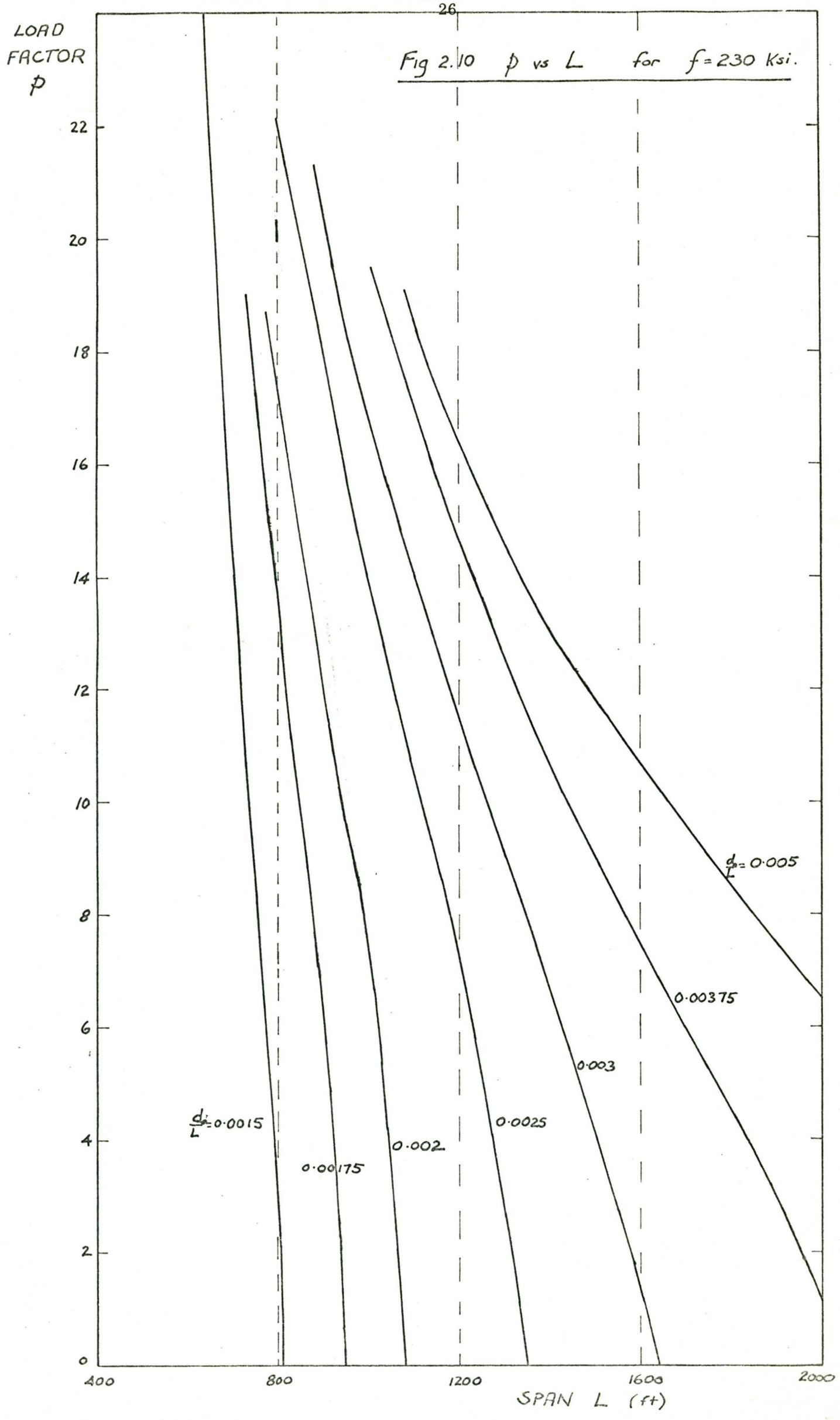
LOAD FACTOR p
Fig 2.10 p vs L for f = 230 ksi.
22
20
18
16
14
12
10
8
6
4
2
0
400
800
1200
1600
2000
SPAN L (ft)
$\frac{d_i}{L}$=0.0015
0.00175
0.002
0.0025
0.003
0.00375
$\frac{d_i}{L}$=0.005

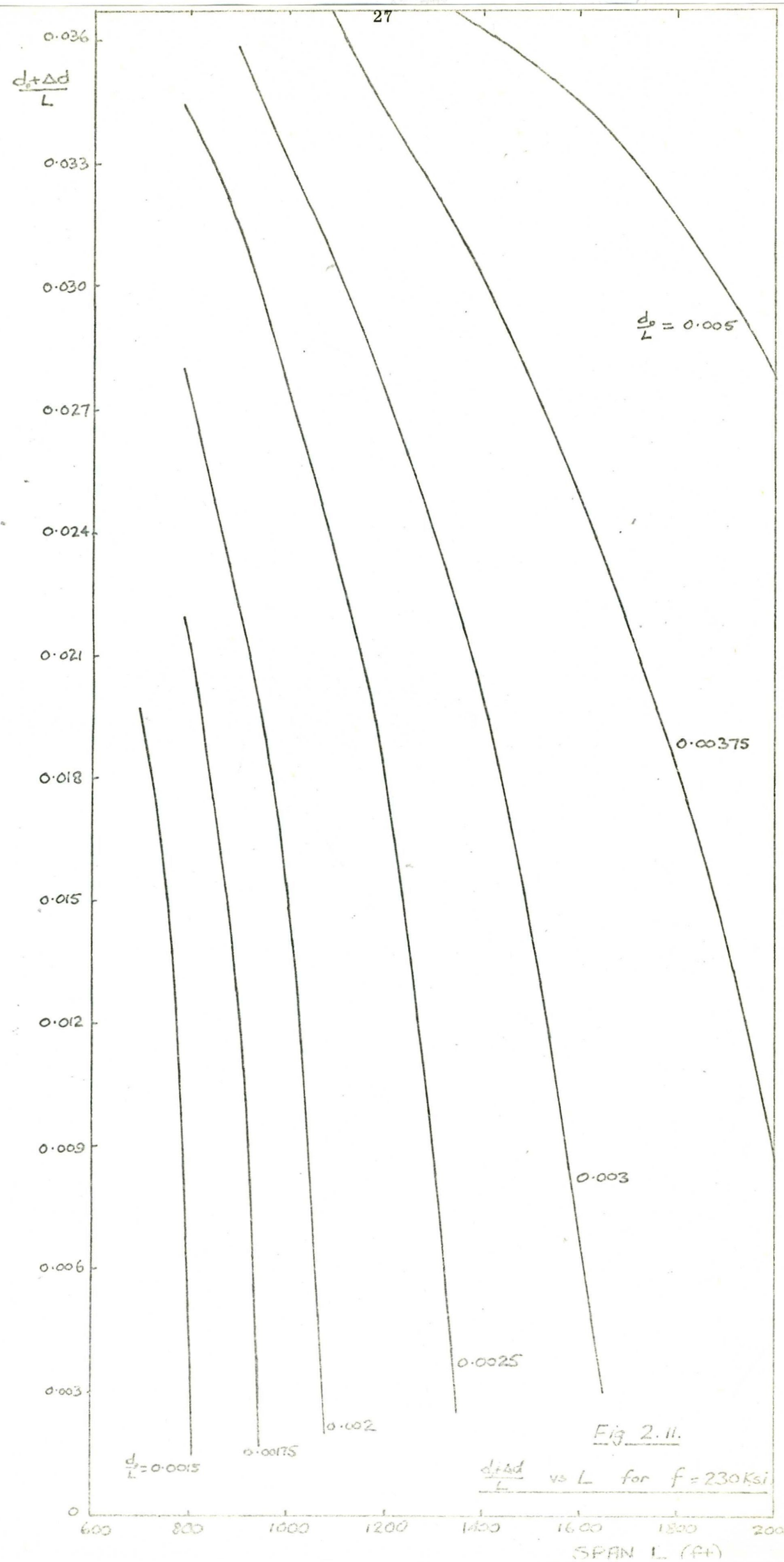

Fig 2.11.

$\frac{d_o+\Delta d}{L}$ vs L for f = 230 Ksi

p = 6). The curve (Δf) represents the stress increment due to the live load. The maximum stress increment occurs at a value of $\left(\frac{d_o}{L}\right)$ = 0.0162 for which

$$\frac{3\,\rho_c\,L}{64\,E_c}\left(\frac{L}{d_o}\right)^3 = 1 \qquad \text{(see Section 2.3)}$$

Figure 2.7 shows the relationship between the span length (L) and the load factor (p) at a deflection $\frac{d_o + \Delta d}{L}$ = 0.015 (as a maximum serviceability criterion) for $\frac{d_o}{L}$ varying from 0.0015 to 0.015. The relative high influence of $\frac{d_o}{L}$ as compared with L on the load-carrying capacity of the catenary member, is obvious. This relationship is only valid provided the yield stress of the cable material has not been reached.

Figures 2.8 and 2.10 show the relationship between the span length (L) and the load factor (p) at maximum stresses of 50 Ksi and 230 Ksi respectively, for various values of $\frac{d_o}{L}$. The span length L has a much greater influence on the load carrying capacity at a specified maximum stress level, and becomes increasingly important as the maximum stress level is raised.

Figures 2.9 and 2.11 show the relationship between the span length (L) and the deflected shape $\left(\frac{d_o + \Delta d}{L}\right)$ at maximum stress levels of 50 Ksi and 230 Ksi respectively, for the values of $\left(\frac{d_o}{L}\right)$ considered in Figures 2.8 and 2.10. Again the span length (L) becomes increasingly important as the maximum stress level is raised.

Further comments regarding cable behaviour, are made in the following section.

2.7 DIRECT METHOD OF CABLE DESIGN

For conventional tension members, the member stress is directly proportional to the applied loading. For the catenary structural member, however, the relationship between applied loading and resulting member stress (as expressed in equation 2.18) is non-linear. This non-linearity is demonstrated in the relevant graphs in Appendix A, and increases with decreasing $\frac{d_o}{L}$ Consequently, the conventional "working stress" approach is not considered satisfactory for the design of catenary structures. Instead, an ultimate strength approach is proposed, employing ultimate load factors similar to those adopted for prestressed concrete design. This subject is covered in Chapter 7.

The basic design method proposed herein uses equations (2.17) and (2.18) in conjunction to satisfy serviceability criteria at working loads, and ultimate strength criteria with appropriate load factors applied to the working loads. Both the initial profile $(\frac{d_o}{L})$ and the cable area for this profile must be determined. Using information from the graphs in Appendix A, it is possible to determine directly suitable values of $\frac{d_o}{L}$ and the load factor p. Knowing absolute values of live loading, the required cable dead load is obtained and hence the cable area. Allowance for temperature variation can also be incorporated in the procedure.

The design procedure can best be illustrated by a series of numerical examples. Four examples are included in this section, all requiring information which can be extracted from Figures 2.7 to 2.11.

EXAMPLE 2.1

A cable is required to carry a uniformly distributed live loading of 1,200 lb/ft. between two fixed points at the same level, 800 feet apart. The maximum slope of the cable is to be limited to 6% under working loads, and at yield point the cable is to resist twice the total working load. The cable material has the following properties Fy = 50 Ksi, E = 30,000 Ksi, ρ = 490 lb/cu.ft. Determine the required area of cable and the unloaded cable profile.

Solution:

At extremities, $(\frac{dy}{dx})_{max} = \frac{4\,d}{L}$

Thus for serviceability, limiting $\frac{d_o + \Delta d}{L} = \frac{0.06}{4} = 0.015$

From Figure 2.7, for L = 800 feet, a plot of p_s vs $\frac{d_o}{L}$ for $\frac{d_o + \Delta d}{L} = 0.015$ can be obtained. This is shown as the "serviceability" curve on Figure 2.12.

Ultimate load conditions are obtained by applying a live load $w_u = w_d + 2w_l$ to the cable. Thus the load factor at ultimate $p_u = 1 + 2p_s$. From Figure 2.8, for L = 800 feet, a plot of p_u vs $\frac{d_o}{L}$ for f_{max} = 50 Ksi, can be obtained. This is shown as the "stress" curve on Figure 2.12.

If the p_u axis is to a scale such that $p_u = 1 + 2p_s$, then the point of intersection of the two curves indicates the best possible solution to the problem. Any solution in the shaded area will satisfy both serviceability and stress criteria.

From Figure 2.12, the optimum solution is:

$$p_s = 0.52 \qquad \frac{d_o}{L} = 0.01215$$

For w_l = 1,200 lb/ft. then $w_d = \frac{1,200}{0.52}$ = 2,310 lb/ft.

For ρ = 490 lb/cu.ft. then $A = \frac{2,310}{490}$ = 4.72 sq.ft.

Thus a cable of area 4.72 sq.ft. and initial dead-load profile of 0.01215 is required.

Total anchorage force at ultimate loading = $A f_y$

= 4.72 x 144 x 50

= 34,000 Kip

EXAMPLE 2.2

For the same location and loading data, determine the cable area and unloaded profile if the cable has fy = 230 Ksi.

Solution: Using the same procedure as in Example 2.1, curves are plotted in Figure 2.13 with serviceability and stress criteria from Figures 2.7 and 2.10 respectively, for L = 800 feet.

From Figure 2.13, the optimum solution is:

$$p_s = 7.6 \qquad \frac{d_o}{L} = 0.0019$$

For w_l = 1,200 lb/ft. then $w_d = \frac{1,200}{7.6}$ = 158 lb/ft.

For ρ = 490 lb/cu.ft. then $A = \frac{158}{490}$ = 0.322 sq.ft.

In this case, a cable area of only 0.322 sq.ft. at an initial dead-load profile of 0.0019, is required.

Total anchorage force at ultimate loading = 0.322 x 144 x 230

= 10,630 Kip

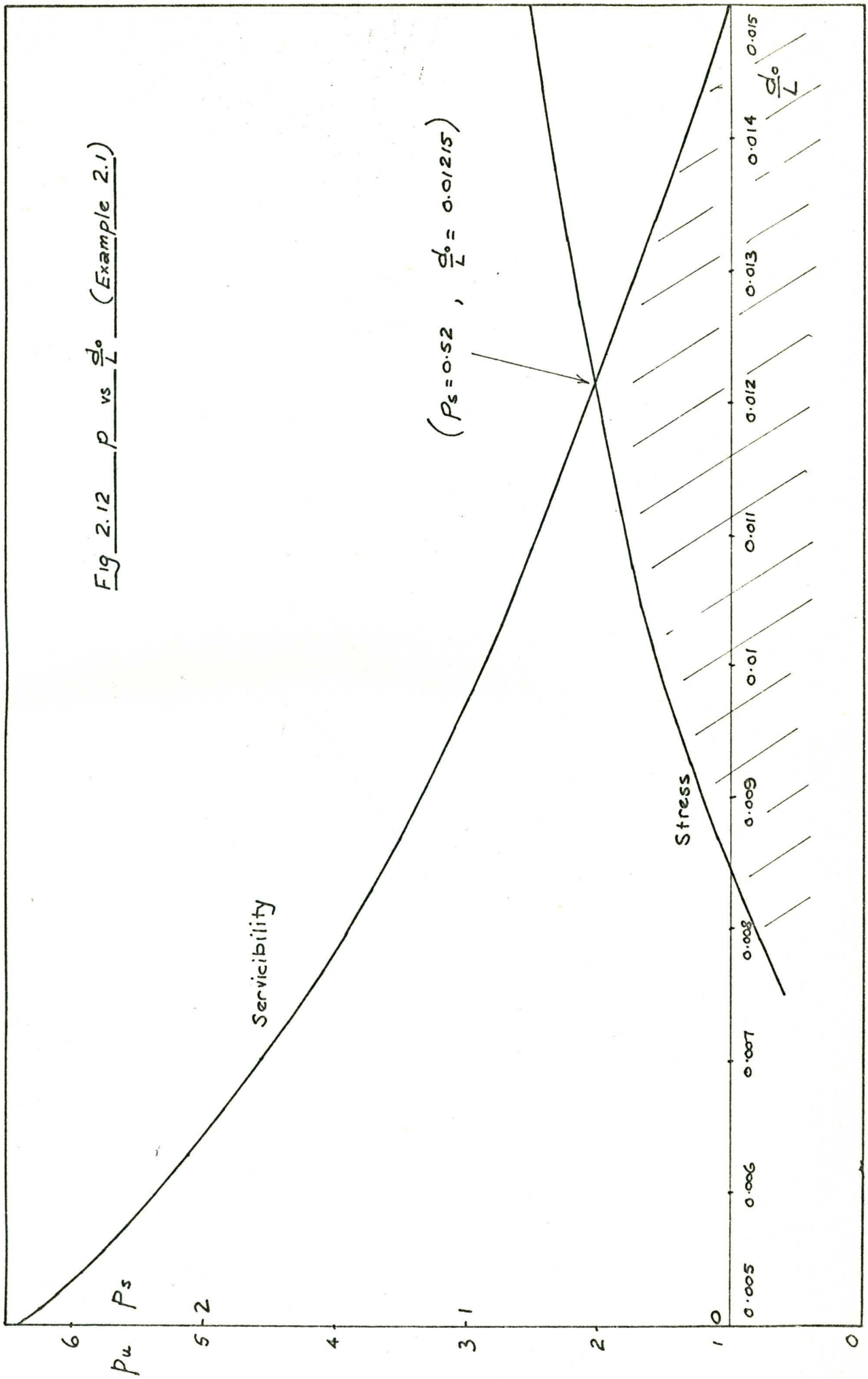

Fig 2.12 P vs $\frac{d_0}{L}$ (Example 2.1)

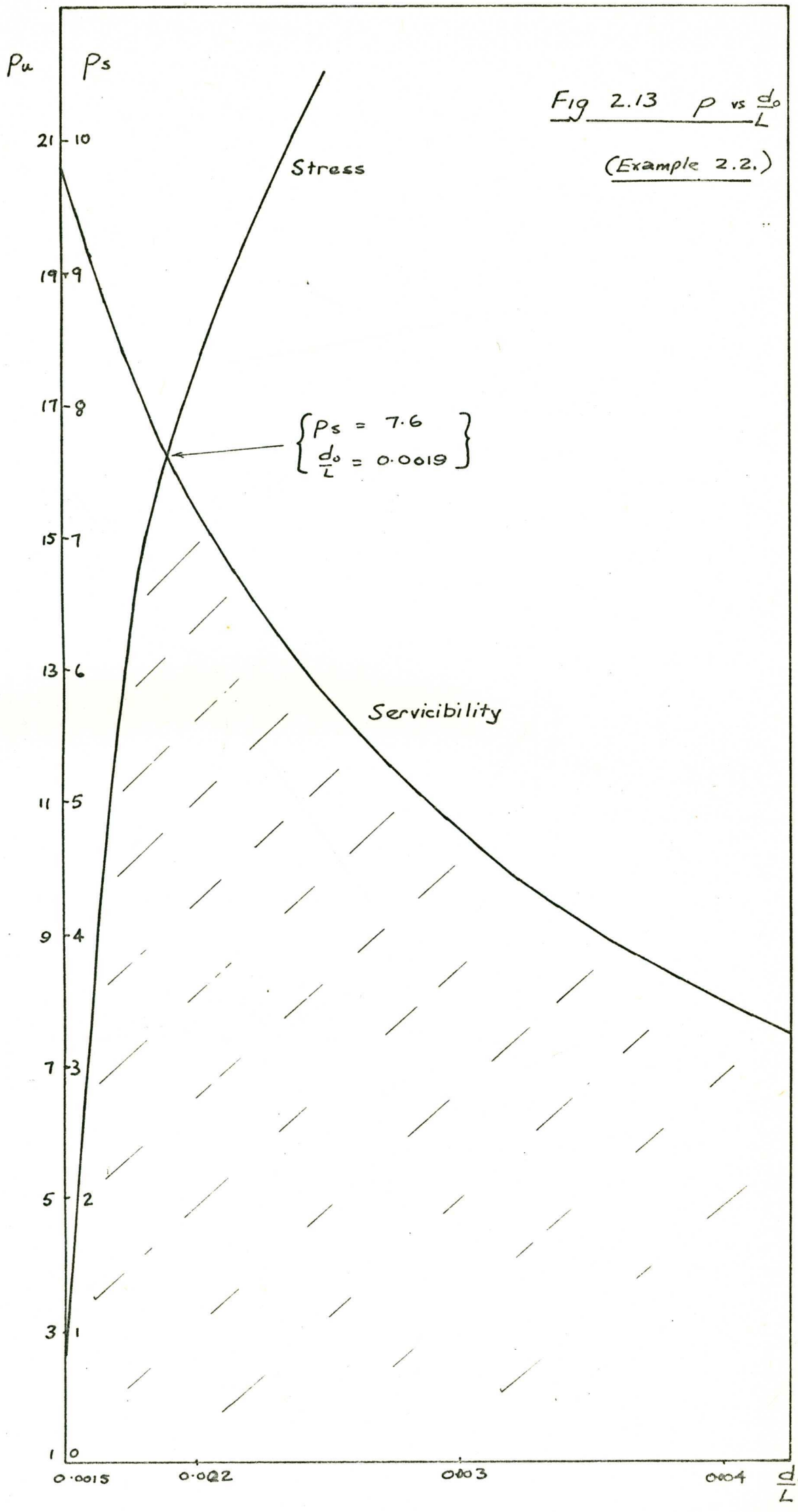

Fig 2.13 p vs $\frac{d_0}{L}$

(Example 2.2.)

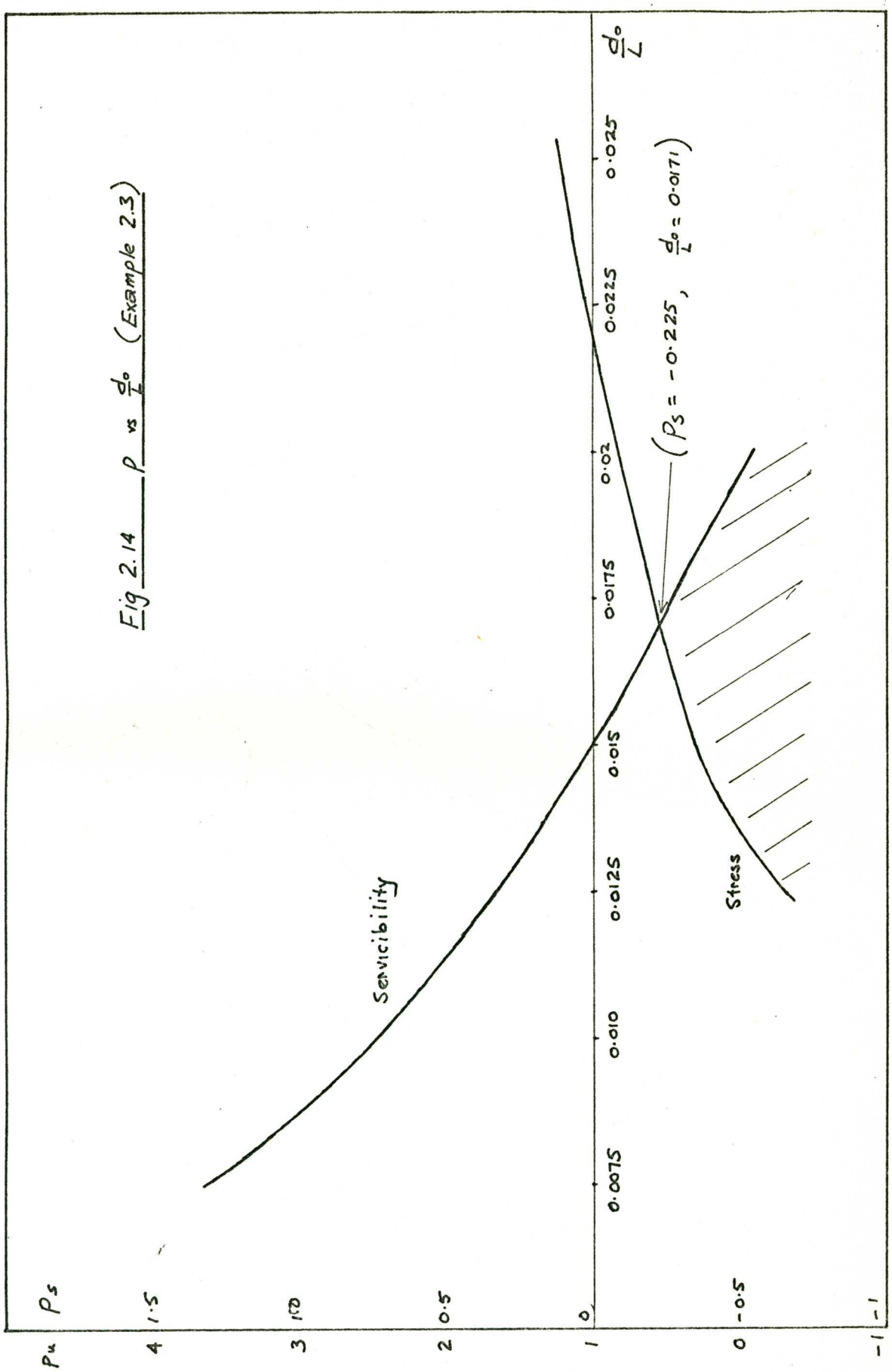
Fig 2.14 ρ vs d₀/L (Example 2.3)
ρu
ρs
4
3
2
1
0
1.5
1.0
0.5
-0.5
-1
0.0075
0.010
0.0125
0.015
0.0175
0.02
0.0225
0.025
d₀/L
Servicibility
Stress
(ρs = -0.225, d₀/L = 0.0171)

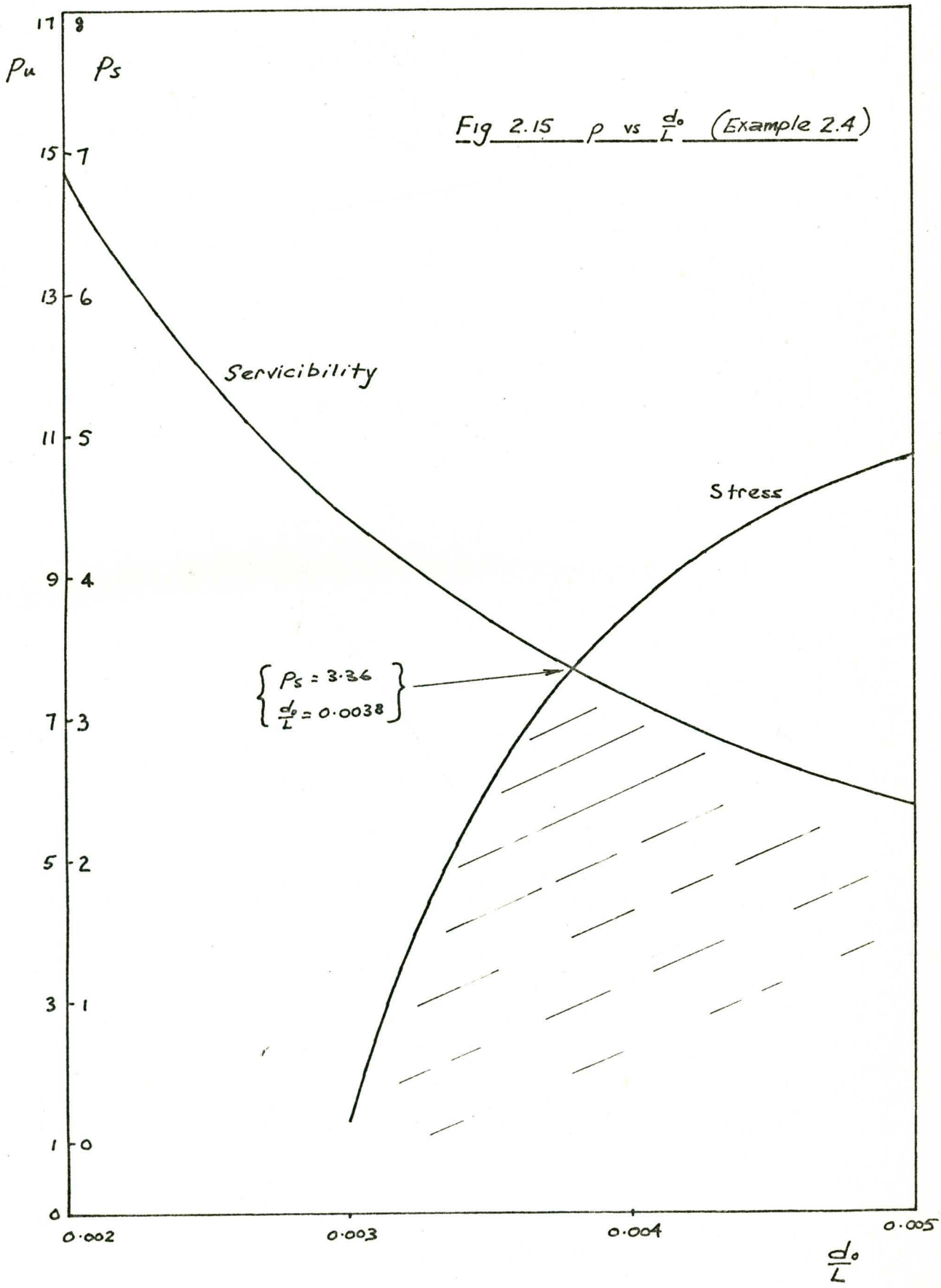

Fig 2.15 ρ vs $\frac{d_0}{L}$ (Example 2.4)

Comparison of solutions for Examples 2.1 and 2.2 shows that an increase in permissible stress by a factor of 4.6 resulted in a decrease in cable area by a factor of 15. Thus the second cable works much more efficiently than the first. A further benefit associated with the second cable is that the required total anchorage force is far lower than that for the first cable.

EXAMPLE 2.3

For the same loading data and cable material as in Example 2.1, determine the cable area and unloaded cable profile for a span length of 1,600 feet.

Solution: Using the same procedure, curves are plotted in Figure 2.14 with serviceability and stress criteria from Figures 2.7, 2.8 and Appendix A for L = 1,600 feet.

From Figure 2.14, the optimum solution is:

$$p_s = -0.225 \qquad \frac{d_o}{L} = 0.0038$$

The negative value of p_s indicates that an upward dead-load would be required. In other words, it is not possible to use this material and satisfy both the serviceability and stress criteria specified in this problem.

EXAMPLE 2.4

For the same loading data and cable material as in Example 2.2, determine the cable area and unloaded cable profile for a span length of 1,600 feet.

Solution: Using the same procedure, curves are plotted in Figure 2.15 with serviceability and stress criteria from Figures 2.7 and 2.10 respectively for L = 1,600 feet.

From Figure 2.15, the optimum solution is:

$$p_s = 3.36 \qquad \frac{d_o}{L} = 0.0038$$

It is a simple matter to check the graphical solution using equations 2.17 and 2.18, as indicated below.

$$m(m+1)(m+2) = \frac{3\rho L}{64 E} \left(\frac{L}{d_o}\right)^3 (p - m) \qquad - (2.17)$$

For $\left(\frac{d_o}{L}\right) = 0.0038$

Then $$\frac{3\rho L}{64 E} \left(\frac{L}{d_o}\right)^3 = \frac{3 \times 490 \times 1600}{64 \times 30,000,000 \times 144} \left(\frac{1}{0.0038}\right)^3$$

$$= 156$$

For $\left(\frac{d}{L}\right)_s = 0.015$ then $m_s = \frac{0.015 - 0.0038}{0.0038} = 2.95$

Thus $$p_s = \frac{2.95 \times 3.95 \times 4.95}{156} + 2.95$$

$$= 0.37 + 2.95 = 3.32$$

For $$p_u = 1 + 2 p_s = 7.64$$

From equation 2.18, an m_u would be required such that

$$230 = \frac{490 \times 1600}{8 \times 144} \times \frac{(8.64)}{1 + m} \times \frac{1}{0.0038}$$

$$m_u = 6.72 - 1 = 5.72$$

Checking in equation 2.17 for m = 5.72

$$p = \frac{5.72 \times 6.72 \times 7.72}{156} + 5.72$$

$$= 1.90 + 5.72 = 7.62$$

Thus there is very good agreement with the graphical solution.

Adopting $p_s = 3.32$ and $= 0.0038$

For $w_l = 1,200$ lb/ft. then $w_d = \frac{1,200}{3.32} = 362$ lb/ft.

For $\rho = 490$ lb/ft. then $A = \frac{362}{490} = 0.738$ sq.ft.

Noting that the cable area A is inversely proportional to the load factor p_s, Figure 2.16 indicates the relationship between span length L and cable area required to satisfy the serviceability and stress criteria considered in these examples. For $p_s < 0$ the cable will yield under its own weight.

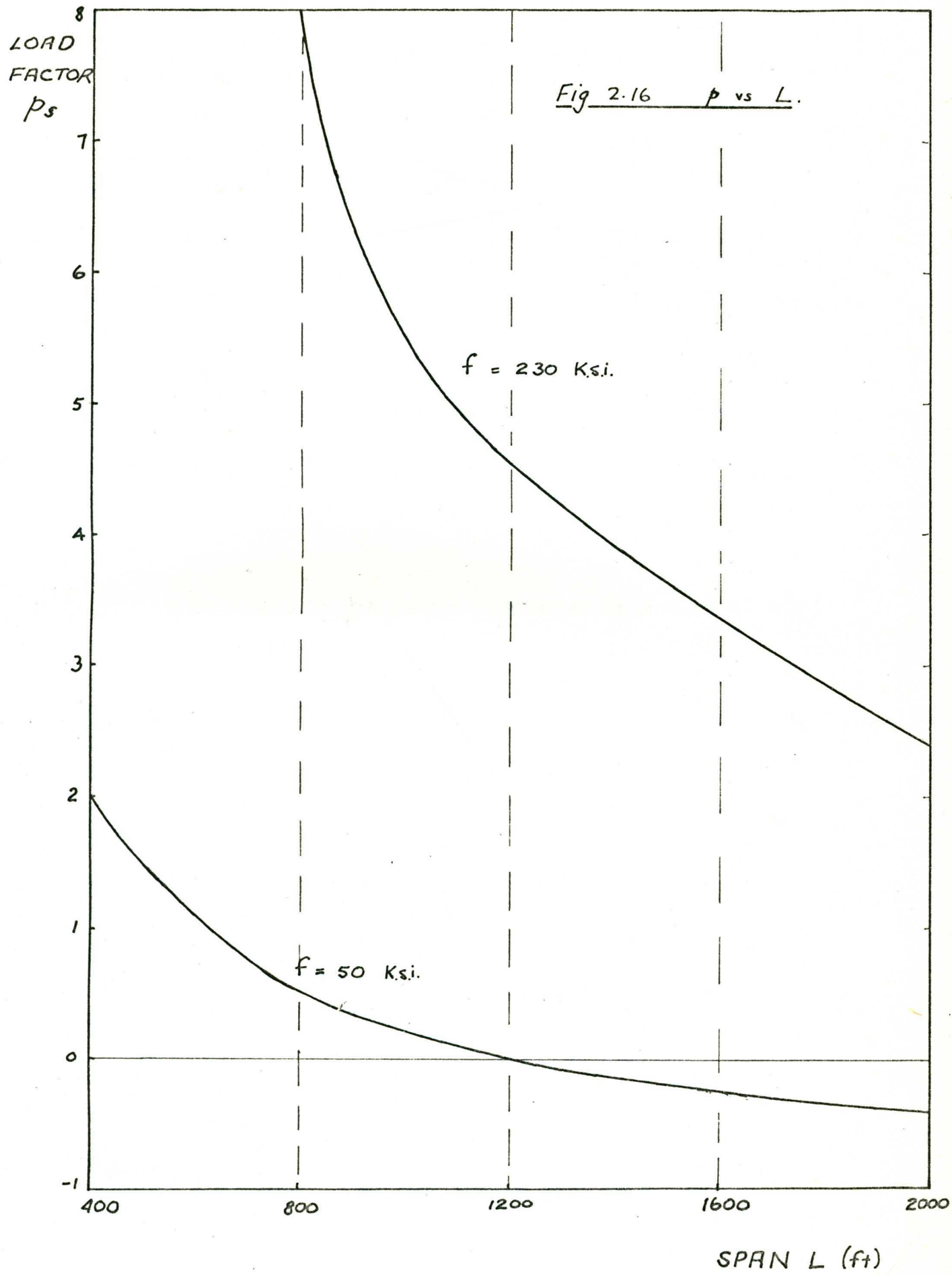
LOAD FACTOR p_s
8
7
6
5
4
3
2
1
0
-1
400
800
1200
1600
2000
SPAN L (ft)
f = 230 K.s.i.
f = 50 K.s.i.

Fig 2.16 p vs L.

CHAPTER 3

EXTENSION TO GENERAL CABLE PROBLEMS

3.1 THE CABLE WITH SUPPORT POINTS AT DIFFERENT LEVELS

Chapter 2 was concerned with the special case where the two fixed anchorage points were at the same level. In practice this is not normally the case, and allowance must be made for the difference in level.

Figure 3.1 shows a cable suspended between two fixed points A and B, at a distance L apart and with B a distance h above A. The cable can be considered as part of the cable between B' and B (at the same level), and will therefore adopt a parabolic profile.

With origin at A, the general equations of the parabola through A and B is: $y = Dx^2 + Ex$

At B, $x = L$ and $y_B = DL^2 + EL$

Also $y_B = h = L \tan\beta$

Thus $E = \tan\beta - DL$

At C, $x = \frac{L}{2}$ and $y_c = \frac{DL^2}{4} + \frac{EL}{2}$

$= \frac{DL^2}{4} + \frac{L}{2}(\tan\beta - DL)$

$= \frac{L}{4}(2\tan\beta - DL)$

Also $y_c = \frac{h}{2} - d$

Then $d = \frac{L}{2}\tan\beta - \frac{L}{4}(\tan\beta - DL)$

$= \frac{DL^2}{4}$

Thus $D = \frac{4d}{L^2}$

and $E = (\tan\beta - \frac{4d}{L})$

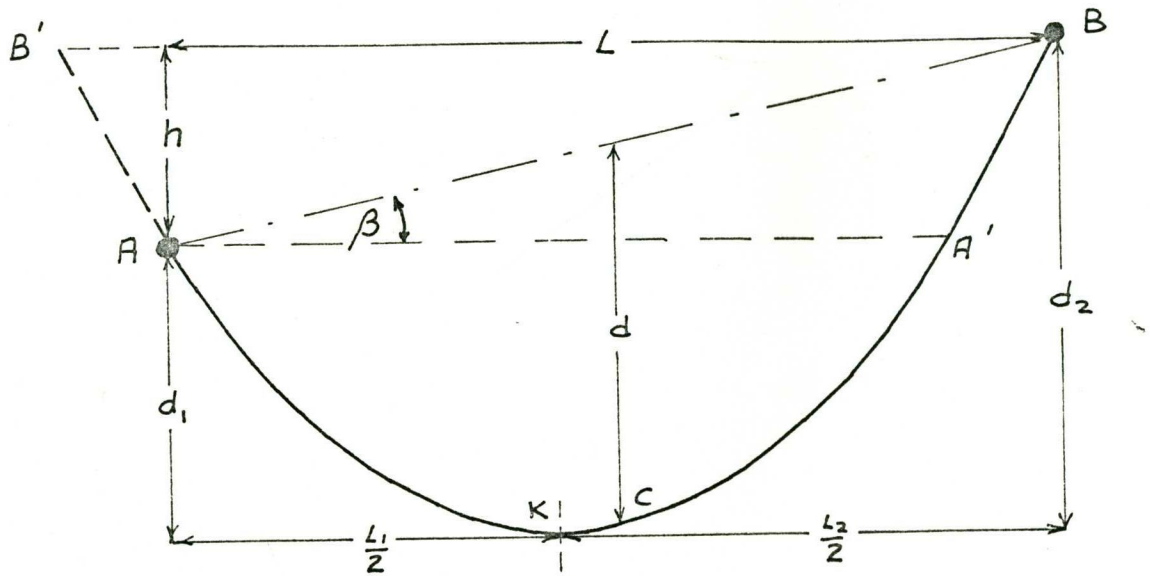

Fig 3.1 GENERAL CABLE PROFILE

So that the equation of the parabola through A and B becomes:

$$y = \frac{4d}{L^2} \cdot x^2 + (\tan\beta - \frac{4d}{L})x \qquad - (3.1)$$

$$\frac{dy}{dx} = \frac{8d}{L^2} \cdot x + (\tan\beta - \frac{4d}{L})$$

At $x = \frac{L}{2}$, $\frac{dy}{dx} = \frac{4d}{L} + \tan\beta - \frac{4d}{L}$

$= \tan\beta$

Thus the maximum vertical dip measured from the chord AB will always occur at mid-span.

In Chapter 2, emphasis was directed towards relationship between serviceability criteria and $\frac{d}{L}$. For the general case considered here, the maximum vertical dip (d) measured from the chord AB, will not coincide with the lowest point on the cable profile, which is obtained when $\frac{dy}{dx} = 0$. The two alternative serviceability criteria have to be considered separately.

At $x = L$, $\frac{dy}{dx} = \frac{8d}{L} + \tan\beta - \frac{4d}{L}$

$= \frac{4d}{L} + \tan\beta$

Thus for a maximum ruling grade, the required maximum $\frac{d}{L}$ for serviceability can be readily calculated.

To find the location of the lowest point K or the cable profile, (i.e. the vertex) put $\frac{dy}{dx} = 0$

Then $x_k = (\frac{L}{2} - \frac{L^2 \tan\beta}{8d})$

Also $y_k = \frac{4d}{L^2}\left\{\frac{L}{2} - \frac{L^2\tan\beta}{8d}\right\}^2 + \left\{\tan\beta - \frac{4d}{L}\right\}\left\{\frac{L}{2} - \frac{L^2\tan\beta}{8d}\right\}$

$= -d\left\{1 - \frac{L\tan\beta}{4d}\right\}^2 \qquad - (3.2)$

from which $(\frac{d}{L})^2 + \frac{d}{L}(\frac{y_k}{L} - \frac{\tan\beta}{2}) + \frac{\tan^2\beta}{16} = 0$

Thus if clearance restrictions are imposed, the required maximum $\frac{d}{L}$ for serviceability can again be readily determined.

In relation to the vertex K, the cable can be considered as two separate portions (see Figure 3.1).

Portion AK is half of the parabola (A A') having central vertical dip d_1 and span L_1

Portion BK is half of the parabola (B' B) having central vertical dip d_2 and span L_2

The horizontal tension at the vertex K is given by: $H = \frac{w L_1^2}{8 d_1} = \frac{w L_2^2}{8 d_2}$

from which $L_1 = \left(\frac{8 d_1 H}{w} \right)^{\frac{1}{2}}$

and $L_2 = \left(\frac{8 d_2 H}{w} \right)^{\frac{1}{2}}$

Now $L = \frac{1}{2} (L_1 + L_2)$

Therefore $L \left(\frac{w}{2H} \right)^{\frac{1}{2}} = (d_1)^{\frac{1}{2}} + (d_2)^{\frac{1}{2}}$

and $$H = \frac{w L^2}{2 \left\{ (d_1)^{\frac{1}{2}} + (d_2)^{\frac{1}{2}} \right\}^2} \qquad - (3.3)$$

Equation (3.3) has been derived for the case where the vertex of the parabola lies between A and B. It remains valid for the case where the vertex lies outside the support points A and B. This situation would correspond to analysis of cable segment B'A in Figure 3.1, which must have the same horizontal tension as segment AB.

Also $V_A = \frac{w L_1}{2}$ and $V_B = \frac{w L_2}{2}$ - (3.4)

Now from equation (3.2) $d_1 = - y_k$

$$= d \left(1 - \frac{L \tan \beta}{4d} \right)^2$$

and $d_2 = - y_k + L \tan \beta$

$$= d \left(1 + \frac{L \tan \beta}{4d} \right)^2$$

Thus $\left\{ (d_1)^{\frac{1}{2}} + (d_2)^{\frac{1}{2}} \right\}^2 = d \left\{ \left(1 - \frac{L \tan \beta}{4d} \right) + \left(1 + \frac{L \tan \beta}{4d} \right) \right\}^2$

$$= 4d$$

Therefore $$H = \frac{w L^2}{4d} \qquad - (3.5)$$

which is identical to the expression derived in Chapter 2 for H, with d defined as the vertical dip at mid-span from the straight line between the support points. This general relationship is most important. Although observed by Steinman (1) in 1922 it does not appear to have been appreciated by more recent writers (2, 3, 4, 12 for example) who do not progress beyond the special case of the symmetrical cable as considered in Chapter 2.

Again considering the two cable segments AK and BK, the total length (l) of cable can be determined as indicated below.

$$l = \tfrac{1}{2} L_1 \left\{ 1 + \frac{8}{3} \left(\frac{d_1}{L_1}\right)^2 \right\} + \tfrac{1}{2} L_2 \left\{ 1 + \frac{8}{3} \left(\frac{d_2}{L_2}\right)^2 \right\}$$

$$= L + \frac{4}{3} \left\{ \frac{d_1^2}{L_1} + \frac{d_2^2}{L_2} \right\}$$

Noting from equation (3.5) that $H = \dfrac{w L_1^2}{8 d_1} = \dfrac{w L_2^2}{8 d_2} = \dfrac{w L^2}{8 d}$

$$\text{Then } \frac{d_1}{(L_1)^2} = \frac{d_2}{(L_2)^2} = \frac{d}{L^2}$$

$$\text{So that } l = L + \frac{4}{3} \left(\frac{d}{L^2}\right)^{\frac{1}{2}} \left(d_1^{3/2} + d_2^{3/2} \right)$$

$$\text{Also } d_1 = d \left(1 - \frac{L \tan\beta}{4d} \right)^2$$

$$\text{and } d_2 = d \left(1 + \frac{L \tan\beta}{4d} \right)^2$$

$$\text{Then } l = L \left\{ 1 + \frac{4}{3} \left(\frac{d}{L}\right)^2 \left[\left(1 - \frac{L \tan\beta}{4d}\right)^3 + \left(1 + \frac{L \tan\beta}{4d}\right)^3 \right] \right\}$$

$$\text{from which } l = L \left\{ 1 + \frac{8}{3} \left(\frac{d}{L}\right)^2 + \tfrac{1}{2} \tan^2\beta \right\} \qquad - (3.6)$$

If the more accurate expression for cable length in equation (2.8) is used, then

$$l = L \left\{ 1 + \frac{8}{3} \left(\frac{d}{L}\right)^2 - \frac{32}{5} \left(\frac{d}{L}\right)^4 + \tan^2\beta \left[\tfrac{1}{2} - \frac{12}{5} \left(\frac{d}{L}\right)^2 \right] - \frac{1}{40} \tan^4\beta \right\}$$

It is now possible to analyse the behaviour of the general cable under loading, using the same procedure as for the simple cable in Section 2.2 and Section 2.3.

Equation (3.6) expressing the cable length is identical with equation (2.9) except for an additional <u>constant</u> term $\frac{L}{2} \tan^2\beta$ When considering the

extension of the cable as the difference between the extended length and the original length, the additional constant term will disappear so that

$$\Delta l = \frac{8\,\Delta d}{3L}\,(2d + \Delta d) \qquad \text{as in equation (2.11)}$$

If Δl is due to the elasticity in the cable

$$\text{then} \quad \Delta l = \frac{H_e}{AE}\int_0^L 1 + \left(\frac{dy_e}{dx}\right)^2 dx$$

$$= \frac{H_e}{AE}\int_0^L 1 + \left\{\frac{8(d+\Delta d)}{L^2}\cdot x + \tan\beta - \frac{4d}{L}\right\}^2 dx$$

$$= \frac{H_e L}{AE}\left\{\operatorname{cosec}^2\beta + \frac{16}{3}\left(\frac{d+\Delta d}{L}\right)^2\right\}$$

$$\doteq \frac{H_e L \operatorname{cosec}^2\beta}{AE} \quad \text{for} \quad \frac{(d+\Delta d)}{L} \quad \text{very small.}$$

This expression is, in fact, the extension of the chord length AB ($L \operatorname{cosec}\beta$) under an axial force $H \operatorname{cosec}\beta$ along AB.

Now $$H = \frac{w L^2}{8d} \qquad - (3.5)$$

ERRATUM

On pages 43, 44, 47, 48, 51, 52

"cosec β " should be read as "sec β "

$$w = w_c \operatorname{cosec}\beta \qquad - (3.7)$$

Thus the expression for the extension of the cable becomes

$$\Delta l = \frac{w_c L^3 \operatorname{cosec}^3\beta}{8AE(d+\Delta d)} = \frac{8\,\Delta d}{3L}(2d + \Delta d)$$

Putting $d = n.d$

$$\text{then} \quad n(n+1)(n+2) = \frac{3 w_c}{64AE}\left(\frac{L}{d}\right)^3 . L \operatorname{cosec}^3\beta \qquad - (3.8)$$

Likewise equations (2.17) and (2.18) become

$$m(m+1)(m+2) = \frac{3\rho_c}{64E_c}\left(\frac{L}{d_o}\right)^3 . (L \operatorname{cosec}^3\beta)(p-m) \qquad - (3.9)$$

and $f_c = \frac{H \operatorname{cosec} \beta}{A_c}$

or $f_c \operatorname{cosec} \beta = \frac{\rho_c}{8} \cdot (L \operatorname{cosec}^3 \beta) \left(\frac{L}{d_o}\right) \frac{(1 + p)}{(1 + m)}$ - (3.10)

In this form, equations (3.9) and (3.10) permit direct use of the graphs in Appendix A, where $(L \operatorname{cosec}^3 \beta)$ may be regarded as the equivalent length of a cable between two support points at the same level. Consequently, the design procedure outlined in Chapter 2 can now be applied to the general case where the support points are at different levels.

3.2 UNIFORMLY DISTRIBUTED HORIZONTAL LOADING

When the cable is subjected to a uniformly distributed horizontal loading in addition to vertical loading, by resolving to find the direction of the resultant load, the cable can be analysed using equations (3.9) and (3.10), as indicated in Figure 3.2. β is considered as the angle of inclination between the supports as in Section 3.1.

3.3 UNIFORMLY DISTRIBUTED LOADING PART-WAY ACROSS SPAN

Preceeding analysis has been concerned solely with loading distributed uniformly across the full length of the span. Figure 3.3 shows a cable initially under a loading system (w_1) uniformly distributed across the span, and subjected to an additional live load (w_2) uniformly distributed across only a portion of the span.

In order to analyse this situation, the cable is divided into two segments AC and BC, corresponding to the two loading systems (w_1) and ($w_1 + w_2$). Each segment is analysed as a cable with support points at different levels. For equilibrium at the common support point C, the tension in the cable segments AC and BC must be equal in magnitude and opposite in direction. In other words there is a common slope at C. Knowing the initial cable profile under loading (w_1), and enforcing compatibility by maintaining a constant unstretched total cable length, the cable profile and stress condition under the additional loading (w_2) can be determined.

At this point it is appropriate to distinguish between two different types of loading:

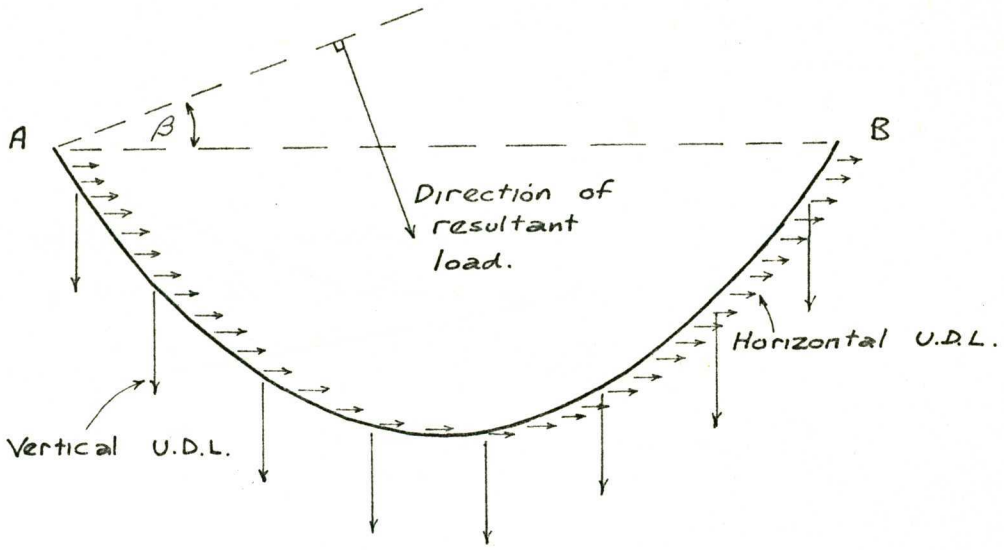

Fig 3.2. VERTICAL AND HORIZONTAL LOADING.

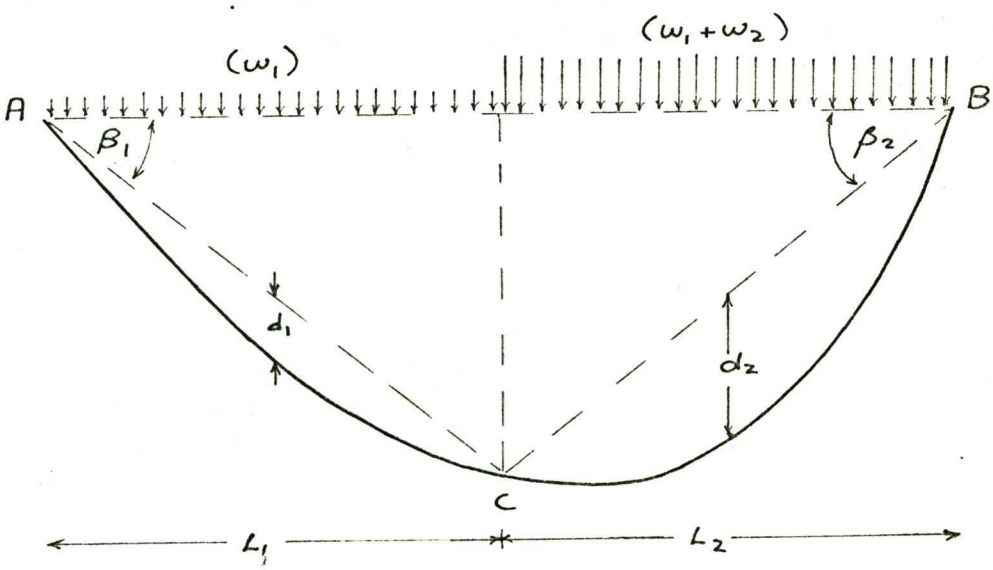

Data for Example 3.1 : $L_1 = L_2 = 800$ ft

$w_1 = 362$ lb/ft

$(w_1 + w_2) = 1562$ lb/ft.

Before applying (w_2) cable has sag/span = 0.0038

$\rho_c = 490$ lb/cuft

$E_c = 30{,}000$ K.s.i.

Fig. 3.3. LIVE LOADING PART-WAY ACROSS SPAN

(i) the fixed load - where the point of attachment of the load to the cable is fully specified,

(ii) the rolling load - where the load maintains a constant horizontal distance from the support point.

The method of analysis outlined above is suitable for both types of loading. It is demonstrated for the rolling load in the following example.

EXAMPLE 3.1

The cable designed in Exercise 2.4 is subjected to a uniformly distributed rolling load of 1,200 lb/ft. over one half of the span. Determine the stress in the cable, the deflection at mid-span, and the maximum slope of the cable.

Relevant cable data is shown in Figure 3.3.

Dead loading in segment AC $= w_1 = 362$ lb/ft.

Total loading in segment BC $= w_1 + w_2 = 4.32\, w_1$

For horizontal equilibrium at C, using equations (3.5) and (3.6)

$$\frac{w_1 \operatorname{cosec}\beta\, L^2}{8D_1} = \frac{(w_1 + w_2)\operatorname{cosec}\beta\, L^2}{8d_2}$$

From which $d_2 = 4.32\, d_1$

For segment AC, slope at C is

$$\frac{dy}{dx} = \frac{4d_1}{L} - \tan\beta$$

For segment BC, slope at C is

$$\frac{dy}{dx} = -\frac{4d_2}{L} + \tan\beta$$

Thus for a common slope at C,

$$\tan\beta = \frac{2}{L}(d_1 + d_2)$$

$$= 10.64\, \frac{d_1}{L}$$

For cable initially under loading (w_1), from equation (2.17)

$$m(m+1)(m+2) = \frac{3\rho L}{64 E}\left(\frac{L}{d_o}\right)^3 (p - m)$$

To determine total unstretched length, put p = -1.

Then $m(m+2) = -156$

or $(m+1)^2 = -155$

Thus unstretched length

$$l_{AB} = L\left\{1+\frac{8}{3}\left(\frac{d}{L}\right)^2 (m+1)^2\right\}$$

$$= 1600\left\{1-\frac{8}{3}(0.0038)^2 \times 155\right\}$$

$$= 1600 - 9.51$$

$$= 1590.49 \text{ ft.}$$

For cable segment AC, using equations (3.6) and (3.9), the unstretched length is given by

$$l_{AC} = L\left\{1+\frac{8}{3}\left(\frac{d_1}{L}\right)^2 - \frac{\rho}{8E}\left(\frac{L}{d_1}\right) L \operatorname{cosec}^3\beta + \tfrac{1}{2}\tan^2\beta\right\}$$

Similarly for cable segment BC, the unstretched length is given by:

$$l_{BC} = L\left\{1+\frac{8}{3}\left(\frac{d_2}{L}\right)^2 - \frac{4.32\rho}{8E}\left(\frac{L}{d_2}\right) L \operatorname{cosec}^3\beta + \tfrac{1}{2}\tan^2\beta\right\}$$

$$l_{AB} = l_{AC} + l_{BC}$$

So that $$1590.49 = L\left\{2+\frac{8}{3L^2}(d_1^2+d_2^2) + \tan^2\beta - \frac{\rho}{8E} L^2 \operatorname{cosec}^3\beta\left(\frac{1}{d_1}+\frac{4.32}{d_2}\right)\right\}$$

$$= 2L\left\{1+\frac{4}{3}\left(\frac{d_1}{L}\right)^2 (19.62) + \tan^2\beta - \frac{\rho}{8E}\left(\frac{L}{d_1}\right) L \operatorname{cosec}^3\beta\right\}$$

As a first approximation, neglect the second and third terms on the right hand side of the expression, and assume $\operatorname{cosec}^3\beta = 1$

Then $$\frac{\rho}{8E}\left(\frac{L}{d_1}\right) 2L^2 \doteq 9.51$$

From which $$\frac{L}{d_1} = 524$$

and $$\tan\beta = 10.64\frac{d_1}{L} = 0.0203$$

Using these figures to recalculate the unextended length,

$$l_{AB} = 1600 + 0.1525 + 0.66 - 9.514$$

$$= 1600 - 8.7015$$

The order of magnitude of the terms initially neglected, is apparent.

Try $\frac{L}{d_1}$ = 569

giving $\tan\beta$ = 0.0187

and l_{AB} = 1600 + 0.129 + 0.559 - 10.326

= 1600 - 9.638

Try $\frac{L}{d_1}$ = 562

giving $\tan\beta$ = 0.01895

and l_{AB} = 1600 + 0.132 + 0.573 - 10.214

= 1600 - 9.509

Thus required $\frac{L}{d_1}$ = 562

Stress in cable $f_c = \frac{H \operatorname{cosec}\beta}{A_c} = \frac{\rho L \operatorname{cosec}^2\beta}{8} \left(\frac{L}{d_1}\right)$

$= \frac{490 \times 800.3}{8 \times 144} \times 562$

= 191.5 Ksi

For comparison;

Stress in cable under dead load only = 179 Ksi

and stress in cable with live load across full span = 196 Ksi

Cable deflection at mid-span = 800 $\tan\beta$

= 15.15 ft.

For comparison;

Central deflection under dead load only = 6.08 ft.

Central deflection with live load across full span = 24.0 ft.

The maximum cable slope will occur at B and will be given by:

$\tan\beta + \frac{4 d_2}{L} = 0.01895 + \frac{4 \times 4.32}{562}$

= 0.0557

For comparison;

Maximum cable slope with live loading across full span = 0.060

3.4 THE CABLE UNDER CONCENTRATED LOADING

The procedure for analysis of a cable under concentrated loading is similar to that outlined in Section 3.3. The cable is divided into segments between the concentrated load points. Each segment is analysed as a cable with support points at different levels. Horizontal and vertical equilibrium and compatibility of the total unstretched length of cable are enforced. For this case, however, the slope of adjacent segments will be different at the common support points.

The method is demonstrated in Example 3.2 which is a problem previously used by Michalos and Birnstiel (8), O'Brien and Francis (10) and Harrison (11).

EXAMPLE 3.2

A cable spanning 1,000 ft. between supports at the same level, has a central sag of 100 ft. under self-weight conditions. For a rolling load of 8 kips applied 400 ft. from one end, determine the cable tension and slope at each support, and the vertical displacement of the load. The cable has an area of 0.85 sq.in., a self-weight of 3.16 lb/ft. and an elastic modulus of 19,000 ksi.

The cable is divided into two segments AP and BP as shown in Figure 3.4.

The total unstretched length of the cable is determined using equations (2.17) and (2.8).

$$(m_u + 1)^2 = 1 - \frac{3\,w\,L}{64AE}\left(\frac{L}{d}\right)^3$$

$$= 1 - \frac{3 \times 3.16 \times 1000\,(10)^3}{64 \times 0.85 \times 19,000,000}$$

$$= 0.99082$$

and

$$l_u = L\left\{1 + \frac{8}{3}(m_u + 1)^2\left(\frac{d}{L}\right)^2 - \frac{32}{5}(m_u + 1)^4\left(\frac{d}{L}\right)^4\right\}$$

$$= 1025.8 \text{ ft.}$$

This compares extremely well with Harrison's computed value for the unstretched length of 1,025.92 ft.

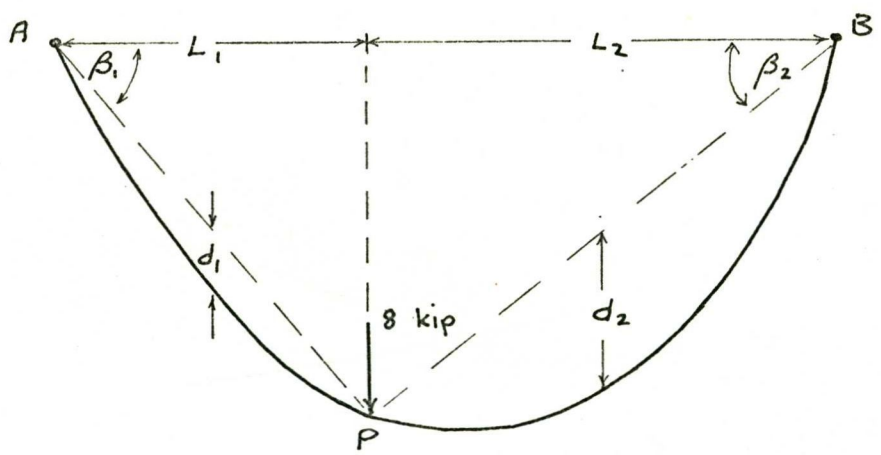

Data for Example 3.2. : $L_1 = 400'$, $L_2 = 600'$
Self weight = 3.16 lb / ft
Area = 0.85 in^2
Modulus = 19,000 K.s.i.
Cable self-weight profile $\frac{d_o}{L} = 0.1$

Fig 3.4 CABLE PROFILE FOR CONCENTRATED LOAD.

METHOD	Final load position y-ordinate	L.H. Support		R.H. Support	
		Slope (degrees)	Tension (Kips)	Slope (degrees)	Tension (Kips)
O'Brien and Francis	114.648'				
Harrison :					
100 elements	113.978'	17.74	20.8013	13.48	20.3735
200 elements	114.600'	17.69	21.1190	13.43	20.6856
Present Method	113.84'	17.584	21.03	13.31	20.60

Table 3.1 EXAMPLE 3.2 - COMPARISON OF SOLUTIONS.

From symmetry: $\tan \beta_2 = \frac{2}{3} \tan \beta_1$ ..... (1)

Horizontal equilibrium: $H_1 = H_2$

therefore $\frac{w}{\cos \beta_1} \cdot \frac{(400)^2}{8d_1} = \frac{w}{\cos \beta_2} \frac{(600)^2}{8d_2}$

from which $\frac{4 d_2}{9 d_1} = \frac{\cos \beta_1}{\cos \beta_2}$ ..... (2)

Vertical equilibrium:

(a) At P $H_1 (\tan \beta_1 - \frac{4 d_1}{L_1}) + H_2 (\tan \beta_2 - \frac{4 d_2}{L_2}) = 8$

(b) Externally $H_1 (\tan \beta_1 + \frac{4 d_1}{L_1}) + H_2 (\tan \beta_2 + \frac{4 d_2}{L_2}) = 8 + w L$

from which $H (\tan \beta_1 + \tan \beta_2) = 8 + \frac{w l_u}{2}$

whence $\frac{5}{3} H \tan \beta_1 = 8 + \frac{w l_u}{2}$

$= 9.621$

and $\frac{\tan \beta_1}{d_1 \cos \beta_1} = 0.09134$ ..... (3)

The unstretched lengths of segments AP and BP are determined using equations (3.6) and (3.9)

For AP: $(m_{1u} + 1)^2 = 1 - \frac{3 w}{64 AE} (\frac{L_1}{d_1})^3 (L_1 \operatorname{cosec}^3 \beta_1)$

Thus $l_{1u} = L_1 \left\{ 1 + \frac{8}{3} (\frac{d_1}{L_1})^2 (m_{1u} + 1)^2 + \frac{1}{2} \tan^2 \beta_1 \right\}$

$= L_1 \left\{ 1 + \frac{8}{3} (\frac{d_1}{L_1})^2 - \frac{w}{8AE} (\frac{L_1}{d_1}) (L_1 \operatorname{cosec}^3 \beta_1) + \frac{1}{2} \tan^2 \beta_1 \right\}$

Similarly for BP: $l_{2u} = L_2 \left\{ 1 + \frac{8}{3} (\frac{d_2}{L_2})^2 - \frac{w}{8AE} (\frac{L_2}{d_2}) (L_2 \operatorname{cosec}^3 \beta_2) + \frac{1}{2} \tan^2 \beta_2 \right\}$

For compatibility $l_{1u} + l_{2u} = l_u = 1025.8$ ft. ..... (4)

As a first approximation, neglect all terms involving $\frac{d_1}{L_1}$ and $\frac{d_2}{L_2}$

Then $l_u = L_1 (1 + \frac{1}{2} \tan^2 \beta_1) + L_2 (1 + \frac{1}{2} \tan^2 \beta_2)$

$= 400 (1 + \frac{1}{2} \tan^2 \beta_1) + 600 (1 + \frac{2}{9} \tan^2 \beta_1)$

from which $\tan\beta_1 = 0.278$

Substituting this value of $\tan\beta_1$ into the full expressions,

$l_{1u} + l_{2u} = 1024.68$ ft.

Try $\tan\beta_1 = 0.285$ This gives $l_{1u} + l_{2u} = 1026.00$ ft.

Try $\tan\beta_1 = 0.2846$ This gives $\tan\beta_2 = 0.1887$

$d_1 = 3.242$ ft., $d_2 = 7.16$ ft.

and $l_{1u} + l_{2u} = 1025.8$ ft. $= lu$

by slide rule calculation.

Thus final position of 8 kip load $= L_1 \tan\beta_1$

$= 113.84$ ft. below supports

Slope at L.H. support $= \tan\beta_1 + \frac{4d_1}{L_1}$

$= 0.2846 + 0.0324 = 0\ 317$

$= 17.584$ degrees

Slope at R.H. support $= \tan\beta_2 + \frac{4d_2}{L_2}$

$= 0.1887 + 0.0477 = 0.2364$

$= 13.31$ degrees

Horizontal tension in cable $H = \frac{w(L_1)^2}{8d_1 \cos\beta_1}$

$= 20.22$ Kip

Thus tension at L.H. support $= H \operatorname{cosec}(17.584^\circ)$

$= 21.03$ Kip

and tension at R.H. support $= H \operatorname{cosec}(13.31^\circ)$

$= 20.6$ Kip

These results are compared with those of O'Brien and Francis, and of Harrison in Table 3.1. Agreement is very good especially when consideration is given to the convenience of solution by slide rule calculation in this method. The discrepancy in the final position of the 8 kip load is only 0.6% while results

for cable tension lie between Harrison's computer solutions using 100 and 200 cable elements.

3.5 THE GENERAL CABLE UNDER ANY LOADING SYSTEM

In Chapters 2 and 3 a procedure has been developed to permit direct analysis of the general cable with support points at different levels and subjected to any system of concentrated and uniformly distributed loads vertically and horizontally in the plane of the cable. Relevant formulae are given in Section 2.5 and Section 3.1. Example 3.1 demonstrates the approach for dealing with uniformly distributed loads, and Example 3.2 that for concentrated loads. The basic procedure is the same in both cases and can readily be applied to any combined system of uniformly distributed and concentrated loads. Allowance can also be made for support flexibilities. Furthermore, calculations may be conveniently carried out by slide rule.

CHAPTER 4

CABLE - DECK INTERACTION

4.1 SOLUTION TO THE INTERACTION PROBLEM

Chapters 2 and 3 have been concerned with the situation where a single cable (or a system of identical cables) is subjected to a variety of loading conditions. Examples in Section 2.7 provide an indication of the effect of variation of material ultimate strength properties on the design of cables (see Figure 2.16). In fact the values of 50 ksi and 230 ksi used, were selected as typical values of normal structural steel and high strength prestressing cable.

In order to examine the feasibility of a steel cellular deck member in catenary prestressed by high strength cables, it is necessary to consider the interaction between two cables of differing material properties acting in combination to carry any specified loading. Analysis is more complicated than previously because the two cables will almost certainly have differing self-weight sag/span ratios ($\frac{d_o}{L}$). As the total load varies, in order to maintain the same cable profiles under load (i.e. in combination), the proportion of load carried by each cable will vary.

In this chapter the cellular deck member will be represented as a cable identified by the suffix "d", while the higher strength prestressing cable will be identified by the suffix "c".

At any particular profile ($\frac{d}{L}$) of the cable combination under a total loading ($w_d + w_c + w_L$), the horizontal tension is given by:

$$H_c + H_d = (w_c + w_d + w_L) \frac{L^2}{8d}$$

or

$$\frac{8d}{L^2} (f_d A_d + f_c A_c) = w_c (1 + p_c) + w_d (1 + p_d) \quad - \quad (4.1)$$

Equation (4.1) has a whole range of possible solutions from $A_d = 0$ to

$A_c = 0$. Thus, in a design problem, it is necessary to specify either A_c or A_d, after which equation (4.1) can be solved for the other cable area and the self-weight profiles of both cables, by consideration of serviceability and stress criteria. It was demonstrated in Chapter 2 that the higher strength material works more efficiently than the lower strength (deck) material. It would therefore be logical to specify the minimum possible deck area satisfying other structural requirements (such as aerodynamic stability) and then determine the required area of prestressing cable.

The design procedure is demonstrated in Examples 4.1, 4.2 and 4.3 which use the data from Examples 2.1 - 2.2, and Examples 2.3 - 2.4. For the two cables in combination yielding simultaneously, and A_d specified, the procedure is:

(i) Select a value of $(\frac{d_o}{L})_d$, the dead-weight profile of the deck.

(ii) Determine p_{ds}, the deck serviceability loading factor
p_{du}, the deck ultimate stress loading factor
$(\frac{d}{L})_u$, the ultimate stress cable profile

(iii) Determine the value of $(\frac{d_o}{L})_c$, the dead-weight profile of the cable, which produces the same $(\frac{d}{L})_u$

(iv) For this value of $(\frac{d_o}{L})_c$ determine p_{cs} and p_{cu}.

(v) At service loading, $w_s = w_c + w_d + w_L$

Also $$w_s = w_c (1 + p_{cs}) + w_d (1 + p_{ds})$$

Thus $$(w_c \cdot p_{cs}) + (w_d \cdot p_{ds}) = w_L$$

Knowing all other values, determine $(w_c)_s$ and hence $(A_c)_s$

At ultimate loading, $w_u = 2w_c + 2w_d + 2w_L$

Also $w_u = w_c (1 + p_{cu}) + w_d (1 + p_{du})$

Thus $w_c (p_{cu} - 1) + w_d (p_{du} - 1) = 2w_L$

Knowing all other values, determine $(w_c)_u$ and hence $(A_c)_u$

(vi) Plot $(\frac{d_o}{L})_d$ vs $(A_c)_s - (A_c)_u$ to eventually converge to a value of $(\frac{d_o}{L})_d$ for which $(A_c)_s = (A_c)_u$

Application of the graphs in Appendix A enables ready determination of all the above values.

EXAMPLE 4.1

A cable-deck system is required to carry a uniformly distributed live loading of 1,200 lb/ft. between two fixed points at the same level, 800 ft. apart. The maximum slope of the structure is to be limited to 6% under working loads. At simultaneous yielding of the cable and deck, the structure is to resist twice the total working load.

The deck material is specified as $A_d = 3.0$ sq.ft., $f_{dy} = 50$ Ksi, $E = 30{,}000$ Ksi, $\rho = 490$ lb/cu.ft.

The cable material is specified as $f_{cy} = 230$ Ksi, $E = 30{,}000$ Ksi, $\rho = 490$ lb/cu.ft.

Determine the required area of cable and the initial self-weight profiles for both the deck and the cable.

This problem comprises the identical design situation and cable types as considered in Examples 2.1 and 2.2. From Appendix A, the following plots are prepared:

(a) For the deck p_s vs $\frac{d_o}{L}$ and p_u vs $\frac{d_o}{L}$
(This has previously been prepared in Figure 2.12.)

(b) For the cable p_s vs $\frac{d_o}{L}$ and p_u vs $\frac{d_o}{L}$
(This has previously been prepared in Figure 2.13.)

(c) For the cable $(\frac{d}{L})_u$ vs $\frac{d_o}{L}$. This plot is shown in Figure 4.1.

The design procedure can now be followed step by step:

Trial No.1 (i) Select $(\frac{d_o}{L})_d = 0.01215$ (solution of Example 2.1).

(ii) Then from Figure 2.12 $p_{ds} = 0.52$

$p_{du} = 2.04$

From equation 2.18 $f_{du} = \frac{\rho L}{8}(1 + p_{du})(\frac{L}{d})_u$

giving $(\frac{d}{L})_u = 0.0207$

(iii) From Figure 4.1, for $(\frac{d}{L})_u = 0.0207$

then $(\frac{d_o}{L})_c = 0.00174$

(iv) From Figure 2.13, for $(\frac{d_o}{L})_c = 0.00174$

then $p_{cs} = 8.4$ and $p_{cu} = 12.6$

(v) Normal loading:

$$w_c \cdot p_{cs} + w_d \cdot p_{ds} = w_L$$

Thus $w_c \times 8.4 = 1,200 - 0.52 \times 3 \times 490$

$= 435$

$$(A_c)_s = \frac{435 \times 144}{8.4 \times 490}$$

$= 15.2$ sq.in.

Ultimate loading:

$$w_c (p_{cu}-1) + w_d (p_{du}-1) = 2 w_L$$

$$w_c (12.6 -1) = 2400 - 3 \times 490 (2.04 -1)$$

$= 870$

$$(A_c)_u = \frac{870 \times 144}{11.6 \times 490}$$

$= 22.0$ sq.in.

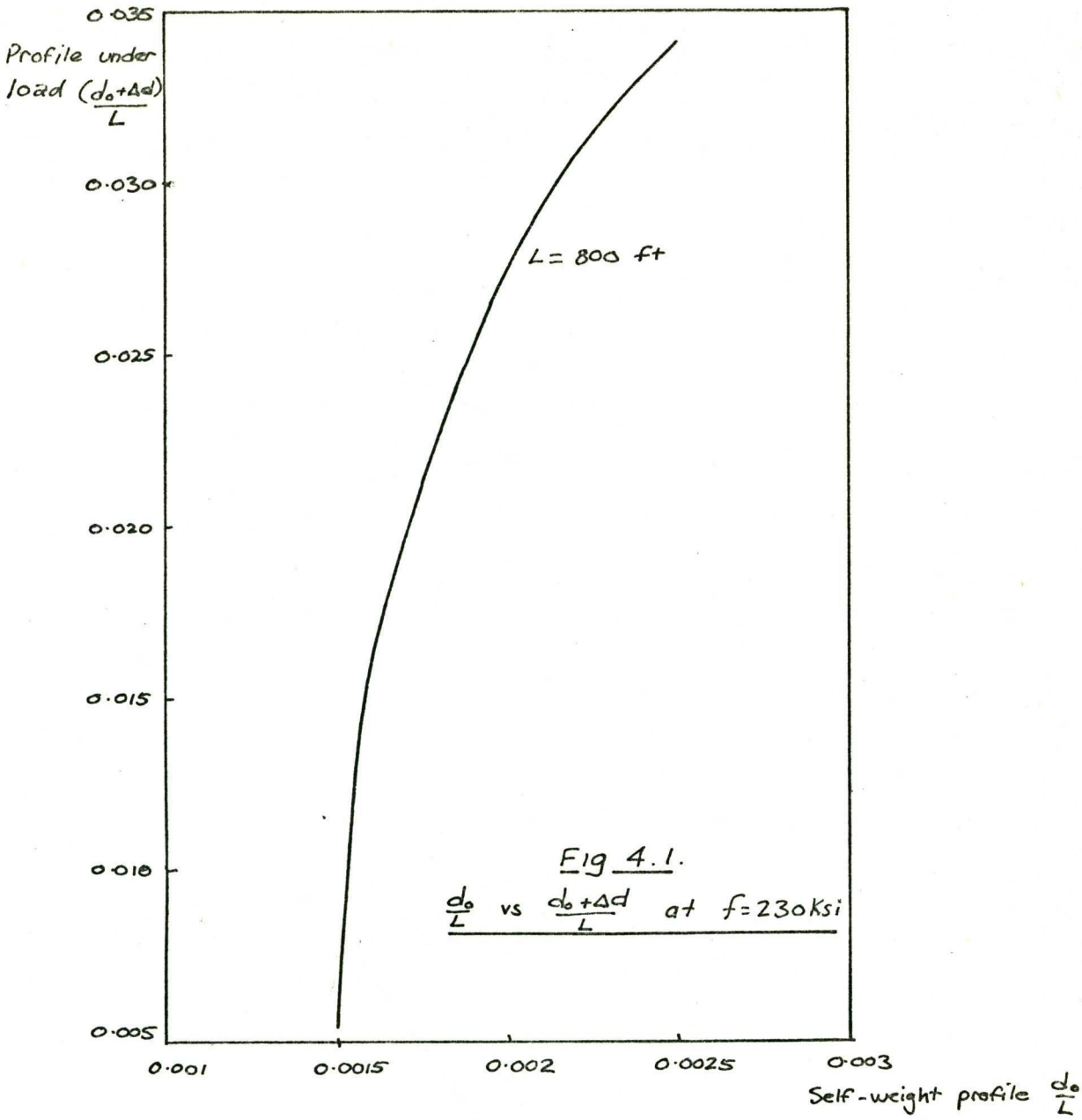

Fig 4.1.
$\frac{d_o}{L}$ vs $\frac{d_o+\Delta d}{L}$ at f = 230 ksi

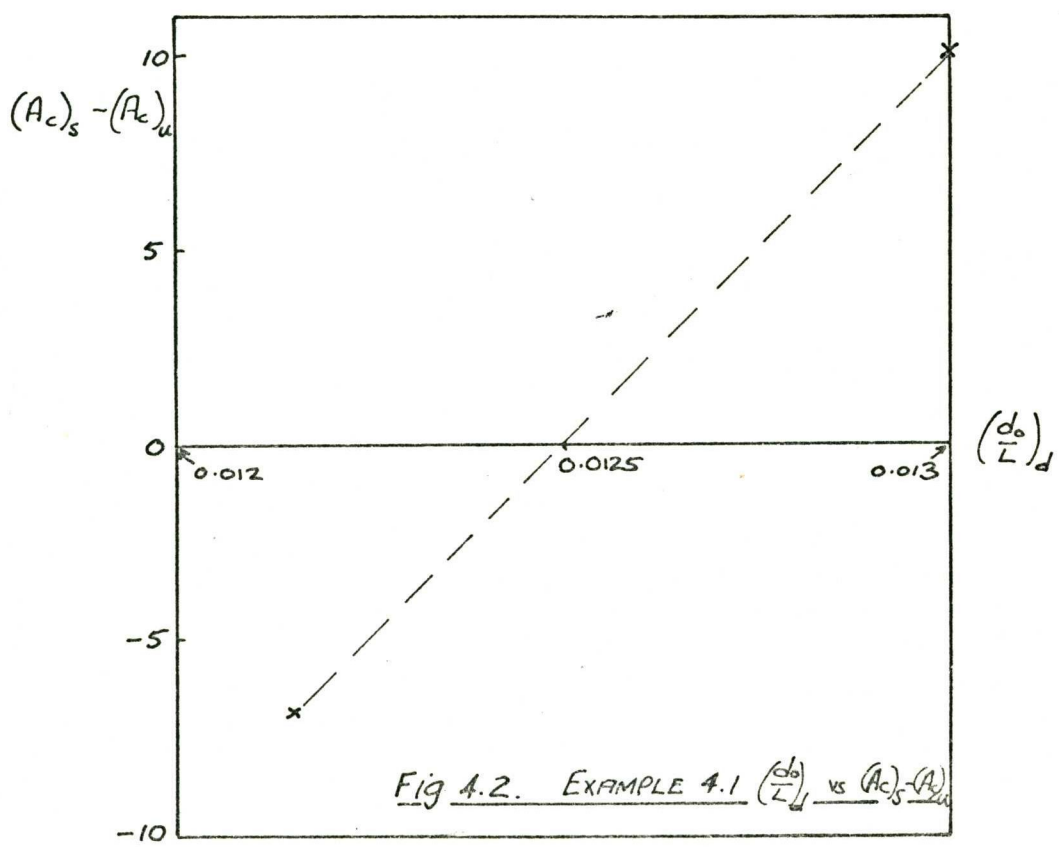

Fig 4.2. EXAMPLE 4.1 $\left(\frac{d_o}{L}\right)_d$ vs $(A_c)_s - (A_c)_u$

(vi) $(A_c)_s - (A_c)_u = 15.2 - 22$

$= -6.8 \text{ in}^2$

Trial No.2 (i) Select $(\frac{d_o}{L})_d = 0.013$

(ii) Then from Figure 2.12 $p_{ds} = 0.36$

$p_{du} = 2.19$

and from equation 2.18 $(\frac{d}{L})_u = 0.02174$

(iii) From Figure 4.1 required $(\frac{d_o}{L})_c = 0.001775$

(iv) From Figure 2.13 $p_{cs} = 8.23$

$p_{cu} = 14.4$

(v) This gives for normal loading:

$(A_c)_s = 24.4$ sq.ins.

and for ultimate loading:

$(A_c)_u = 14.3$ sq.ins.

(vi) $(A_c)_s - (A_c)_u = 24.4 - 14.3$

$= 10.1$ sq.ins.

Trial No.3 (i) Results of Trials 1 and 2 are plotted in Figure 4.2.

From Figure 4.2 select $(\frac{d_o}{L})_d = 0.0125$

(ii) From Figure 2.12 $p_{ds} = 0.45$

and $p_{du} = 2.1$

From equation 2.18 $(\frac{d}{L})_u = 0.0211$

(iii) From Figure 4.1 required $(\frac{d_o}{L})_c = 0.00175$

(iv) From Figure 2.13 $p_{cs} = 8.36$

$p_{cu} = 13.2$

(v) This gives for normal loading:

$$(A_c)_s = 18.9 \text{ sq.ins.}$$

and for ultimate loading:

$$(A_c)_u = 18.85 \text{ sq.ins.}$$

(vi) $(A_c)_s - (A_c)_u = 0.05$ sq.ins.

The solution has now converged sufficiently and should be checked using equation (2.17).

$$m\ (m+1)\ (m+2) = \frac{3\rho L}{64E} \left(\frac{L}{d_o}\right)^3 (p - m)$$

For the deck; $\left(\frac{d_o}{L}\right)_d = 0.0125$

So that $\frac{3\rho L}{64E} \left(\frac{L}{d_o}\right)^3 = 2.18$

For $\left(\frac{d}{L}\right)_s = 0.015$, $m_{ds} = \frac{0.015 - 0.0125}{0.0125}$

$= 0.20$

and $p_{ds} = \frac{(0.2)(1.2)(2.2)}{2.18} + 0.20$

$= 0.442$

For $\left(\frac{d}{L}\right)_u = 0.0211$, $m_{du} = \frac{0.0211 - 0.0125}{0.0125}$

$= 0.688$

and $p_{du} = \frac{(0.688)(1.688)(2.688)}{2.18} + 0.688$

$= 2.12$

For the cable, $\left(\frac{d_o}{L}\right)_c = 0.00175$

So that $\frac{3\rho L}{64E} \left(\frac{L}{d_o}\right)^3 = 798$

For $\left(\frac{d}{L}\right)_s = 0.015$, $m_{cs} = \frac{0.015 - 0.00175}{0.00175}$

$= 7.58$

and $p_{cs} = \frac{(7.58)(8.58)(9.58)}{798} + 7.58$

$= 8.36$

$$\text{For } \left(\frac{d}{L}\right)_u = 0.0211, \quad m_{cu} = \frac{0.0211 - 0.00175}{0.00175}$$

$$= 11.06$$

$$\text{and} \quad p_{cu} = \frac{(11.06)(12.06)(13.06)}{798} + 11.06$$

$$= 13.24$$

These "exact" values give for normal loading:

$$(A_c)_s = 19.3 \text{ sq.in.}$$

and for ultimate loading:

$$(A_c)_u = 18.03 \text{ sq.in.}$$

Thus $(A_c)_s - (A_c)_u = 1.27$ sq.in.

Checking stresses at ultimate loading:

$$f_{du} = \frac{490}{144} \cdot \frac{3.12}{0.211} = 50.3 \text{ Ksi}$$

$$f_{cu} = \frac{490}{144} \cdot \frac{14.24}{0.211} = 230 \text{ Ksi}$$

Trial No.4 Because $f_{du} > 50$ Ksi, reduce $\left(\frac{d}{L}\right)_u$ to 0.0210 keeping all other values constant.

Then $m_{du} = 0.68$, $p_{du} = 2.084$

and $m_{cu} = 11.0$, $p_{cu} = 13.15$

from which $(A_c)_u = 19.5$ sq.in.

so that $(A_c)_s - (A_c)_u = -0.2$ sq.in.

Checking stresses

$$f_{du} = 50 \text{ Ksi}$$

$$f_{cu} = 229.4 \text{ Ksi}$$

Thus a safe solution which is sufficiently close to optimum, is:

$$A_d = 3.00 \text{ sq.ft.}, \quad \left(\frac{d_o}{L}\right)_d = 0.0125$$

$$A_c = 19.5 \text{ sq.in.}, \quad \left(\frac{d_o}{L}\right)_c = 0.00175$$

The sensitivity of the interaction behaviour to variation in self-weight profiles, is evident. This is reflected in the sharp "peak" at optimum solution in Figure 2.13. The sensitivity increases with decreasing span length.

STRUCTURAL SYSTEM	S/W. PROFILE		AREA		ULTIMATE ANCHORAGE FORCE.
	$\left(\frac{d_o}{L}\right)_c$	$\left(\frac{d_o}{L}\right)_d$	A_c	A_d	
DECK ONLY (Ex 2.1)		0.01215		4.72 sq ft	34,000 Kip
CABLE ONLY (Ex. 2.2)	0.0019		0.322 sq ft		10,630 Kip
CABLE – DECK INTERACTION	0.00175	0.0125	0.135 sq ft	3.00 sq ft	26,070 Kip
CABLE WITH DECK AS DEAD LOAD	0.0019	N.A.	0.713 sq ft	3.00 sq ft	23,750 Kip.

Table 4.1.

COMPARISON OF STRUCTURAL SYSTEMS.

Total anchorage force at ultimate loading = $A_d f_{du} + A_c f_{cu}$

= 26,070 Kip

If the deck was to be carried by the cable as dead loading, then the solution to Example 2.2 would apply giving a required cable area of 103.2 sq.ins., and a total anchorage force at ultimate loading of 23,750 Kip.

These results are compared with Examples 2.1 and 2.2 in Table 4.1. The benefit of a deck member with a load-carrying capacity can be readily appreciated. The one disadvantage is the increase in anchorage force as compared with the high strength cable carrying the deck as additional dead loading.

EXAMPLE 4.2

For a span length of 1,600 ft., a deck area of 4.5 sq.ft., and other data as for Example 4.1, determine the required area of cable and the initial self-weight profiles of both the deck and the cable.

Following the same procedure as in Example 4.1, a satisfactory solution is:

$(\frac{d_o}{L})_d$ = 0.0185 $(\frac{d_o}{L})_c$ = 0.00358

p_{ds} = -0.395 p_{cs} = 3.685

p_{du} = 0.653 p_{cu} = 6.61

f_{du} = 49.95 Ksi f_{cu} = 230 Ksi

= 0.02255

$(A_c)_s$ = 165.3 sq.in.

$(A_c)_u$ = 165.7 sq.in.

Total anchorage force at ultimate loading = 70,300 Kip.

If the cable had to carry the entire deck plus live loading, then total live load = 1,200 + (4.5 x 490) = 3,400 lb/ft. for which (from Example 2.4), required A_c = 297 sq.ins. and total anchorage force at ultimate loading = 68,300 Kip.

Whereas it was shown in Example 2.3 that for a 1,600 ft. span, the deck material alone was not capable of supporting the specified loading, there is (in this example) a 44% saving in cable area by accounting for the load-carrying capacity of the deck. At working load the cable provides an upward loading on the deck so that the deck is only required to support part of its dead weight, while at ultimate loading the deck supports its full dead weight plus a part of the live load. However, as in the previous example, this benefit does not extend to the anchorage requirements.

EXAMPLE 4.3

Determine the required area of cable and the initial self-weight profiles of both the deck and the cable if for the site conditions specified in Example 4.2, a deck area of 3.0 sq.ft. is nominated.

Following the same procedure as in the previous two examples, a satisfactory solution is:

$$\left(\frac{d_o}{L}\right)_d = 0.0187 \qquad \left(\frac{d_o}{L}\right)_c = 0.0036$$

$$p_{ds} = -0.4165 \qquad p_{cs} = 3.543$$

$$p_{du} = 0.683 \qquad p_{cu} = 6.715$$

$$f_{du} = 50 \text{ Ksi} \qquad f_{cu} = 230 \text{ Ksi}$$

$$\left(\frac{d}{L}\right)_u = 0.02285$$

$$A_d = 3.0 \text{ sq.ft.}$$

$$A_c = 1.04 \text{ sq.ft.}$$

Total anchorage force at ultimate loading = 56,100 Kip

Comparison of these figures with the alternative solution in Example 4.2 indicates the trend as the area of deck is reduced. Where the deck is unable to support its own weight fully, a decrease in the area of deck produces a decrease in the required cable area and a decrease in the anchorage requirements.

4.2 ECONOMIC APPRAISAL OF THE INTERACTION CONCEPT

It is appropriate at this point to discuss the basis for economic comparison of the two alternative structural systems under consideration in this thesis.

System 1: The deck with some load-carrying capacity interacting with the high strength cables.

System 2: The deck with no load-bearing function apart from local load distribution, fully supported by the cables.

Comparative assessment was demonstrated in Examples 4.1 and 4.2 using the same deck section for both Systems. This will normally not be the case. The first consideration, therefore, is the minimum satisfactory deck section required for each system (see Chapters 5 and 6). A stiffened steel plate cellular section is envisaged as typical of System 1, while a concrete deck section, i.e. the stress ribbon concept, might well be proposed for System 2. Economic comparison will involve the cost of supply and fabrication of each deck section.

As seen in Examples 4.1 and 4.2, System 1 will normally require a much smaller cable area than System 2. Account must be taken of the saving in supply and erection of cables associated with System 1.

It was demonstrated in Chapter 2 that the high strength cables work more efficiently than the lower strength material as suitable for the deck section in System 1. Thus the interaction behaviour in System 1 could required a larger total anchorage force to resist ultimate loading. Again this will depend on the relative deck sections for each System. This may be an important factor, especially where anchorage has to be developed in poor ground.

CHAPTER 5

ANALYSIS OF THE "STIFF" DECK

5.1 THE DECK SUBJECTED TO CHANGING CURVATURE

Solution of the cable-deck interaction problem in Chapter 4, was based on the assumption of perfect flexibility in both the cable and the deck. This assumption is valid for the cable, but account must be taken of the stiffness of the deck member in determining the actual behaviour of the structure under load. The following analysis is applicable to both System 1 and System 2 discussed in Section 4.2.

For a structural member that is not perfectly flexible, a change in curvature will induce bending stresses in the member, which may be calculated using equation (5.1).

$$f_b = E Y \left(\frac{1}{R} - \frac{1}{R_o} \right) \qquad - (5.1)$$

where f_b = bending stress at distance Y from neutral axis

E = elastic modulus

$\frac{1}{R_o}$ = initial curvature of member

$\frac{1}{R}$ = new curvature of member.

In conventional beam analysis the initial curvature is usually zero.

The curvature of the member is given by equation (5.2).

$$\frac{1}{R} = \frac{d^2y/dx^2}{\left\{1 + \left(\frac{dy}{dx}\right)^2\right\}^{3/2}} \qquad - (5.2)$$

The general equation of the catenary structure is given by equation (2.6) as

$$y = \frac{4d}{L^2} \cdot x^2$$

So that

$$\frac{1}{R} = \frac{8d/L^2}{\left\{1 + \frac{64d^2 x^2}{L^4}\right\}^{3/2}}$$

For the range of $\frac{d}{L}$ under consideration herein, the maximum value of $\left\{1 + \frac{64d^2 x^2}{L^4}\right\}$ will be approximately 1.01.

Hence it is sufficiently accurate to assume $\frac{1}{R} = \frac{8d}{L^2}$ - (5.3)

Thus change in curvature $= \frac{1}{R_1} - \frac{1}{R_2} = \frac{8}{L}\left(\frac{d_1}{L} - \frac{d_2}{L}\right)$

and bending stress $f_b = \frac{8 E Y}{L}\left(\frac{d_1}{L} - \frac{d_2}{L}\right)$ - (5.4)

The stiffness of the deck will provide a restraint against increase in curvature from the initial curvature of the member, and therefore tend to reduce the overall deflection of the structure as obtained by assuming perfect flexibility. The importance of this restraint can be appreciated by comparing the change in bending energy and the change in axial strain energy as a catenary structure deflects under load.

This comparison will be made for the cable in Example 2.1 deflecting from working load profile to ultimate profile. Relevant figures from Example 2.1 are:

$\left(\frac{d}{L}\right)_s = 0.015$, $H_s = 23{,}400$ Kip

$\left(\frac{d}{L}\right)_u = 0.02065$, $H_u = 34{,}000$ Kip

Area of cable A = 4.72 sq.ft., L = 800 ft.

Moment of inertia $I = 20 \text{ ft.}^4$ (assumed typical value)

Change in bending energy $E_b = \int_0^L \frac{M^2}{2EI}\, dx$

$$= \frac{EI}{2} \int_0^L \left(\frac{1}{R_u} - \frac{1}{R_s}\right)^2 dx$$

$$= 32 \frac{EI}{L} \left\{ \left(\frac{d}{L}\right)_u - \left(\frac{d}{L}\right)_s \right\}^2$$

$$= 110 \text{ Kip ft.}$$

Change in axial strain energy $E_s \doteq \frac{L}{2EA} (H_u^2 - H_s^2)$

$$= 11{,}920 \text{ Kip ft.}$$

For the above situation the energy required to overcome the flexural restraint of the deck is only 1% of the strain energy involved in the deflection of the structure. An increase in the span length L will reduce E_b and increase E_s so that E_b/E_s will decrease.

On the basis of this example it is concluded that the stiffness of the deck has very little effect on the deflection of the structure under load for the order of dimensions under consideration herein. For practical purposes the deck may be regarded as a flexible member in order to calculate deformations of the structure. However the bending stress in the deck as computed by equation (5.4) should be added to the tensile stress in the deck as computed by the flexible cable analysis to determine the resultant stress state of the deck.

Adopting as a typical value of ultimate profile $\left(\frac{d}{L}\right)_u = 0.020$, then from equation (5.3), for L = 800 ft.

$$\text{Curvature} = \frac{1}{R} = 0.0002$$

$$\text{or radius } R = 5{,}000 \text{ ft.}$$

It is not practicable to fabricate a segment to this curvature. Adopting an initial zero curvature of the deck, the bending stresses induced at ultimate profile are given by equation (5.1) as

$$f_b = EY \cdot \frac{1}{R_u}$$

For a steel section having $Y_{max} = 3$ ft. and $(\frac{d}{L})_u = 0.020$

then $f_b = 30{,}000 \times 3 \times 0.0002$

$= 18$ Ksi

Thus a situation similar to the ultimate buckling behaviour of beam-columns will occur. The bottom side of the deck will yield in advance of the top side. As yielding gradually propagates across the deck section, the effective modulus of the section is reduced. Again, this effect is somewhat akin to the classical reduced modulus theory for buckling of a perfect uniform column of strain-hardening material. The response of the structure under increasing load will of course differ from the elastic response, but the ultimate tensile capacity of the yielded deck will remain constant, no matter what (realistic) magnitude of bending stress is applied.

This does not mean that the yielded deck will deflect indefinitely under constant applied load. Any increase in deflection at constant applied load will reduce the tensile force in the deck. If the structure is subjected to an increase in the applied load, the deck will accommodate a portion of the extra loading such that it remains at its tensile capacity, and the cable will accommodate the remainder of the additional loading. At the ultimate profile $(\frac{d}{L})_u$ obtained from the elastic interaction analysis (Section 4.1), despite any bending effects to which the deck has been subjected, the structure will have the same load-carrying capacity as if the deck had remained elastic.

A cellular deck section up to six feet deep is envisaged. For such a deck, bending stresses induced by increasing the deck curvature, can be ignored in the determination of suitable sectional areas and profiles for the cable and deck. Provided that under working load the maximum tensile stress (including bending) of the deck is lower than the yield stress, the elastic interaction solution should prove satisfactory. However, it is evident that the depth of the deck section should be as shallow as practicable in order to reduce the magnitude of any bending effects.

For the interaction solutions obtained in Examples 4.1 and 4.2 the maximum tensile stress in the deck is shown below:

Example 4.1 $A_d = 3.0$ sq.ft. $Y_{max} = 2.0$ ft. (assumed)

$f_{ds} = 32.75$ Ksi

$f_b = 9.0$ Ksi

$f_{tot} = 41.75$ Ksi < 50 Ksi

Example 4.2 $A_d = 4.5$ sq.ft. $Y_{max} = 3.0$ ft. (assumed)

$f_{ds} = 27.5$ Ksi

$f_b = 6.75$ Ksi

$f_{tot} = 34.25$ Ksi < 50 Ksi

Thus both interaction solutions would be satisfactory.

5.2 EFFECT OF DIFFERENTIAL TEMPERATURE

The effect of differential temperature can be assessed by considering the profile of the deck at some mean temperature, with the top flange at a higher temperature and the bottom flange at a lower temperature, restraining each other from movement so that the deck retains its mean temperature profile. A temperature strain will exist across the deck cross-section which will result in an additional compressive stress in the top flange and an additional tensile stress in the bottom flange.

Temperature strain $= \alpha t$

where t is the variation from the mean temperature. Differential temperature stress increment $\Delta f = E \alpha t$

For steel, $\alpha = 6 \times 10^{-6} /F^{o}$

So that $\Delta f = 30 \times 10^{3} \times 6 \times 10^{-6} \times t$

$= 0.18\ t$ Ksi

For a temperature difference of 40 F^{o} across the deck cross-section,

$t = 20\ F^{o}$

giving $\Delta f = 3.6$ Ksi

The stresses resulting from differential temperature are therefore not a major consideration. It will only be necessary to take account of them in checking the maximum tensile stress in the bottom flange of the deck under working load (see previous Section).

5.3 DISTRIBUTION OF LOCAL LOADS

So far, the catenary structure has been considered as a cable system carrying uniformly distributed live loading between abutments. In reality, the live loading on a traffic carriageway will consist of a large number of individual wheels. The force exerted by each wheel on the deck plate has to be distributed to the cables and over the whole deck cross-section. The cellular deck section envisaged is one having a stiffened top plate, with diaphragms at regular intervals which rest on the cables. The top plate can therefore be treated as an "orthotropic deck" in order to analyse the local effect of the concentrated wheel loads.

In 1963 the American Institute of Steel Construction published a "Design Manual for Orthotropic Steel Plate Deck Bridges" (13), which included some very useful design charts. For girder bridges, the following general design procedure is used. The bridge deck, consisting of a flat deck plate and longitudinal stiffening ribs, is treated as a continuous orthotropic plate supported on infinitely rigid main girders and on uniformly spaced elastic floor beams. On the initial assumption that the floor beams are also infinitely rigid, the maximum values of the bending moments in the longitudinal ribs and the floor beams are computed. The second step is to determine the effects of the elastic flexibility of the floor beams and to adjust the values of the bending moments previously obtained. The stresses in the deck due to its action as a flange of the main girders are then computed separately by normal beam analysis, and superimposed on the stresses obtained from the first two steps.

The equivalent steps in determining the longitudinal stresses for the cellular deck in catenary are:

(i) Consider the deck with zero initial curvature and infinitely rigid diaphragms. Compute the maximum value of bending moment in the longitudinal ribs.

(ii) Determine the effect of diaphragm flexibility. This effect may be analysed by considering the diaphragm resting on the cables as a beam

on elastic foundations. For the rigid diaphragm arrangement envisaged in a practical situation, diaphragm flexibility will have a negligible effect in adjusting the values obtained from Step (i).

(iii) Allow the structure to adopt its cable profile under load and superimpose the curvature stresses from Section 5.1 on the bending stresses derived from Step (i) above.

Because the deck member is essentially a tension member, only tensile bending stresses need be considered. The curvature stresses in the top flange of the deck will be compressive and therefore oppose the local tensile bending stresses.

The following example gives an indication of the magnitude of the local tensile bending stresses (Step (i)) which were evaluated using the design charts in Reference (13).

For the orthotropic-type section shown in Figure 5.1, with diaphragms at a spacing of 15 feet, under a N.A.A.S.R.A. standard H-S truck plus 30% impact loading, the maximum tensile bending stress occurs at mid-span in the trough of the ribs and has a value of 11.6 Ksi.

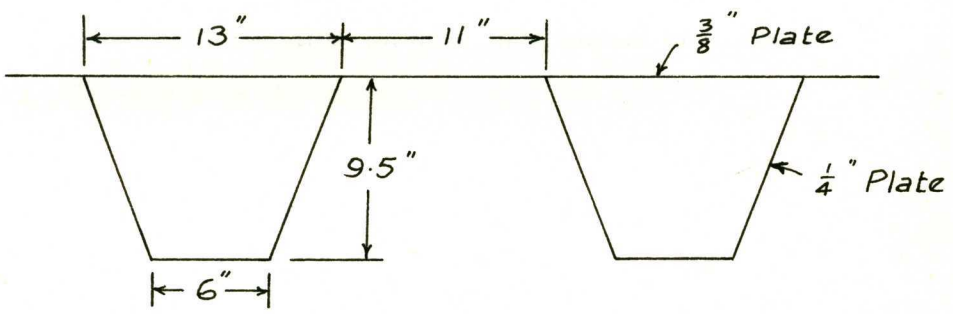

Fig 5.1.

Account should be taken of the local bending stresses in checking the maximum tensile stress in the top flange of the deck under working load. However, the local bending stresses will not alter the ultimate load-carrying capacity of the structure.

5.4 CONCENTRATED LOADING

In highway bridge design, an overload provision is applied to allow for infrequent heavy loads. The N.A.A.S.R.A. Highway Bridge Design Code specifies in any single lane an H or H-S truck increased 100%, and without concurrent loading of any other lanes. The cable analysis for concentrated loads in Section 3.4 assumed an instantaneous break in curvature at the point of application of the concentrated load. For the flexible cable this assumption is justified. However for the "stiff" deck, an instantaneous break in curvature is unacceptable. The change in slope will be much more gradual, and the deck will be subjected to a significant bending moment.

The maximum value will occur at mid-span with the concentrated load at mid-span. For a long span bridge, the concentrated overloading will equal at most a few percent of the total uniformly distributed lane loading across the bridge. The deformation of the catenary bridge deck under the concentrated overloading will be extremely small, and for the purpose of evaluating the bending moment in the deck, the structure may be approximated by an inextensible pin-ended parabolic arch. The value of the bending moment at the centre of such an arch, centrally loaded, is given by equation (5.5).

$$M = \frac{7}{128} P.L. \qquad - (5.5)$$

where P is the concentrated load.

It should be noted that equation (5.5) is independent of the actual profile of the arch, or in other words of the sag d.

The maximum stress state for the deck cross-section will to a good approximation be given by the summation of:

(i) the axial stress as determined from Section 3.4.

(ii) the bending stresses derived using equation (5.5).

(iii) the curvature stresses for the dead load profile from Section 5.1.

(iv) the local bending stress effects on the top plate from Section 5.3.

It is necessary to ensure that the deck remains in the elastic state under the concentrated loading case.

Calculation of the bending stresses in the stiff deck due to a central concentrated load, is demonstrated in Example 5.3.

EXAMPLE 5.3

The cable-deck system determined in Example 4.3 has a deck comprising a hollow box 30 feet wide, 6 feet deep and with walls 1/2 inch thick. The structure is subjected to a concentrated load of 144 Kip (twice the standard H-S truck load) at mid-span. Determine the total stress in the bottom flange of the deck due to this load.

For the deck, moment of inertia $I = 24 \text{ ft.}^4$

From the interaction solution with the concentrated load acting, axial stress in deck = 21 Ksi.

Dead load profile of structure $(\frac{d}{L})_d = 0.01067$. At this profile, the curvature stress is determined using equation (5.4).

$$\text{Curvature stress in deck} = \frac{8\,EY}{L}\left(\frac{d}{L}\right)_d$$

$$= 4.8 \text{ Ksi.}$$

For the concentrated load, from equation (5.5)

$$M = \frac{7}{128} PL$$

$$\text{Thus bending stress } f_b = \frac{MY}{I} = \frac{7\,PLY}{128I}$$

$$= \frac{7 \times 144 \times 1600 \times 3}{128 \times 24 \times 144}$$

$$= 10.9 \text{ Ksi}$$

$$\text{Thus total stress in bottom flange} = 21 + 4.8 + 10.9$$

$$= 36.7 \text{ Ksi}$$

The use of equation (5.5) to determine the bending stress in the deck due to a concentrated load, is only a convenient approximation. However, provided the deck has a sufficiently large moment of inertia, the concentrated loading case will not be critical. In Example 5.3, an increase of 100% in the bending stress determined from equation (5.5) would still give a total stress in the bottom flange, less than 50 Ksi (i.e. still in the elastic range).

CHAPTER 6

AERODYNAMIC BEHAVIOUR OF THE CATENARY STRUCTURE

6.1 GENERAL STATEMENT OF AERODYNAMIC ANALYSIS

Prior to 1940 little attention was paid in the design of civil engineering structures to the dynamic action of wind. Then, in November 1940, the Tacoma Narrows Bridge collapsed in a steady 40 m.p.h. wind. After vibrating in vertical motion with moderate amplitude for two hours, the entire motion changed to a violent torsional oscillation which continued for about an hour until the bridge finally yielded. Subsequent to this catastrophe, a considerable volume of literature has been published concerning the dynamic instability of suspension bridges.

The type of catenary structure under consideration herein has certain advantages, aerodynamically, over the suspension bridge. Pugsley (2) observed in 1948 that the natural frequencies of a suspension cable tended to vary inversely as $\sqrt{d}$, the sag at mid-span, and was almost independent of the cable length. Because the catenary profile is much flatter than that normally provided for suspension bridge cables, the natural frequencies of the catenary structure will be appreciably higher and therefore associated with a lower wind energy and higher critical speeds. Thus the deck will not be required to provide as much torsional and flexural restraint against dynamic oscillation and a smaller deck section may be permitted. Further, since the cables are contained within the deck, out-of-phase oscillation of the cables should be more difficult to establish than for a suspension bridge.

Wind tunnel tests on models of truss-stiffened suspension bridges with thin closed decks, and observations of full-size structures have indicated that the aerodynamic behaviour of these structures closely resembles that of an airplane wing. Bleich (14) in 1948 applied Theodorsen's classical flutter theory of thin airfoils in a study of the aerodynamic stability of the second Tacoma Bridge. A flutter vibration in an airfoil occurs due to "coupling" between different modes of vibration, when the airfoil has at least two degress of freedom. The flutter velocity V_F is the critical wind velocity at which flutter vibrations commence for an airfoil in a windstream parallel to it.

Selberg (15) carried out a systematic investigation in 1954-1958 on the critical wind velocity at the initial stage of catastrophic oscillation, for a number of bridge cross-sections. He derived a simple empirical formula for the flutter velocity and found that this gave a critical wind velocity very close to the measured airspeed at the commencement of vibrations with catastrophic amplitude. The critical velocities were very sensitive to changes in wind incidence. Normally a wind incidence of $\pm 10^{o}$ gives a critical airspeed very much lower than that attained with horizontal wind direction. This effect can be appreciably decreased by streamlining the structure. For example, model tests of a sharp wedge-shaped box section proposed for the new Lillebaelt Bridge in Denmark gave a critical wind velocity for coupled catastrophic oscillations, which varied only slightly for wind incidences in the range $+ 5^{o}$ to $- 5^{o}$. These critical velocities were approximately equal to those calculated by Selberg's flutter velocity formula.

Frandsen (16) in 1966 published a direct solution to the theoretical flutter equations for the simple deflection-torsion case which applies to normal suspension bridge vibration. His solution is in close agreement with that of Selberg. The cellular deck in catenary is envisaged as similar to the streamlined box sections gaining popularity in modern suspension bridge design (e.g. the Severn Bridge and the new Lillebaelt Bridge) for which the classical flutter theory gives very satisfactory results. Frandsen's method will therefore be used for analysis of the catenary structure, to determine the critical wind velocity at which aerodynamic instability might be expected. Frandsen's expression for the critical flutter speed V_F is:

$$V_F = b.\ \omega_T \sqrt{\frac{\nu}{\mu}}\ \sqrt{\frac{1 - (\omega_v/\omega_T)^2}{\nu A + B}} \qquad - (6.1)$$

where ω_T = fundamental torsional frequency (radians/sec)

ω_v = fundamental vertical frequency

b = half width of deck

$$\mu = \frac{2\pi \rho_A b^2}{w}$$

$$\nu = \frac{2r^2}{b^2}$$

ρ_A = specific weight of air - assumed as 0.0805 lb/cu.ft.

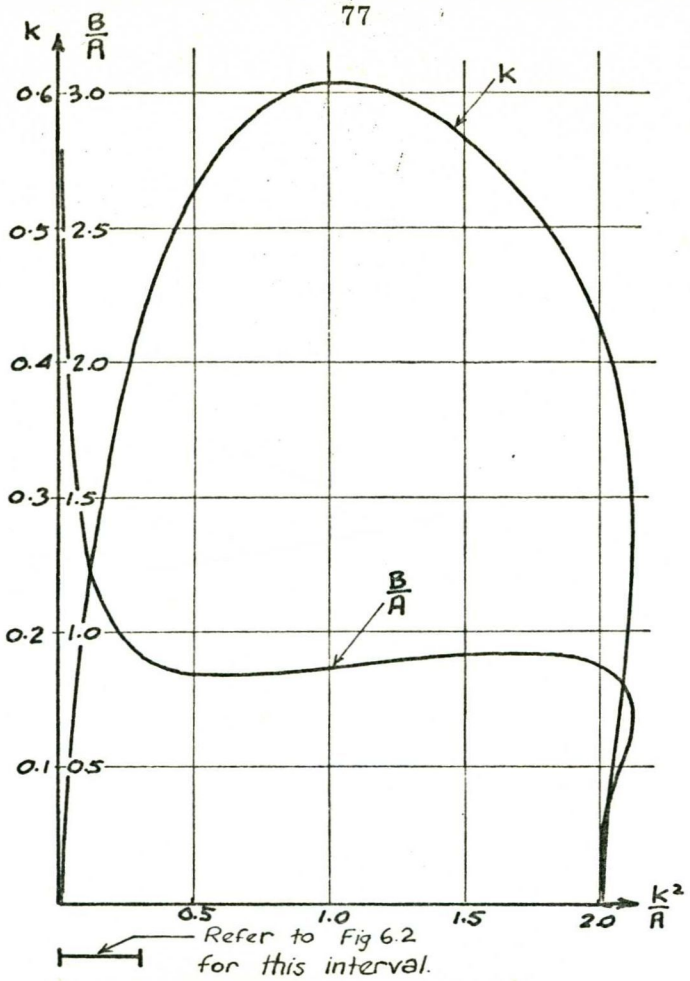

Fig 6.1. - Ex Frandsen (16)

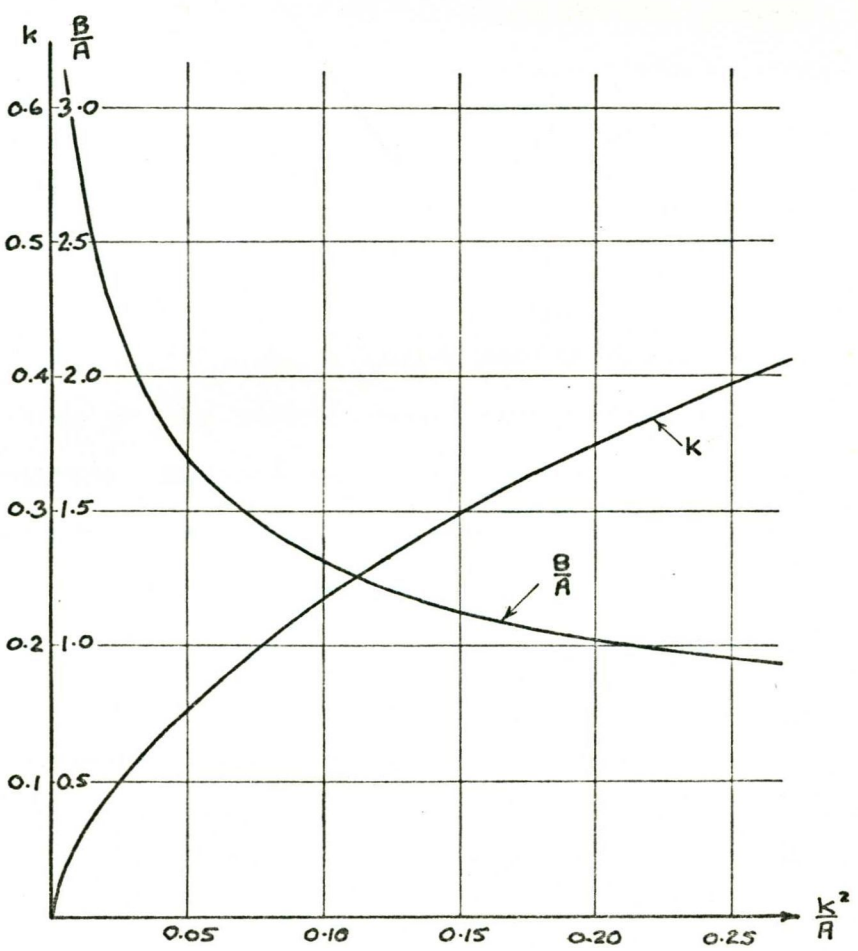

Fig 6.2. - Ex Frandsen (16)

w = weight of bridge per foot length

r = mass radius of gyration.

A, B are factors determined from the following equation and Figures 6.1 and 6.2 (reproduced from Frandsen's paper).

$$\frac{K^2}{A} = \frac{\mu}{1-(\omega_V/\omega_T)^2} + \frac{\frac{\mu}{\nu}\cdot\left(\frac{\omega_V}{\omega_T}\right)^2\cdot\frac{B}{A}}{1-(\omega_V/\omega_T)^2}$$

The natural frequencies and modes of vibration of the structure, required in equation (6.1), can be determined using an energy approach as in Bleich (14). Applying Hamilton's minimum principle of mechanics -

$$\int_{t_1}^{t_2} (T - V)\, dt = \text{minimum} \qquad - (6.2)$$

where T and V are the kinetic and potential energy respectively of the vibrating system and may be considered as functions of the amplitude "a" at the time "t" and of the associated frequency "ω". In other words, under all possible configurations of the vibrating structure, the shape of the deflection curve Z (x) must be chosen which makes the time integral (equation 6.1) a minimum. Based on the premise that a number of basic functions (deflected shapes) - say $\phi_1(x)$, $\phi_2(x)$ ...., $\phi_n(x)$ - may be superimposed to obtain a closer approximation to the true fundamental mode shape, then the deflected shape Z (x) may be represented as:

$$Z(x) = C_1\,\phi_1(x) + C_2\,\phi_2(x) + \ldots\ldots + C_n\,\phi_n(x) \qquad - (6.3)$$

The constants C_1, C_2, ... C_n must then be determined such that the best approximations to the natural modes are obtained. Ritz deduced that this requirement was equivalent to choosing C_1, C_2 ..... C_n so that the frequency (or ω^2) is made stationary at the natural modes. That is, the partial derivatives

$$\frac{\partial \omega^2}{\partial C_1}, \quad \frac{\partial \omega^2}{\partial C_2} \cdots, \quad \frac{\partial \omega^2}{\partial C_n}$$ should be set equal to zero,

in the derivative of equation (6.2), viz:

$$\frac{d}{dC_n}(T - V) = 0 \qquad - (6.4)$$

A system of n linear equations is then formed, determining the co-efficients C_n. These equations are homogeneous, and solutions exist only when the determinant of the system vanishes. Solution of the determinant yields values

of ω^2 corresponding to each of the n modes. This energy approach is usually called the Rayleigh-Ritz method.

6.2 CALCULATION OF NATURAL FREQUENCIES AND MODES OF VIBRATION

The success of the Rayleigh-Ritz method depends largely on the choice of the basic functions ϕ_n. Knowing that the transverse vibrations of a tightly stretched string are sinusoidal, the deflected shape of the catenary structure will be chosen as -

$$Z(x) = \sum C_n \sin \frac{n\pi x}{L} \qquad - (6.5)$$

This is superimposed on the equilibrium shape $(\frac{d}{L})$ under loading w.

Equation (6.5) has the advantage that symmetric and antisymmetric modes are independent and may be analysed separately by considering only even values of n for the symmetric modes and only odd values of n for the anti-symmetric modes. Furthermore, these basic functions belong to a "system of orthogonal functions" characterized by the fact that -

$$\int_0^L \sin \frac{m\pi x}{L} \sin \frac{n\pi x}{L} \, dx = 0 \qquad \text{for } m \neq n$$

and

$$\int_0^L \sin^2 \left(\frac{n\pi x}{L}\right) dx = \frac{L}{2}$$

6.2.1 VERTICAL OSCILLATION

The potential energy of the system is composed of an energy of resistance to bending, an axial strain energy and the potential energy due to gravity.

The energy of resistance to bending, is approximately equal to that of a straight member subject to the deflection Z (x).

Thus potential bending energy $E_b = \frac{EI}{2} \int_0^L \left(\frac{d^2Z}{dx^2}\right) dx$

$$= \frac{EI}{2} \int_0^L \left\{ \sum C_n \left(\frac{n\pi}{L}\right)^2 \sin \frac{n\pi x}{L} \right\}^2 dx$$

$$= \frac{EI}{2} \int_0^L \sum C_n^2 \left(\frac{n\pi}{L}\right)^4 \sin^2 \left(\frac{n\pi x}{L}\right) dx$$

$$= \sum \frac{EIL}{4} \cdot C_n^2 \left(\frac{n\pi}{L}\right)^4 \qquad - (6.6)$$

The potential energy due to gravity is -

$$E_g = \int_0^L w\, Z(x)\, dx$$

$$= - \sum \frac{wLC_n}{n\pi} \left[\cos \frac{n\pi x}{L}\right]_0^L$$

$$= \sum \frac{wLC_n}{n\pi} (1 - \cos n\pi) \qquad - (6.7)$$

To obtain the potential strain energy of the structure it is necessary to consider the increase in tension and in length as the structure deforms from its equilibrium position.

Final deflected shape of structure $y = y_o + Z$. Taking the origin at the left-hand support, the equilibrium profile is given by:

$$y_o = 4d \left\{ \left(\frac{x}{L}\right)^2 - \frac{x}{L} \right\}$$

Thus $$y = 4d \left\{ \left(\frac{x}{L}\right)^2 - \frac{x}{L} \right\} + \sum C_n \sin \frac{n\pi x}{L}$$

Increase in length $$\Delta l = \int_0^L \sqrt{1 + \left(\frac{dy}{dx}\right)^2}\, dx - \int_0^L \sqrt{1 + \left(\frac{dy_o}{dx}\right)^2}\, dx$$

$$\doteq \int_0^L 1 + \tfrac{1}{2} \left(\frac{dy}{dx}\right)^2 dx - \int_0^L 1 + \tfrac{1}{2} \left(\frac{dy_o}{dx}\right)^2 dx$$

$$= \int_0^L \left(\frac{dy_o}{dx}\right)\left(\frac{dz}{dx}\right) dx + \tfrac{1}{2} \int_0^L \left(\frac{dz}{dx}\right)^2 dx$$

On evaluation $$\Delta l = \sum \left\{ \left(\frac{n\pi C_n}{L}\right) \cdot \frac{L}{4} + \frac{8d C_n}{n\pi L} (\cos n\pi - 1) \right\}$$

if only even values of n or odd values of n are considered.

Horizontal tension in cable at equilibrium $$H = \frac{wL^2}{8d}$$

Increase in cable tension $$\Delta h = EA \left(\frac{\Delta l}{L}\right)$$

giving $$\Delta h = \frac{EA}{L} \sum \left\{ \left(\frac{n\pi C_n}{L}\right)^2 \cdot \frac{L}{4} + \frac{8d C_n}{n\pi L} (\cos n\pi - 1) \right\}$$

Potential axial strain energy $E_s = \frac{L}{2EA}\left\{(H + \Delta h)^2 - H^2\right\}$

$$= \left(\frac{L}{EA}\right)\left\{H\ \Delta h\right\} + \frac{L}{2EA}(\Delta h)^2 \qquad - (6.8)$$

Evaluating the two terms on the R.H.S. of this expression:

$$\left(\frac{L}{EA}\right) H\ \Delta h = \sum \frac{HL}{4}\left(\frac{n\pi C_n}{L}\right)^2 + \sum' \frac{wLC_n}{n\pi}\left(\cos n\pi - 1\right)$$

so that $$\left(\frac{L}{EA}\right) H\ \Delta h + Eg = \sum \frac{HL}{4}\left(\frac{n\pi C_n}{L}\right)^2 \qquad - (6.9)$$

$$\left(\frac{L}{EA}\right)(\Delta h)^2 = \left(\frac{EA}{2L}\right)\left\{\sum\left(\frac{n\pi C_n}{L}\right)^2\left(\frac{L}{4}\right) + \sum \frac{8C_n d}{n\pi L}(\cos n\pi - 1)\right\}^2$$

$$= \frac{EA}{2L}\left\{\sum \frac{8C_n d}{n\pi L}(\cos n\pi - 1)\right\}^2 \qquad - (6.10)$$

neglecting terms which include $(C_n)^3$ and higher, and giving first-order accuracy.

Total potential energy $E_T = E_b + E_g + E_s$

The kinetic energy of the system when vibrating at a frequency is:

$$T = \tfrac{1}{2}\int_0^L m\left\{\omega . Z(x)\right\}^2 dx \qquad - (6.11)$$

$$= \frac{w\omega^2}{2g}\int_0^L \left\{Z(x)\right\}^2 dx$$

$$= \frac{w\omega^2}{2g}\int_0^L \left\{\sum C_n \sin\frac{\pi nx}{L}\right\}^2 dx$$

$$= \frac{wL}{4g}\cdot\omega^2\sum C_n^2 \qquad - (6.12)$$

A. First and Second Symmetric Modes.

Putting $Z(x) = C_1 \sin\frac{\pi x}{L} + C_3 \sin\frac{3\pi x}{L}$

then $\cos n\pi = -1$

Equation (6.6) becomes $E_b = \frac{EIL}{4}\left(\frac{\pi}{L}\right)^4\left\{C_1^2 + 81 C_3^2\right\}$

Equation (6.9) becomes $\left(\frac{L}{EA}\right)H\ \Delta h + Eg = \frac{\pi^2 H}{4L}\left\{C_1^2 + 9C_3^2\right\}$

Equation (6.10) becomes $\left(\frac{L}{2EA}\right)(\Delta h)^2 = \frac{128\,EA\,d^2}{\pi^2 L^3}\left\{C_1 + \frac{C_3}{3}\right\}^2$

Equation (6.12) becomes $T = \frac{wL}{4g}\omega^2\left\{C_1^2 + C_3^2\right\}$

Substituting into equation (6.4)

$$\frac{d(T-E)}{dC_1} = 2C_1\left\{\frac{wL}{4g}\omega^2 - \frac{EIL}{4}\left(\frac{\pi}{L}\right)^4 - \frac{\pi^2 H}{4L} - \frac{128\,EA\,d^2}{\pi^2 L^3}\right\} - \frac{2C_3}{3}\left\{\frac{128\,EA\,d^2}{\pi^2 L^3}\right\}$$

$$= 0 \qquad - (6.13)$$

$$\frac{d(T-E)}{dC_3} = 2C_3\left\{\frac{wL}{4g}\cdot\omega^2 - \frac{81\,EIL}{4}\left(\frac{\pi}{L}\right)^4 - \frac{9\,\pi^2 H}{4L} - \frac{128\,EA\,d^2}{9\pi^2 L^3}\right\} - \frac{2C_1}{3}\left\{\frac{128\,EA\,d^2}{\pi^2 L^3}\right\}$$

$$= 0 \qquad - (6.14)$$

A non-trivial solution of equations (6.13) and (6.14) exists only if the determinant of the equations is zero. Evaluation of the determinant gives two values of as the natural frequencies for the first and second symmetric modes.

B. First and Second Antisymmetric Modes.

Putting $Z(x) = C_2 \sin\frac{2\pi x}{L} + C_4 \sin\frac{4\pi x}{L}$

then $\cos n\pi = 1$

Equation (6.6) becomes $E_b = \frac{EIL}{4}\left(\frac{\pi}{L}\right)^4\left\{16C_2^2 + 256C_4^2\right\}$

Equation (6.9) becomes $H\,\Delta h\left(\frac{L}{EA}\right) + Eg = \frac{\pi^2 H}{4L}\left\{4C_2^2 + 16C_4^2\right\}$

Equation (6.10) becomes $(\Delta h)^2\,\frac{L}{2EA} = 0$

Equation (6.12) becomes $T = \frac{wL}{4g}\omega^2\left\{C_2^2 + C_4^2\right\}$

From the above results

$$\frac{d(T-E)}{dC_2} = 2C_2\left\{\frac{wL}{4g}\cdot\omega^2 - 4\,EIL\left(\frac{\pi}{L}\right)^4 - \frac{\pi^2 H}{L}\right\}$$

$$= 0 \qquad - (6.15)$$

$$\frac{d(T-E)}{dC_4} = 2C_4\left\{\frac{wL}{4g}\cdot\omega^2 - 64\,EIL\left(\frac{\pi}{L}\right)^4 - \frac{4\pi^2 H}{L}\right\}$$

$$= 0 \qquad - (6.16)$$

Equations (6.15) and (6.16) are independent, and consequently the first and second antisymmetric modes are independent. The evaluation of the natural frequency ω for each mode is straight forward.

6.2.2 TORSIONAL OSCILLATION

The potential energy of the system is made up of the energy associated with torsional deformations of the deck, and an axial strain energy component. Oscillation of the structure in this mode involves only rotation of the cross-section. The deflected shape will therefore be chosen as:

$$\phi(x) = \sum C_n \sin \frac{n\pi x}{L} \qquad \text{- (6.17)}$$

where $\phi(x)$ is the angle of rotation at any point x along the deck.

Potential energy due to torsional rigidity of the deck is

$$E_T = \frac{1}{2} \int_0^L M_T d\phi$$

where twisting moment $M_T = (GJ + G\bar{J}) \frac{d\phi}{dx}$

The term $G\bar{J}$ represents an additional torque due to the interaction between the axial load and the twisting action of the member, and is only applicable when the deck carries an axial load. For a compression member the additional torque acts in the same direction as the twisting moment and reduces the effective torsional rigidity, while for a tension member the effective torsional rigidity is increased. This is called the Wagner effect.

$$\text{Thus} \quad E_T = \frac{1}{2} (GJ + G\bar{J}) \int_0^L \left(\frac{d\phi}{dx}\right)^2 dx$$

$$= \frac{1}{2} (GJ + G\bar{J}) \int_0^L \left\{ \sum C_n \cdot \frac{n\pi}{L} \cos \frac{n\pi x}{L} \right\}^2 dx$$

$$= \frac{1}{2} (GJ + G\bar{J}) \int_0^L \sum C_n^2 \left(\frac{n\pi}{L}\right)^2 \cos^2 \frac{n\pi x}{L} \, dx$$

if only even values of n or odd values of n are considered.

Integrating, $$E_T = \frac{1}{2} (GJ + G\bar{J}) \sum \frac{n^2 \pi^2 C_n^2}{2L} \qquad \text{- (6.18)}$$

In order to apply the formulae already derived for the potential axial strain energy, consider an elemental width db at a distance b from the centre of a plate whose total width is 2B.

For a small rotation ϕ of the plate, then vertical displacement of this element is approximately -

$$Z'(x) = b\,\phi(x)$$

If the element has H', A', $\Delta l'$, $\Delta h'$

and the plate has H, A, Δl, Δh as in Section 6.2.1.

$$\text{then} \quad H' = H\frac{db}{2B}, \qquad A' = A\frac{db}{2B}$$

$$\Delta l' = \int_0^L \left(\frac{dy_o}{dx}\right)\left(\frac{dz'}{dx}\right)dx + \tfrac{1}{2}\int_0^L \left(\frac{dz'}{dx}\right)^2 dx$$

$$= b\int_0^L \left(\frac{dy_o}{dx}\right)\left(\frac{d\phi}{dx}\right)dx + \frac{b^2}{2}\int_0^L \left(\frac{d\phi}{dx}\right)^2 dx$$

$$= b^2 \Sigma \left(\frac{n\pi C_n}{L}\right)^2 \cdot \frac{L}{4} + b\Sigma \frac{8dC_n}{n\pi L}(\cos n\pi - 1)$$

$$\Delta h' = \frac{EA'\,\Delta l'}{L}$$

giving for the terms in equation (6.8)

$$H'\,\Delta h'\left(\frac{L}{EA'}\right) = H'\,\Delta l'$$

$$= \Sigma \left(\frac{n\pi C_n}{L}\right)^2 \frac{L}{4} \cdot H \cdot \frac{b^2\,db}{2B} + \Sigma \frac{8dC_n}{n\pi L}(\cos n\pi - 1) \cdot \frac{H\,bdb}{2B}$$

$$(\Delta h')^2 \left(\frac{L}{2EA'}\right) = (\Delta l')^2 \left(\frac{EA'}{2L}\right)$$

$$= \left(\frac{EA}{2L}\right)\left\{\Sigma \frac{8C_n d}{n\pi L}(\cos n\pi - 1)\right\}^2 \frac{b^2\,db}{2B}$$

neglecting terms which include $(C_n)^3$ and higher, as before.

Integrating with respect to b across the plate to find the total axial strain energy:

$$E_s = \frac{B^2}{3}\left\{\Sigma \frac{HL}{4} \cdot \left(\frac{n\pi C_n}{L}\right)^2\right\} + \frac{B^2}{3}\left\{\left(\frac{EA}{2L}\right)\left(\Sigma \frac{8C_n d}{n\pi L}(\cos n\pi - 1)\right)^2\right\} \quad - \quad (6.19)$$

where the co-efficients C_n refer to $\phi(x)$ - equation (6.17)

A cellular section can be divided into its various elements and each element treated as indicated above.

The kinetic energy of the system when vibrating at a frequency ω is:

$$T = \frac{1}{2} \int_0^L I_p \{\omega \phi(x)\}^2 dx$$

$$= \frac{I_p L}{4} \omega^2 \Sigma C_n^2 \qquad - (6.20)$$

From this point, the procedure is the same as for vertical oscillations, putting

$$\frac{d(T - E)}{d C_n} = 0$$

to determine the natural frequency associated with each mode.

6.3 NUMERICAL EVALUATION

Inspection of equation (6.1) indicates that the critical flutter speed is dependent on three basic factors, viz -

the magnitude of the torsional frequency ω_T

the ratio of the vertical to the torsional frequency ω_v/ω_T

the weight of the bridge w.

In order to ascertain the relative importance of these factors four numerical examples are included below. Examples 6.1 and 6.2 employ the numerical solution of Example 4.2 where a deck area of 4.5 sq.ft. was nominated. The influence of ω_T and the ratio ω_v/ω_T are examined by maintaining the same deck area in each example but varying the torsional rigidity. In Example 6.3 the effect of a reduction in the deck area (economically desirable as discussed in Section 4.2) is examined using the solution to Example 4.3. This is an alternative solution to that of Example 4.2, employing a deck area of 3.0 sq.ft. The effect of a concrete deck section (in lieu of steel) is demonstrated in Example 6.4 for the same site conditions and live loading as in Examples 4.2 and 4.3.

Relevant details from the solution to Example 4.2 are:

Dead load profile of the structure $\left(\frac{d}{L}\right)_d = 0.01375$

ERRATUM

The data from Example 4.2 required for Examples 6.1 and 6.2 (pages 85, 86) should read as:

Dead load profile of the structure	$(\frac{d}{L})_d$	=	0.0119
Tension in deck	H_{dd}	=	13,500 Kip
Tension in cable	H_{dc}	=	33,100 Kip
Total tensile force in structure		=	46,600 Kip

These altered values produce small variations in the numerical evaluation of Examples 6.1 and 6.2. However the net result is to increase the flutter velocity in Example 6.1 from 41.75 ft/sec to 42 ft/sec (page 89). The flutter velocity of 584 ft/sec in Example 6.2 is unchanged (page 92).

Weight of cable w_c = 563 lb/ft.

Total dead weight of structure = 2765 lb/ft.

EXAMPLE 6.1

Considering the deck as a flat plate 30 ft. wide by 1.8 inches thick (A_d = 4.5 sq.ft.) and employing the above results, then

$$EI = 144 \times 30 \times 10^3 \times \frac{30}{12} \times (\frac{3}{20})^3 = 3.65 \times 10^4 \text{ Kip ft.}^2$$

$$GJ = 11.53 \times 10^3 \times 144 \times \frac{30}{3} \times (\frac{3}{20})^3 = 5.61 \times 10^4 \text{ Kip ft.}^2$$

$$G\bar{J} = \frac{H_{dd}}{A_d} \int r^2 \, d_A \quad \text{(where r = distance from shear centre)}$$

$$= H_{dd} \cdot \frac{B^2}{3}$$

$$= 6550 \times \frac{15^2}{3} = 49.2 \times 10^4 \text{ Kip ft.}^2$$

Then: $(GJ + G\bar{J}) = 54.8 \times 10^4$ Kip ft.^{2}

It is of interest to note the proportion of the total torsional rigidity $(GJ + G\bar{J})$ contributed by the tension in the deck.

In computing the polar moment of inertia of the cross-section, account must be taken of the cable weight as well as the deck. Including the weight of

the cable, assumed uniformly distributed across the width, gives an equivalent plate of thickness 2.26 inches.

$$I_p = \frac{w B^2}{3g} = \frac{2.765 \times 15^2}{3 \times 32.2} = 6.45 \text{ Kip sec.}^2$$

A. Symmetric Modes

Substituting the above values into equations (6.13) and (6.14) for the vertical oscillation:

$$C_1 \left\{ 34.4\ \omega^2 - 5.15 \times 10^{-4} - 62 - 29.7 \right\} - 9.9\ C_3 = 0$$

$$- 9.9\ C_1 + C_3 \left\{ 34.4\ \omega^2 - 4.16 \times 10^{-2} - 558 - 3.3 \right\} = 0$$

Therefore, for a non-trivial solution,

$$(34.4\ \omega^2 - 91.7)\ (34.4\ \omega^2 - 561.3) - (9.9)^2 = 0$$

or $$(\omega^2 - 2.67)\ (\omega^2 - 16.3) - (0.29)^2 = 0$$

Hence $\omega^2 = 2.67$ or 16.3

giving $\omega_{1v} = 1.632$ radians/sec.

$f_{1v} = \frac{1.632}{2\pi} = 0.26$ cycles/sec.

$\omega_{3v} = 4.045$ radians/sec.

$f_{3v} = 0.643$ cycles/sec.

Substituting into equations (6.18), (6.19) and (6.20) for the torsional oscillation:

$$C_1 \left\{ 25.8 \times 10^2\ \omega^2 - 8.43 \times 10^2 - 68.8 \times 10^2 \right\} - (7.425 \times 10^2)\ C_3 = 0$$

$$- (7.425 \times 10^2)\ C_1 + C_3 \left\{ 25.8 \times 10^2\ \omega^2 - 75.87 \times 10^2 - 421 \times 10^2 \right\} = 0$$

Therefore, for a non-trivial solution,

$$(25.8\,\omega^2 - 77.23)\,(25.8\,\omega^2 - 497) - (7.425)^2 = 0$$

Hence $\omega^2 = 3.0$ or 19.3

giving $\omega_{1T} = 1.732$ radians/sec.

$f_{1T} = 0.276$ cycles/sec.

$\omega_{3T} = 4.4$ radians/sec.

$f_{3T} = 0.7$ cycles/sec.

Inspection of these calculations indicates that the restraint of flexural rigidity of this deck is insignificant while the torsional rigidity is responsible for the difference between the torsional and vertical natural frequencies:

B. Antisymmetric Modes.

By the same procedure:

$\omega_{2V} = 2.69$ radians/sec.

$f_{2v} = 0.428$ cycles/sec.

$\omega_{4V} = 5.38$ radians/sec.

$f_{4v} = 0.856$ cycles/sec.

and $\omega_{2T} = 2.92$ radians/sec.

$f_{2T} = 0.466$ cycles/sec.

$\omega_{4T} = 5.86$ radians/sec.

$f_{4T} = 0.933$ cycles/sec.

The lowest value of torsional frequency is $\omega_{1T} = 1.732$

The highest ratio of vertical/torsional frequency is $\omega_{1V}/\omega_{1T} = 0.943$

The first symmetric mode is therefore the fundamental mode of vibration for determination of the critical flutter velocity.

For Frandsen's analysis:

$$\mu = \frac{2\pi \cdot 0.0805 \times 15^2}{2765} = 0.0412$$

$$\nu = \frac{2\ r^2}{b^2} = \frac{2}{b^2} \cdot \frac{I_p g}{W} = \frac{2}{3}$$

Putting $V_D = \omega_T \cdot b \cdot \sqrt{\frac{\nu}{\mu}}$ (V_D is the divergence velocity)

$$= 1.732 \times 15 \times \sqrt{\frac{0.667}{0.0412}}$$

$$= 104 \text{ ft./sec.}$$

Now $$\frac{k^2}{A} = \frac{\mu}{1 - (\omega_v/\omega_T)^2} + \frac{}{1 - (\omega_v/\omega_T)^2} \frac{B}{A}$$

$$= \frac{0.0412}{0.107} + \frac{0.0142}{0.667} \times \frac{0.893}{0.107} \times \frac{B}{A}$$

$$= 0.385 + 0.515 \frac{B}{A}$$

From Figure 6.1, at $\frac{B}{A} = 0.85$, $\frac{k^2}{A} = 0.823$

Hence $k = 0.6$, $A = 0.438$, $B = 0.372$

So that $(\nu \cdot A + B) = 0.292 + 0.372 = 0.664$

$$V_F = V_D \sqrt{\frac{1 - (\omega_v/\omega_T)^2}{\nu \cdot A + B}}$$

$$= V_D \sqrt{\frac{0.107}{0.664}}$$

$$= 41.75 \text{ ft./sec.}$$

EXAMPLE 6.2

For the same data as in Example 6.1, if the deck used is a hollow box 30 feet wide and 6 feet deep with all walls 3/4 inch thick ($A_d = 4.5$ sq.ft.), then

$$EI = 15.55 \times 10^7 \quad \text{Kip ft.}^2$$

$$GJ = 187 \times 10^6 \quad \text{Kip ft.}^2$$

$$G\bar{J} = 71.9 \times 10^4 \quad \text{Kip ft.}^2$$

$$\text{then } GJ + G\bar{J} = 187.7 \times 10^6 \quad \text{Kip ft.}^2$$

Considering for computation of I_p the cable area distributed uniformly around the box section, then

$$I_p = 9.26 \quad \text{Kip sec.}^2$$

A. Symmetric Modes

Substituting the above values into equations (6.13) and (6.14) for the vertical oscillation.

$$C_1 \left\{ 34.4\,\omega^2 - 0.923 - 62 - 29.7 \right\} - 9.9\,C_3 = 0$$

$$-9.9\,C_1 + C_3 \left\{ 34.4\,\omega^2 - 74.8 - 558 - 3.3 \right\} = 0$$

Therefore, for a non-trivial solution:

$$(34.4\,\omega^2 - 92.6)\,(34.4\,\omega^2 - 636.1) - (9.9)^2 = 0$$

from which $\omega^2 = 2.695$ or 18.5

giving $\omega_{1v} = 1.64$ radians/sec.

$f_{1v} = 0.261$ cycles/sec.

$\omega_{3v} = 4.3$ radians/sec.

$f_{3v} = 0.685$ cycles/sec.

Substituting into equations (6.18), (6.19) and (6.20) for the torsional oscillation.

$$C_1 \left\{ 37.04 \times 10^2\,\omega^2 - 289 \times 10^3 - 99 \times 10^2 \right\} - 10.7 \times 10^2\,C_3 = 0$$

$$-C_1\,10.7 \times 10^2 + C_3 \left\{ 37.04 \times 10^2\omega^2 - 2601 \times 10^3 - 617 \times 10^2 \right\} = 0$$

Therefore for a non-trivial solution:

$$(37.04\ \omega^2 - 2989)\ (37.04\ \omega^2 - 26627) - (10.7)^2 = 0$$

from which $\omega^2 = 80.4$ or 720

giving $\omega_{1T} = 8.97$ radians/sec.

$f_{1T} = 1.427$ cycles/sec.

$\omega_{3T} = 26.8$ radians/sec.

$f_{3T} = 4.27$ cycles/sec.

B. Antisymmetric Modes

By the same procedure:

$\omega_{2V} = 3.40$ radians/sec.

$f_{2V} = 0.54$ cycles/sec.

$\omega_{4V} = 9.9$ radians/sec.

$f_{4V} = 1.575$ cycles/sec.

and $\omega_{2T} = 17.87$ radians/sec.

$f_{2T} = 2.84$ cycles/sec.

$\omega_{4T} = 35.74$ radians/sec.

$f_{4T} = 5.68$ cycles/sec.

Lowest value of torsional frequency is $\omega_{1T} = 8.97$ radians/sec.
Highest ratio of vertical/torsional frequency is $\frac{\omega_{1V}}{\omega_{1T}} = 0.183$

The first symmetric mode is therefore the fundamental mode of vibration for determination of the critical flutter velocity.

For Frandsen's analysis:

$\mu = 0.0412$

$$= \frac{2}{b^2} \cdot \frac{I_p g}{W} = \frac{2}{225} \times \frac{9.26 \times 32.2}{2.765}$$

$$= 0.958$$

Divergence velocity $V_D = \omega_T \cdot b\sqrt{\frac{\gamma}{\mu}}$

$$= 647 \text{ ft./sec.}$$

$$\frac{k^2}{A} = \frac{0.0412}{1-0.0334} + \frac{0.0412}{0.958} \times \frac{0.0334}{0.967} \times \frac{B}{A}$$

$$= 0.0426 + 0.00149 \frac{B}{A}$$

From Figure 6.2, at $\frac{B}{A} = 1.78$, $\frac{k^2}{A} = 0.0452$

Hence $k = 0.14$, $A = 0.433$, $B = 0.77$

So that $(\gamma A + B) = 0.415 + 0.77 = 1.185$

Flutter velocity $V_F = V_D \sqrt{\frac{0.967}{1.185}}$

$$= 584 \text{ ft./sec.}$$

EXAMPLE 6.3

The aerodynamic stability of the structure in Example 6.2 (V_F = 584 ft./sec.) was more than adequate. A more economical solution involving a smaller area of deck may also prove satisfactory with respect to aerodynamic stability. The solution of Example 4.3 will therefore be analysed to indicate the trend as the area of deck is reduced.

Relevant data from Example 4.3 is:

Dead load profile of structure	= 0.01067	
Tension in deck H_{dd}	= 7,610	Kip
Tension in cable H_{dc}	= 29,600	Kip
Total tensile force in structure	= 37,200	Kip

Area of deck A_d	=	3.0 sq.ft.
Weight of deck W_d	=	1470 lb/ft.
Area of cable A_c	=	1.04 sq.ft.
Weight of cable W_c	=	510 lb/ft.
Total dead weight of structure	=	1980 lb/ft.

Using the same overall dimensions for the deck as in Example 6.2, consider the deck as a hollow box 30 feet wide and 6 feet deep with all walls 1/2" thick (A_d = 3.0 sq.ft.). Then

$$EI = 10.35 \times 10^7 \quad \text{Kip ft.}^2$$

$$GJ = 124.7 \times 10^6 \quad \text{Kip ft.}^2$$

$$G\bar{J} = 83.5 \times 10^4 \quad \text{Kip ft.}^2$$

$$\text{then } GJ + G\bar{J} = 125.5 \times 10^6 \quad \text{Kip ft.}^2$$

Considering for computation of I_p the cable area distributed uniformly around the box section, then

$$I_p = 6.63 \text{ Kip sec.}^2$$

A. Symmetric Modes

Substituting the above values into equations (6.13) and (6.14) for the vertical oscillation:

$$C_1 \left\{ 24.6\,\omega^2 - 0.615 - 57.3 - 11.94 \right\} - 3.98\, C_3 = 0$$

$$-3.98\, C_1 + C_3 \left\{ 24.6\,\omega^2 - 49.8 - 515 - 1.33 \right\} = 0$$

Therefore, for a non-trivial solution:

$$\left(24.6\,\omega^2 - 69.9\right)\left(24.6\,\omega^2 - 566.1\right) - (3.98)^2 = 0$$

from which $\omega^2 = 2.84$ or 22.9

giving $\omega_{1V} = 1.684$ radians/sec.

$f_{1V} = 0.268$ cycles/sec.

$$\omega_{3V} = 4.79 \text{ radians/sec.}$$

$$f_{3V} = 0.761 \text{ cycles/sec.}$$

Substituting into equations (6.18), (6.19) and (6.20) for the torsional oscillation:

$$C_1 \left\{ 26.52 \times 10^2 \omega^2 - 192 \times 10^3 - 74.6 \times 10^2 \right\} - 4.3 \times 10^2 \; C_3 = 0$$

$$- 4.3 \times 10^2 \; C_1 + C_3 \left\{ 26.52 \times 10^2 \omega^2 - 1555 \times 10^3 - 557 \times 10^2 \right\} = 0$$

Therefore for a non-trivial solution:

$$(26.52\,\omega^2 - 1994.6)\,(26.52\,\omega^2 - 16107) - (4.3)^2 = 0$$

from which $\omega^2 = 75$ or 607

giving

$$\omega_{1T} = 8.65 \text{ radians/sec.}$$

$$f_{1T} = 1.376 \text{ cycles/sec.}$$

$$\omega_{3T} = 24.6 \text{ radians/sec.}$$

$$f_{3T} = 3.92 \text{ cycles/sec.}$$

As in Example 6.2 the first symmetric mode will be the fundamental mode of vibration for determination of the critical flutter velocity.

For Frandsen's analysis:

$$\mu = \frac{2\pi \times 0.0805 \times 15^2}{1980} = 0.0575$$

$$\nu = \frac{2}{225} \times \frac{6.63 \times 32.2}{1.98} = 0.958$$

Divergence velocity $V_D = \omega_T b \sqrt{\frac{\nu}{\mu}}$

$$= 529 \text{ ft./sec.}$$

$$\frac{k^2}{A} = \frac{0.0575}{1-0.0379} + \frac{0.575}{0.958} \cdot \frac{0.0379}{0.9621} \cdot \frac{B}{A}$$

$$= 0.0598 + 0.00236 \frac{B}{A}$$

From Figure 6.2 at $\frac{B}{A} = 1.55$, $\frac{k^2}{A} = 0.06346$

Hence $k = 0.19$, $A = 0.58$, $B = 0.88$

So that $(\nu A + B) = 0.542 + 0.88 = 1.422$

Flutter velocity $V_F = V_D \sqrt{\frac{0.9621}{1.422}}$

$= 435$ ft./sec.

EXAMPLE 6.4

For the same site conditions as in Examples 6.1 - 6.3 a cellular concrete section is proposed having a width of 30 feet, a depth of 6 feet and all walls 6 inches thick. Determine the critical flutter velocity for the concrete deck. For the concrete E = 3,000 Ksi, G = 1,500 Ksi, ρ = 165 lb/cu.ft. Assuming the deck to act as dead load only, the required area of cable can be obtained from the solution of Example 2.4.

Relevant data from Example 2.4 is:

Area of deck A_d	= 36 sq.ft.
Weight of deck W_d	= 5945 lb/ft.
Area of cable A_c	= 4.31 sq.ft.
Weight of cable W_c	= 2115 lb/ft.
Total dead weight of structure	= 8,060 lb/ft.
Dead load profile of structure	= 0.014
Tension in cable H_{cd}	= 114,700 Kip
EI	= 124.5×10^6 Kip ft.^{2}
GJ	= 194.4×10^6 Kip ft.^{2}

Considering for computation of I_p the cable area distributed across the netural axis of the deck section, then

$$I_p = 19.9 + 4.92 = 24.82 \text{ Kip sec.}^2$$

A. Symmetric Modes

Substituting the above values into equations (6.13) and (6.14) for the vertical oscillation.

$$C_1 \left\{ 100\,\omega^2 - 0.742 - 177 - 29.6 \right\} - 9.9\,C_3 = 0$$

$$-9.9\,C_1 + C_3 \left\{ 100\,\omega^2 - 60.1 - 531 - 3.3 \right\} = 0$$

Therefore for a non-trivial solution:

$$\left(100\,\omega^2 - 207.3\right)\left(100\,\omega^2 - 594.4\right) - (9.9)^2 = 0$$

from which $\omega^2 = 2.073$ or 5.944

giving $\omega_{1V} = 1.44$ radians/sec.

$f_{1V} = 0.231$ cycles/sec.

$\omega_{3V} = 2.44$ radians/sec.

$f_{3V} = 0.388$ cycles/sec.

Substituting into equations (6.18), (6.19) and (6.20) for the torsional oscillation.

$$C_1 \left\{ 99.28 \times 10^2\,\omega^2 - 30 \times 10^4 - 205.2 \times 10^2 \right\} - 9.83 \times 10^2\,C_3 = 0$$

$$-9.83 \times 10^2\,C_1 + C_3 \left\{ 99.28 \times 10^2\,\omega^2 - 270 \times 10^4 - 530 \times 10^2 \right\} = 0$$

Therefore for a non-trivial solution:

$$\left(99.28\,\omega^2 - 3205.2\right)\left(99.28\,\omega^2 - 27530\right) - 9.83^2 = 0$$

from which $\omega^2 = 32.3$ or 278

$\omega_{1T} = 5.69$ radians/sec.

$f_{1T} = 0.905$ cycles/sec.

ω_{3T} = 16.66 radians/sec.

f_{3T} = 2.65 cycles/sec.

As in Example 6.2 the first symmetric mode will be the fundamental mode of vibration for determination of the critical flutter velocity.

For Frandsen's analysis:

$$\mu = \frac{2\pi \times 0.0805 \times 15^2}{8060} = 0.0141$$

$$\nu = \frac{2}{225} \times \frac{24.82 \times 32.2}{8.06} = 0.882$$

Divergence velocity $V_D = \omega_T b \sqrt{\frac{\nu}{\mu}}$

= 675 ft./sec.

$$\frac{k^2}{A} = \frac{0.0141}{1-0.0642} + \frac{0.0141}{0.882} \times \frac{0.0642}{0.9358} \times \frac{B}{A}$$

$$= 0.01506 + 0.0011 \frac{B}{A}$$

From Figure 6.2 at $\frac{B}{A} = 2.4$ $\frac{k^2}{A} = 0.0177$

Hence k = 0.08, A = 0.362, B = 0.868

So that $(\nu . A + B) = 0.319 + 0.868 = 1.187$

Flutter velocity $V_F = V_D \sqrt{\frac{0.9336}{1.187}}$

= 599 ft./sec.

It is concluded from Examples 6.1 and 6.2 that for a constant total dead weight or area of deck, an increase in the torsional rigidity of the deck,

(i) increases the value of ν

(ii) increases ω_T in magnitude and increases ω_T/ω_ν

(iii) considerably increases the divergence frequency V_D

(iv) increases the factor by which V_D is multiplied to yield a larger increase in the critical flutter velocity V_F.

(v) in practice, a substantial torsional rigidity is required for adequate aerodynamic stability. This can be achieved most effectively using a closed cellular section. However, the validity of the "thin airfoil" analysis decreases as the depth of section increases relative to the breadth (i.e. to increase the torsional rigidity). In this respect Selberg (15) reports good agreement between the theoretical flutter velocity and experimental results for a streamlined section having a width-depth ratio of 5.5.

Choice of the same external dimensions in Examples 6.2 and 6.3 gave the same value of ν and also of $\frac{GJ + G\bar{J}}{I_p}$ ($GJ + G\bar{J}$ and I_p are both linearly proportional to the wall thickness of a simple box). ω_T and ω_T/ω_V both showed a slight decrease in Example 6.3, mainly due to the smaller dead load sag/span ratio. The value of μ was decreased in Example 6.3 and produced a significant decrease in the divergence velocity V_D. The net results was a decrease in the critical flutter velocity V_F.

Although the concrete deck in Example 6.4 gave lower values of ω_v, ω_T and ω_T/ω_v than the steel decks of Examples 6.2 and 6.3, the effect of its greater weight (i.e. lower μ) was sufficient to yield a higher value of the critical flutter velocity.

It is of interest to compare the above results with those of the new Severn Suspension Bridge as reported by Walshe (17). The fundamental frequencies for the deck section adopted were:

Fundamental Symmetric Mode

$$f_{1V} = 0.143 \text{ cycles/sec.}$$

$$f_{1T} = 0.374 \text{ cycles/sec.}$$

$$f_{1T}/f_{1V} = \omega_{1T}/\omega_{1V} = 2.62$$

Fundamental Antisymmetric Mode

f_{2V} = 0.128 cycles/sec.

f_{2T} = 0.510 cycles/sec.

f_{2T}/f_{2V} = 4.00

The critical flutter velocity was in the vicinity of 150 M.P.H.

6.4 GUST EXCITATION

A second aspect of the aerodynamic problem is that of gust excitation of the structure. If the structure is aerodynamically stable, the response to wind gusts in the horizontal, torsional and vertical modes can generally be considered independently (18). In other words, the structure can be analysed as having a single degree of freedom in each mode. The gusty wind can be described statistically by a spectrum of turbulence which defines the distribution in energy in the wind as a function of the frequency of the fluctuations in the wind. Wind loads contain the bulk of their energy at frequencies of the order of one cycle per minute. With increasing frequency the energy levels decrease to negligible magnitude at frequencies in excess of a few cycles per second.

Gust excitation of the structure is dependent on the energy level of the wind at the natural frequencies in each mode of vibration, the mass of the bridge and its damping capacity. The sensitivity of the structure to gust excitation will decrease as its fundamental natural frequencies increase. The cellular deck member in catenary will generally have appreciably higher natural frequencies than an equivalent suspension bridge, and buffeting of the structure by turbulent wind is therefore likely to be less significant than is the case for a conventional suspension bridge. Gust excitation is nevertheless a significant aspect in design since turbulence-induced accelerations will probably determine the range of wind speeds over which the bridge can be used in comfort and safety. The evaluation of the response to turbulence is however a problem best solved by model testing in a wind tunnel and is beyond the scope of this study.

CHAPTER 7

GENERAL PRACTICAL ASPECTS

The analysis developed in the preceeding chapters has established that design of a cable-deck catenary system is possible. The purpose of this chapter is to establish whether such a structure can be built in practice. The chapter covers practical aspects such as actual material behaviour, provision of a traffic running surface, safety of the structure against collapse and fabrication and erection considerations.

7.1 MATERIALS PERFORMANCE

To this point, all numerical examples have been based on a steel of density ρ_s = 490 lb/cu.ft. and an elastic modulus E_s of 30,000 Ksi. The charts in Appendix A have also been prepared using these values. If a material having different properties, is proposed, the existing charts can be adapted as indicated below. The charts show particular solutions of the general equations (2.17) and (2.18).

Equation 2.17 $$m\,(m+1)\,(m+2) = \frac{3\rho L}{64E}\left(\frac{L}{d_o}\right)^3 \cdot \{p - m\}$$

Equation 2.18 $$f = \frac{\rho L}{8}\left(\frac{L}{d_o}\right)\left(\frac{1+p}{1+m}\right)$$

To use the prepared charts for any material having ρ and E, a factor M is introduced where

$$M = \frac{\rho}{\rho_s} \times \frac{E_s}{E} \qquad - (7.1)$$

so that in equation 2.17 (ML) is the equivalent span length of a steel cable, to give the same solution for p and m.

Thus in equation (2.17) $$m\,(m+1)(m+2) = \frac{3\rho_s}{64\,E_s}(ML)\left(\frac{L}{d_o}\right)^3 \{p - m\}$$

and in equation (2.18) $$\frac{E_s}{E} \cdot f = \frac{\rho_s (ML)}{8}\left(\frac{L}{d_o}\right)\left(\frac{1+p}{1+m}\right)$$

For $M < 1$ there will be an increase in p for the same value of m. Figure 2.7 shows typical relationships between span L and load factor p for constant m. Varying the span length is equivalent to varying M.

If fy is the tensile strength at the elastic limit, then the term $\frac{E_s}{E}$. fy is called the "equivalent stress level". This value is used as the stress criterion (see Section 2.7) for the prepared charts.

The relative performance of materials having different properties can be assessed by comparing the value of M and the equivalent stress level for each material. Table 7.1 shows a comparison between typical values for structural steel, aluminium, stress-relieved prestressing cable and galvanised bridge wire.

The aluminium (M = 1.07) is equivalent to a steel cable having a slightly larger span length (7% larger) and would therefore show a slightly poorer performance in response to load than a steel cable having the same self-weight profile $(\frac{d_o}{L})$ over the original span length (L). However, because the aluminium has a higher equivalent stress level than the steel, a smaller value of the self-weight profile can be employed to satisfy the same serviceability and stress criteria. (Compare the self-weight profiles for the 50 Ksi and 230 Ksi stress levels in Examples 2.1 and 2.2.) This will have a beneficial effect on the performance of the aluminium cable. On economic grounds, however, any overall benefits in performance for the aluminium are far outweighed by the extra cost of the aluminium (cost per ton 4-5 times greater than that for structural steel).

The stress-relieved prestressing cable has a lower value of M and a higher equivalent stress level than the galvanized bridge strand and will therefore show a superior performance in comparison with the galvanized bridge strand. However if it is to be used in preference to the galvanized bridge strand, adequate protection against corrosion must be ensured. In this regard it is noted (19) that a plastic cable covering has been developed by the Bethlehem Steel Corporation which is claimed to be simple and economical to apply, unquestionably weathertight, sufficiently elastic to deflect with the cable, and has an indefinite life virtually free of maintenance.

TABLE 7.1

MATERIAL	DENSITY ρ (lb/cuft)	ELASTIC MODULUS (K.S.I)	"M"	TENSILE STRENGTH AT ELASTIC LIMIT (K.S.I)	EQUIVALENT STRESS LEVEL (Ks.i.)
Structural Steel	490	30×10^3	1·0	50	50
Duralumin	175	10×10^3	1·07	19	57
Stress-relieved prestressing cable	490	28×10^3	1·07	230	244
Galvanized bridge strand	520	24×10^3	1·326	160	200

7.2 STRESS RELAXATION

In prestressed concrete design, account is taken of the tendency for steel prestressing cable to creep under sustained high stresses. This behaviour is normally referred to as stress relaxation, which is the loss of stress when the cable is prestressed and maintained at a constant strain for a period of time. An alternative approach is to measure the creep strain of the cable under constant load. For practical purposes, the two approaches are equivalent, since the loss of stress is directly proportional (via Young's Modulus) to the decrease in elastic strain, which balances the positive creep strain.

For the long-span cable at a particular profile $(\frac{d}{L})$ maintaining constant span length and applied load, creep strain is accommodated by increasing the length of the cable. This in turn increases the sag/span ratio of the cable, and under the constant applied load the stress in the cable is reduced. This stress reduction will affect the rate of creep strain, resulting in an interaction behaviour similar to the interaction of prestress losses which occurs in prestressed concrete.

Relaxation tests on prestressing wires at constant length (20) have indicated that as the initial stress increases, the relaxation loss increases at an increasing rate. A similar trend is expected for the interaction behaviour of the long-span cable. As the stress in the cable decreases, the rate of creep strain is also expected to decrease. A simple modification of the normal stress relaxation test is suggested to determine the effect of decreasing the cable tension. If a heavy load is suspended from the mid-point of the cable under test, the cable will creep and increase the deflection of the central load, rather than "relaxing". As deflection increases, the tension in the cable will decrease, and the interaction behaviour can be readily assessed.

The consequences of creep in the long-span cable are two-fold. The resulting increase in the sag/span ratio will give the cable a higher load-carrying capacity. However if a maximum sag or cable slope is specified as a design criterion, allowance for the increase in sag due to creep will be necessary.

AS CA 35 Section 4.5.2 nominates stress relaxation losses in pre-stressing steel tendons for initial stresses at approximately 70% of the tensile strength of the steel.

For stress-relieved strand, nominated stress loss = 12 Ksi

For stabilized strand, nominated stress loss = 4 Ksi.

Converting these relaxation losses to creep strain;

$$\text{For stress-relieved strand, creep strain} = \frac{12}{30{,}000} = 4 \times 10^{-4}$$

$$\text{For stabilized strand, creep strain} = \frac{4}{30{,}000} = 1.33 \times 10^{-4}$$

Assuming for a long-span cable having a profile $\frac{d}{L} = 0.015$ under service loading, that this amount of creep strain occurred, then the new profile can be determined using equation (2.11).

$$\text{Strain} = \frac{\Delta l}{L} = \frac{8}{3}\left\{\left(\frac{d + \Delta d}{L}\right)^2 - \left(\frac{d}{L}\right)^2\right\}$$

$$\text{Thus for stress-relieved strand} \quad \left(\frac{d + \Delta d}{L}\right)^2 = \frac{3}{8} \times 4 \times 10^{-4} + (0.015)^2$$

$$= 0.00015 + 0.000225$$

$$\text{giving} \quad \left(\frac{d + \Delta d}{L}\right) = 0.0194$$

This is a significant increase in sag, and would produce a reduction in stress of 23%. The 12 Ksi nominated in AS CA 35 for stress-relieved strand is approximately a 6% stress relaxation.

$$\text{For stabilized strand,} \quad \left(\frac{d + \Delta d}{L}\right)^2 = 0.00005 + 0.000225$$

$$\text{giving} \quad \left(\frac{d + \Delta d}{L}\right) = 0.0166$$

and a reduction in stress of 10% as compared with the value of approximately 2% nominated in AS CA 35 for stabilized strand.

On the basis of these comparisons, it is concluded that the stress relaxation losses nominated in AS CA 35 Section 4.5.2 are not meaningful for the case of the long-span cable where vertical deflection is not restrained. This conclusion endorses the desirability of a modified stress relaxation test such as proposed above.

For a practical design situation, a knowledge of the interaction behaviour and the stress level at which the cable is working are necessary in assessing the

importance of the creep behaviour. This could be a critical factor in determining the type of prestressing cable to be used. In a suggested erection procedure outlined in Section 7.5.2 allowance for the creep behaviour is made by adjusting the cable profile after all significant creep strain deformation has taken place.

7.3 TRAFFIC RUNNING SURFACE

Because of the low skid-resistance of steel and the inherent wavy surface of the fabricated orthotropic steel plate deck, a superior traffic running surface must be provided on top of the steel plate decking. Normal requirements for a traffic running surface are surface smoothness, skid-resistance, wear resistance, stability under all working conditions, and placement of surfacing material without undue difficulty. The flexibility of the orthotropic steel plate deck places additional demands on the surfacing material. It must have adequate resilience and fatigue resistance to accommodate the flexing of the orthotropic plate, but be sufficiently rigid to resist deformation due to traffic and hot weather. A good bond must be developed between the running surface and the steel plate, and reliable protection of the steel plate against corrosion must be provided. Consideration should also be given to the removal and re-application of the running surface.

At the symposium on wearing surfaces for steel bridge decks of lightweight construction, conducted in 1968 by the International Association for Bridge and Structural Engineering (21), satisfactory performance was reported for asphaltic wearing surfaces 2" - 2 1/2" thick on orthotropic steel decks of girder-type bridges. The running surface on a steel cellular deck in catenary will not be subject to conditions any worse than on an orthotropic deck of a girder bridge. Provision of a satisfactory traffic running surface for the steel cellular deck in catenary should therefore be possible using an asphaltic material. However, consideration should be given to the thermal effects induced in the deck due to the high temperatures associated with the laying of the asphalt.

7.4 ULTIMATE BEHAVIOUR AND DESIGN LOAD FACTORS

In Chapters 2 - 4, analysis was based on elastic behaviour, with ultimate conditions equated to the limit of the elastic range. In Section 5.1, the behaviour of the cable-deck catenary system following yielding of the deck, was briefly discussed.

For structural steel in tension, as intended for the deck, the initial linear stress-strain relationship or elastic region is followed by a plastic region of considerable deformation with practically no increase in stress, and then by a region of strain hardening where the increasing deformation is accompanied by some increase in stress. The total strain to failure will be in the order of 30%.

For the high strength prestressing cable, the elastic limit is normally defined by the 0.2 percent proof stress which is usually required to be not less than 0.85 times the minimum specified tensile strength of the cable. Beyond the elastic range, increasing strain is accompanied by some increase in stress. Australian Standard Codes for Steel Tendons for Prestressed Concrete specify a minimum percentage elongation at fracture. For example, in AS A 142 for seven-wire stress-relieved steel strand, a minimum strain of 3.5% is specified.

Assuming that the steel deck is in the plastic region when the cable reaches its maximum strain, then the collapse load of the structure will be determined by the profile of the cable on the point of fracture. The cable profile can be obtained using equation (2.11).

$$\frac{\Delta l}{l} = \frac{8}{3}\left\{\left(\frac{d+\Delta d}{L}\right)^2 - \left(\frac{d}{L}\right)^2\right\}$$

For a strain of 3.5%

$$\left(\frac{d+\Delta d}{L}\right)^2 \doteqdot \frac{3}{8} \times 0.035$$

$$\text{giving } \frac{d+\Delta d}{L} = 0.1145$$

This corresponds to a cable end slope of 46%.

If in Example 4.2, the cable has a tensile strength of 270 Ksi and a strain of 3.5% at fracture, and the deck is at yield stress at the same profile, then the load capacity of the cable-deck catenary system at collapse would be

$$w_{collapse} = \frac{8 \times 0.1145}{1600}\left\{(270 \times 1.15 \times 144) + (50 \times 4.5 \times 144)\right\}$$

$$= 44 \text{ Kip/ft.}$$

The ultimate load at the limit of the elastic range in Example 4.2 was

$$w_{ult.} = 2\,(2.765 + 1.2) = 8 \text{ Kip/ft.}$$

Obviously there is an enormous margin of safety against collapse of the structure. However the collapse load is associated with excessive deformations and is of little value in the design situation where deformation is limited by serviceability criteria. The approach developed in Chapters 2 - 4 is considered more suitable, adopting the elastic limit of each material as the maximum stress criterion. The purpose of specifying load factors for the maximum stress criterion, then, will be to ensure that the structure remains in the elastic range under service loading so that a permanent set will not occur.

Some discussion of the traffic loading is appropriate at this point. The uniformly distributed design lane load of 640 lb/ft. in the NAASRA Highway Bridge Design Code is generally accepted as applicable to spans up to 400 feet. However for long spans, the probability of full traffic loading with a succession of the heaviest vehicles on all lanes is practically zero, and it is reasonable to choose a design live load of smaller intensity. Ivy et al (22) investigated this problem in 1954 for the lower deck of the San Francisco - Oakland Bay Bridge in California, which is devoted entirely to heavy vehicular traffic. From a two-day peak hour traffic count, the maximum lane load obtained was only 145 lb/ft. The average spacing between vehicles was 8 feet. By comparison, the average lane load for an engineer combat battalion, one of the heaviest common military convoys likely to use the highways, was 620 lb/ft. Ivy et al recommended a design lane loading of 640 lb/ft. for spans up to 1,000 feet, 600 lb/ft. for spans 1,000 feet - 1,200 feet, and 560 lb/ft. for spans greater than 1,200 feet. These values were based largely on the consideration of the military convoy occupying the entire length of a structure. The British Code BS 153 : Part 3A : 1954, on the other hand, gives a smooth decreasing curve for design lane loading with increasing span. This curve is included as Figure 7.1.

A design lane loading of 640 lb/ft. up to a span of 1,200 feet and the British curve thereafter, is suggested as reasonable for the long-span bridge.

The emphasis in selection of a design lane load appears to be in catering for infrequent heavy loading of the magnitude of a military convoy. However for the military convoy and other infrequent heavy loading, it is not considered essential that the maximum traffic grade be limited to about 6%. It is considered reasonable to apply this maximum traffic gradient or serviceability criterion for the maximum traffic intensity to which the bridge will be regularly subjected, and a "normal traffic loading" equal to 75% of the design lane load is suggested.

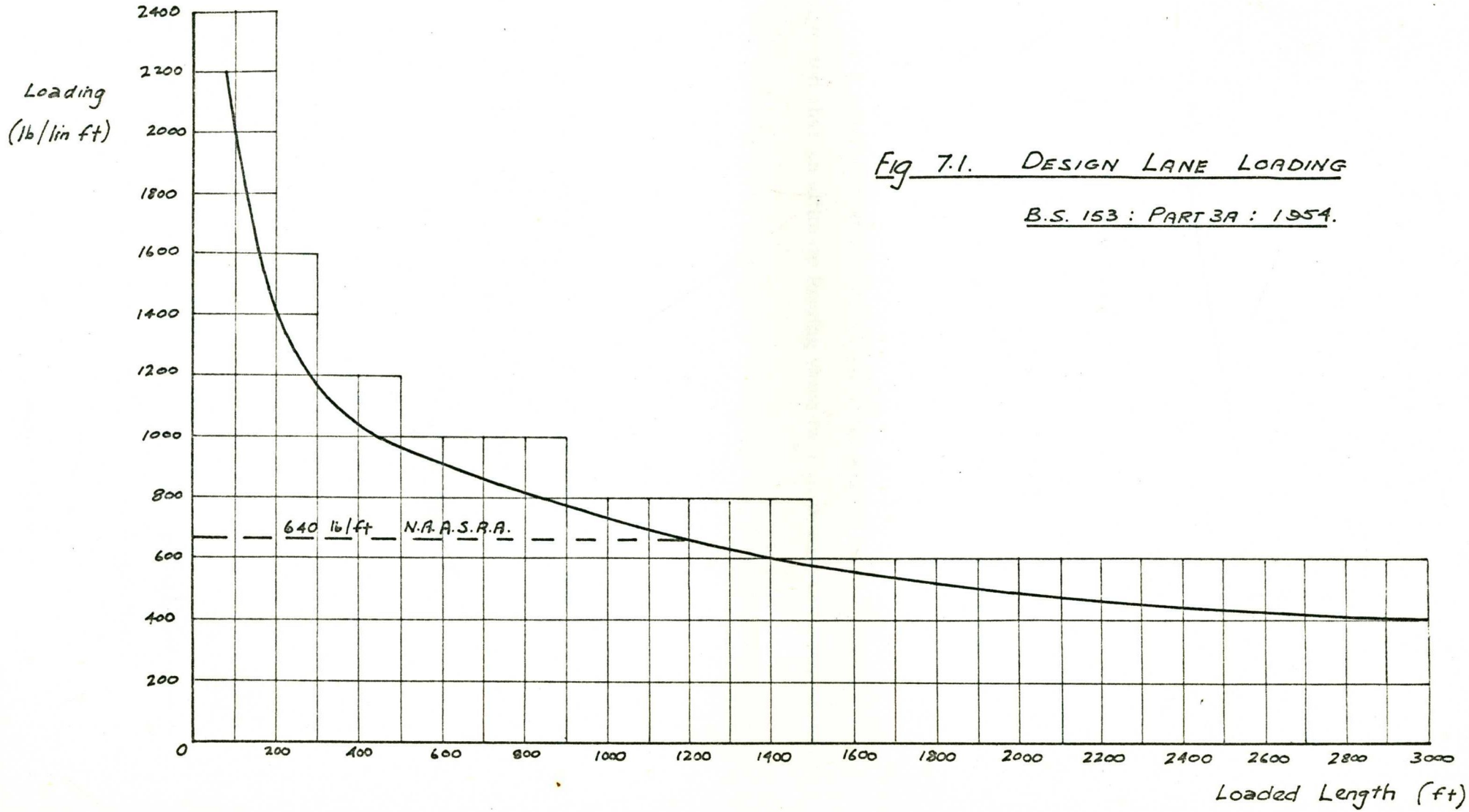

Fig 7.1. DESIGN LANE LOADING

B.S. 153 : PART 3A : 1954.

Having established a "normal traffic loading" the question of load factors is again raised. The ultimate load factors specified for prestressed concrete in AS CA 35 Section 4.10.1 give an indication of the accuracy of prediction of the various load components - i.e. dead load, live load due to traffic including impact, and wind loading. The same approach is suggested in the selection of load factors for the cable-deck catenary system. Aerodynamic behaviour due to wind loading was analysed in Chapter 6, and the loading factors will therefore be restricted to the dead load of the structure (w_D) and the traffic loading (w_L) as determined conventionally using the design lane load.

For normal working conditions, adopting a maximum traffic gradient under the "normal traffic loading", it is suggested that the total service loading (w_s) be determined using equation (7.2).

$$w_c = w_D + 0.75\, w_L \qquad - (7.2)$$

For a maximum stress criterion at the elastic limit of each material, it is suggested that an ultimate loading value (w_u) be determined using equation (7.3).

$$w_u = 1.2\, w_D + 1.5\, w_L \qquad - (7.3)$$

These load factors will ensure that the structure remains elastic under the design lane loading, and adequate safety against collapse of the structure will still be achieved.

7.5 FABRICATION AND ERECTION CONSIDERATIONS

The basic construction procedure for the catenary structure using the closed cellular deck is envisaged as:

(i) Erection of cables.

(ii) Shop fabrication of the deck in segments, each cellular segment comprising several open sections which will be assembled around the cables at the bridge site.

(iii) Field assembly and connection of segments by welding.

(iv) Final tensioning or "tuning" of the structure.

7.5.1 SELECTION OF DECK CROSS-SECTION

Use of the closed cellular section for the deck was confirmed in Chapter 6 where aerodynamic considerations required a deck having a substantial torsional rigidity. As discussed in Section 5.3, provision of an orthotropic top deck plate will be necessary for distribution of the local loading. To achieve the required torsional rigidity of the deck with a minimum deck area, it is possible to use thin stiffened plate for all walls. However the cost of fabrication and connection of the stiffened plate segments will be considerable, and it may be more economical to use thicker unstiffened plate for the side walls and bottom flange.

Sufficient access must be provided inside the cellular segments for field assembly and also for maintenance of the structure in service. Hence a minimum section depth of about 5 - 6 feet is suggested.

7.5.2 ERECTION AND TUNING OF STRUCTURE

The major objective of steps (i), (iii) and (iv) of the basic construction procedure, is to achieve in practice the design profiles for the cables and deck. This process will be termed "tuning" the structure. It was demonstrated in Chapter 4 that the interaction behaviour of the cables and deck is quite sensitive to small variations of profile. To avoid the complications of this interaction in tuning the structure, it is preferable to tune the cables and deck independently. Construction steps (i), (iii) and (iv) are amplified below to explain a suggested procedure whereby independent tuning is achieved. This involves only a limited amount of tensioning to adjust the cable and deck profiles.

(i) Erection of cables. If it was possible to set the profile with perfect precision and if the cable material behaved ideally, it would be expedient to install the cables at the design self-weight profile $(\frac{d_o}{L})_c$. Any nominated profile can be obtained by controlling the cable sag at mid-span, using precision levelling instruments. Permitting the same levelling tolerance at any cable sag, a large sag can be set to a higher order of accuracy than a very small sag. The cable self-weight profile will be very small and it is preferable that the cable profile be finally set at a larger sag when the cable is carrying additional load.

The other problem encountered in immediate tuning of the cables, is the effect of creep strain of the cable material as discussed in Section 7.2. On the basis of tests as suggested in Section 7.2, allowance can be made for the creep strain deformation by setting the cable at a sag/span ratio a little smaller than the self-weight profile $(\frac{d_o}{L})_c$. Later adjustments to the cable profile (in performing the final tuning of the cable) will then be minimized.

(iii) Field assembly and connection of deck segments. It is proposed to attach the deck member to the bridge abutments using high tensile cables anchored in the end segments of the deck and stressed against the abutments. The arrangement is described further in Section 7.5.3. The order of erection would then be to tie one end segment to its abutment and progressively connect segments across the span to the other abutment. The cables provide direct support for the deck segments during the assembly and connection.

The aerodynamic behaviour of the structure at various stages of completion should be checked, and if necessary, restraints such as anchors can be provided along the span to stabilize the aerodynamic motion.

(iv) Final tuning of the structure. With all deck segments connected, and prior to tying the deck to the other abutment, the initial tie at the first abutment is released. The deck will then be acting fully as dead load on the cables. By this time, the deformation of the cables due to creep strain may be regarded as complete. The cables can now be finally tuned at the large sag resulting from the dead load of the deck. This should involve only small adjustment of the cable profile.

With the cables tuned, the deck is then anchored to one abutment, and stressed against the other abutment until the dead load profile of the cable-deck system is achieved. Anchorage is then secured at this abutment to complete the tuning of the deck.

This method of erection involving tuning of the structure, permits actual material properties rather than assumed design values to be used in calculations for the final tuning operations. This is considered an important feature of the structural concept employing the steel cellular deck in catenary.

Appropriate figures for tuning the cable-deck system of Example 4.2 are included below:

Self-weight profile of cables $(\frac{d_o}{L})_c$	=	0.00358
Total cable tension at this profile	=	31,500 Kip
Cable profile with deck as dead load	=	0.0161

ERRATUM

On page 112, values for the cable-deck system should be:

Dead load profile of cable-deck system	=	0.0119
Total cable tension at this profile	=	33,100 Kip
Total tension in deck at this profile	=	13,500 Kip

7.5.3 ANCHORAGE

In the proposed anchorage arrangement, anchorage points are provided around the perimeter of the end deck segment. Prestressing cables are led from these anchorage points back through ducts in a large concrete stressing block along with the main cables, as shown in Figure 7.2. The stressing block is itself stressed down into rock using prestressed rock anchors. The detailing of reinforcement, cable ducts and anchor plates will be practicable for such an arrangement. This arrangement can also be adapted for prestressed concrete approach spans.

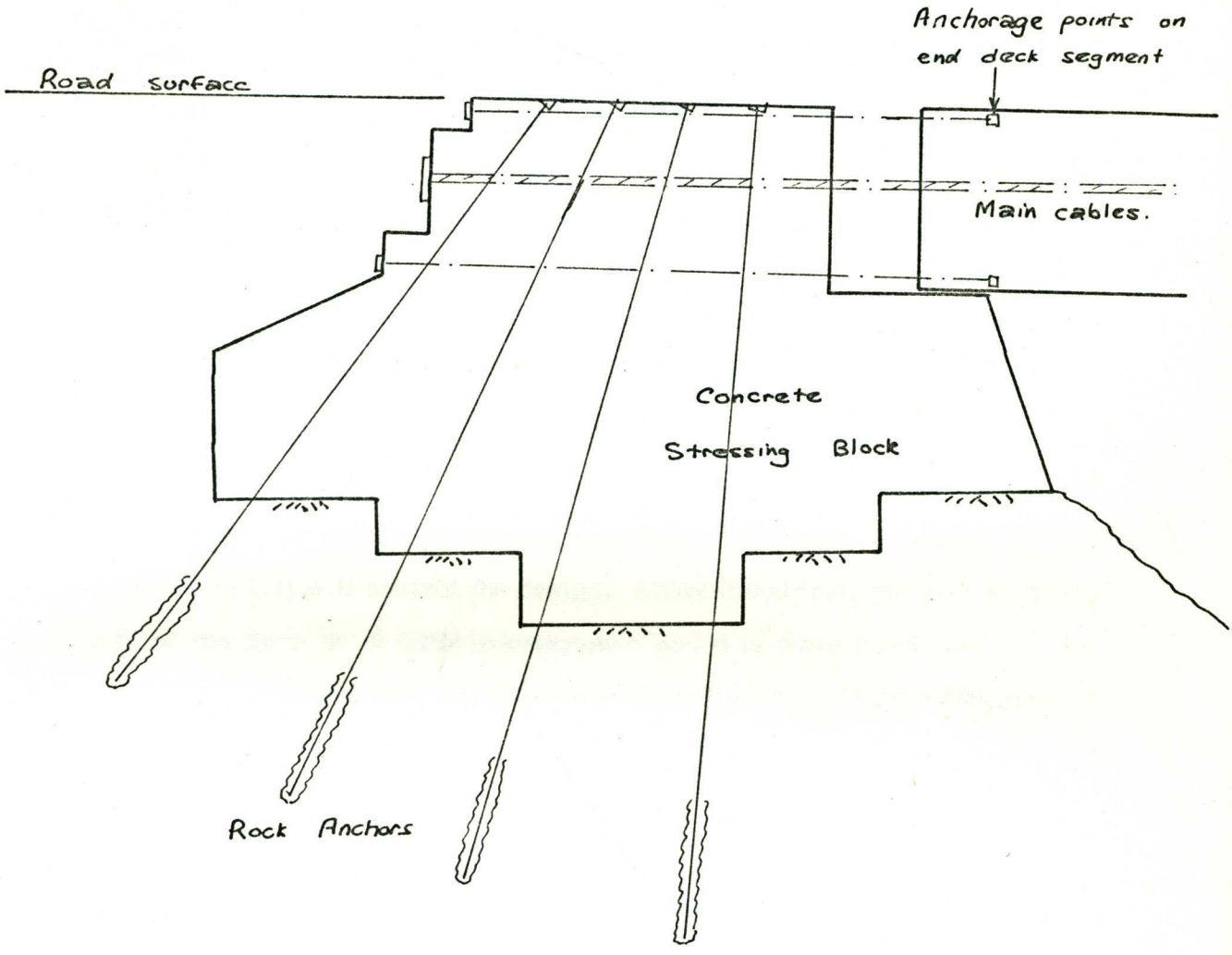

Fig 7.2. PROPOSED ANCHORAGE ARRANGEMENT

CHAPTER 8

COMPARISON WITH ALTERNATIVE BRIDGE TYPES

The final consideration in the feasibility study is whether the steel cellular deck in catenary is economically competitive with other long-span bridge concepts. This is largely dependent on the actual span length and also the anchorage foundation conditions for a particular design situation.

For the cable-deck catenary system, as the span length increases, the deck's contribution to the total load-carrying capacity of the structure decreases. The cable-deck catenary system is considered suitable for spans from about 600 feet to 2,000 feet. Below 600 feet, the structure is particularly sensitive to variations in profile, and requires extremely accurate tuning. Secondary stress effects (Section 5.1) will control the design. Above 2,000 feet, the load-carrying capacity of the deck is of little consequence and it is more economical for the cables to fully support the deck as dead loading. As such, the structure is essentially a degenerate form of the suspension bridge.

For spans from 600 feet - 1,000 feet, the depth of section of the deck may prove a critical factor. The tensile bending stresses induced by the curvature of the deck (Section 5.1) could control the design. This effect can be minimized by selecting a deck cross-section having the neutral axis close to the bottom flange. This may require a slightly greater area of deck, but the deck will be carrying load more efficiently than at longer spans.

The most promising range appears to be from 1,200 feet to 1,600 feet, where secondary bending stress effects are relatively unimportant in regard to selection of the deck area. It is only necessary to provide sufficient torsional rigidity for aerodynamic stability. Maximum use can then be made of the cables which work much more efficiently than the deck.

In comparison with the suspension bridge, the cable-deck catenary system offers the following advantages. Towers and hangers are eliminated, and a lighter deck section can be utilized. The major disadvantage is the higher anchorage force to be accommodated. With favourable anchorage conditions it

is expected that the cable-deck catenary system would prove very competitive economically against the suspension bridge for spans from 1,200 feet to 1,600 feet.

In comparing the cable-deck catenary system with the cable stayed box girder bridge, it is appropriate to quote some general comments from the report of the Royal Commission into the failure of the West Gate Bridge (23) concerning the design of the cable stayed box girder bridge.

"The proper structural analysis of box girders is found to be a complex matter ....

A review of the research literature on the subject of box girders shows that this is still an area where much work is currently being undertaken, and that some aspects of the stress analysis of these structures remain so far unresolved.

It is true that the use of simple theory will give answers which in many cases are sufficiently accurate for normal design requirements. In view of all the imponderables to be encountered in such sophisticated structures, and with theory pushed to the limits of engineers' knowledge, it is essential to include safety factors high enough to provide sufficient allowance to cover the inevitable crudities of the analysis and other unavoidable factors and imponderables which may arise."

The steel cellular deck in catenary is essentially a simple tension member and the possibility of buckling of the thin walls (a critical factor for the cable stayed box girder) is of very little concern. The cable-deck catenary system provides a more confident design with a greater safety against collapse, towers are eliminated and erection is simpler. These advantages are partly offset by the high cost of anchorage. Overall, the cable-deck catenary system is expected to compete most favourably against the cable stayed box girder bridge.

Reference (5) reports a proposed stress ribbon bridge over Lake Geneva, for which the deck is a concrete slab about 10 inches thick with approximately 25% reinforcing steel. The span of the stress ribbon is in the order of 1,400 feet. A basis for comparison between the steel cellular deck in catenary and the stress ribbon concept (employing a concrete deck), was outlined in Section 4.2. The concrete deck was considered as dead load only, the implication

being that the deck was unaffected by deformations of the cable. In practice, however, grouting of the cables would produce an interaction between the cables and the deck. For the concrete to accommodate the tensile stresses resulting from this interaction and also those due to the stiffness of the deck (Chapter 5) it would be necessary to precompress the deck longitudinally. This would require an increase in cable area above that when the interaction is ignored.

The following comment is made in Reference (5) about the aerodynamic behaviour of the stress ribbon bridge ....

"The aerodynamic stability of the stress ribbon bridge was thoroughly investigated with model tests in a wind tunnel. The critical wind speed is about 110 miles per hour for the projects which were tested."

If in Example 6.4 a solid concrete deck 30 feet wide and 14.4 inches thick was used to provide the 36 sq.ft. deck area, the value of its torsional rigidity would be 370×10^4 Kip ft.^{2} (using torsional modulus G = 1,500 Ksi for concrete). On comparison of this value with the torsional rigidity of the concrete box section (194×10^6 Kip ft.^{2}), it is apparent that the thin concrete slab will fare little better than the steel plate of Example 6.1 does against the steel cellular section of Example 6.2.

The above quotation is therefore not considered valid for the section depth of 10 inches and span of 1,400 feet proposed in Reference (5). Such a section, under the analysis of Chapter 6, would have a very low critical flutter velocity. As the span decreases, the torsional rigidity contributes a greater portion of the total potential energy of torsional oscillation. For very short spans, a solid deck 10 inches thick may be acceptable. However for the range of spans under consideration herein, a concrete box section is recommended. A section depth of 5 - 6 feet is suggested to facilitate erection and internal maintenance, while a minimum wall thickness of 6 inches would be required.

It would be possible to avoid the interaction problem by sitting the cellular concrete deck on the main cables (as with the steel deck) and prestressing it independently of the main cables. The concrete would then only be required to accommodate the tensile bending stresses resulting from its own flexural rigidity (Chapter 5) and the comparison of Section 4.2 would be valid.

The steel and concrete deck systems analysed in Examples 6.3 and 6.4 represent the order of dimensions which one might expect in practice for a two-lane highway bridge. The following rates will be used in an economic comparison of these two systems:

Deck steel	. . . .	\$600/ton in place
Main cables	. . . .	\$350/ton in place
Prestressed concrete deck	. . . .	\$120/cu.yd. in place
Anchorage	. . . .	\$0.50/Kip

Example 6.3 (System I):

Steel deck	3.0 sq.ft.	=	\$400/lin.ft.
Main cables	1.04 sq.ft.	=	\$ 80/lin.ft.
Anchorage	35 Kip/ft. of span	=	\$ 20/lin.ft.
Total cost of System I		=	\$500/lin.ft.

Example 6.4 (System II):

Concrete deck	36 sq.ft.	=	\$160/lin.ft.
Main cables	4.31 sq.ft.	=	\$375/lin.ft.
Anchorage	91 Kip/ft. of span	=	\$ 45/lin.ft.
Total cost of System II		=	\$580/lin.ft.

Although the rates are approximate, this exercise does indicate that for a practical design situation the cable-deck catenary system with a steel cellular deck (i.e. System I) should generally be more economical than a catenary system employing a concrete deck (i.e. System II).

ERRATUM

On page 117, for the anchorage unit rate a value of \$2.00/Kip appears to be more realistic than the \$0.50/Kip used. This would result in:

Total cost of System I	=	\$560/lin.ft.
Total cost of System II	=	\$715/lin.ft.

CHAPTER 9

FEASIBILITY EVALUATION - CONCLUSION

Feasibility of the cable-deck system in catenary using a steel cellular deck, has been established in the following respects:

(i) A satisfactory method has been developed to enable optimum design of such a structure. (Chapters 2 - 4)* For a nominated area of deck, the required area of cable and the profiles of both deck and cable can be determined.

(ii) Aerodynamic stability can be achieved, a major requirement being a deck having substantial torsional rigidity (Chapter 6). A cellular section, shallow in depth, is suggested.

(iii) The depth of section should be kept to a minimum to limit the magnitude of bending stresses due to the curvature of the deck (Section 5.1). However, practical considerations such as assembly of the deck and internal maintenance would suggest a minimum section depth of about 5 - 6 feet (Section 7.5.1).

(iv) An orthotropic-type top deck plate is required for distribution of local wheel loads without excessive deflection (Section 5.3).

(v) It is considered that an asphaltic traffic running surface on the catenary deck will give satisfactory performance (Section 7.3).

(vi) A relatively simple erection procedure is possible, including allowance for non-ideal behaviour of materials such as creep strain deformation of the high-strength prestressing tendons (Section 7.5). A major feature is that the structure can be "tuned" in accordance with the actual material properties rather than assumed design values.

Note: The direct method of design and analysis developed herein is not restricted to just the cable-deck catenary system as a traffic carriageway. It can be readily applied to a wide range of cable problems - suspended pipe structures, transmission lines, aerial ropeways, cable supported roof structures and anchorage cables, for example.

(vii) The structure has a very large margin of safety against collapse (Section 7.4).

(viii) The structure is considered to be economically competitive with alternative long-span bridge types (Chapter 8).

CONCLUSION

It is therefore concluded that the structural concept of a steel cellular deck in catenary partially supported by high strength prestressing cable, is practicable as a traffic carriageway.

BIBLIOGRAPHY

1. STEINMAN, D.B. "A Practical Treatise on Suspension Bridges". New York, 1922.

2. PUGSLEY, A.G. "The Theory of Suspension Bridges". 2nd edn, London, 1968.

3. SCHNEIGERT, Z. "Aerial Ropeways and Funicular Railways". Warsaw, 1966.

4. BRESLER, B., LIN, T.Y. and SCALZI, J.B. "Design of Steel Structures". 2nd edn, New York, 1968.

5. - "Stress Ribbon Bridge". J. Am. Concr. Inst., Vol. 62, No.9, September, 1965, pp. 1042-1045.

6. WALTHER, R. "Stress Ribbon Bridges". Schweizerische Bauzeitung, 20th February, 1968.

7. PIPPARD, A.J.S. and CHITTY, L. "The Stresses in an Extensible Suspension Cable". J. Instn Civ. Engrs, Vol. 18, No. 7, June, 1942.

8. MICHALOS, J. and BIRNSTIEL, C. "Movements of a Cable due to Changes in Loading". Trans. Am. Soc. Civ. Engrs, Vol. 127, Part 2, 1962.

9. JENNINGS, A. "The Free Cable". The Engineer, 28th December, 1962, pp. 1111-12.

10. O'BRIEN, W.T. and FRANCIS, A.J. "Cable Movements under Two Dimensional Loads". Proc. Am. Soc. Civ. Engrs, J. Struct. Div., Vol. 90, No. ST3, June, 1964.

11. HARRISON, H.B. "Suspension Cable Movement Analysis". Civ. Engng Trans. Instn Engrs Aust., Vol. CE12, No. 1, April, 1970.

12. SHAW, F.S. "Some Notes on Cable Suspension Roof Structures". J. Instn Engrs Aust., April-May, 1964.

13. AM. INST. STEEL CONSTRN, "Design Manual for Orthotropic Steel Plate Deck Bridges". 1963.

14. BLEICH, F. et al, "The Mathematical Theory of Vibration in Suspension Bridges". 1950.

15. SELBERG, A. and HJORTH-HANSEN, E. "Aerodynamic Stability and Related Aspects of Suspension Bridges". Paper No. 20, Int. Symp. on Suspension Bridges. Lisbon, 1966.

16. FRANDSEN, A.G. "Wind Stability of Suspension Bridges - Application of the Theory of Thin Airfoils". Paper No. 43, Int. Symp. on Suspension Bridges. Lisbon, 1966.

17. WALSHE, D.E. "A Resume of the Aerodynamic Investigation for the Fourth Road and Severn Bridges". Proc. Instn Civ. Engrs, Vol. 37, 1967, pp. 87-108.

18. DAVENPORT, A. "The Action of Wind on Suspension Bridges". Int. Symp. on Suspension Bridges. Lisbon, 1966.

19. DURKEE, J.L. "Advancements in Suspension Bridge Cable Construction". Int. Symp. on Suspension Bridges. Lisbon, 1966.

20. MAGURA, D.D., SOZEN, M.A. and SIESS, C.P. "A Study of Stress Relaxation in Prestressing Reinforcement". J. Prestress. Concr. Inst., Vol. 9, No. 2, April, 1964.

21. INT. ASS. BRIDGE STRUCT. ENGNG, "Symposium on Wearing Surfaces for Steel Bridge Decks of Lightweight Construction, New York, 1968 - Final Report".

22. IVY, R.J. et al, "Live Loading for Long-Span Highway Bridges". Trans. Am. Soc. Civ. Engrs, Vol. 119, 1954.

23. - "Report of Royal Commission into the Failure of West Gate Bridge". Melbourne, 1971.

APPENDIX A

containing twenty-six figures showing the relationship p vs $\frac{d_o + \Delta d}{L}$ and p vs f

for values of $\frac{d_o}{L}$ from 0.0015 to 0.025 and span L from 200 feet to 2,000 feet, and for a steel having E = 30,000 Ksi and ρ = 490 lb/cu.ft.

where $\frac{d_o}{L}$ = self-weight profile of cable.

$\frac{d_o + \Delta d}{L}$ = cable profile under a loading (1 + p) times the cable self-weight.

f = stress in cable under a loading (1 + p) times the cable self-weight.

p = loading factor (non-dimensional).

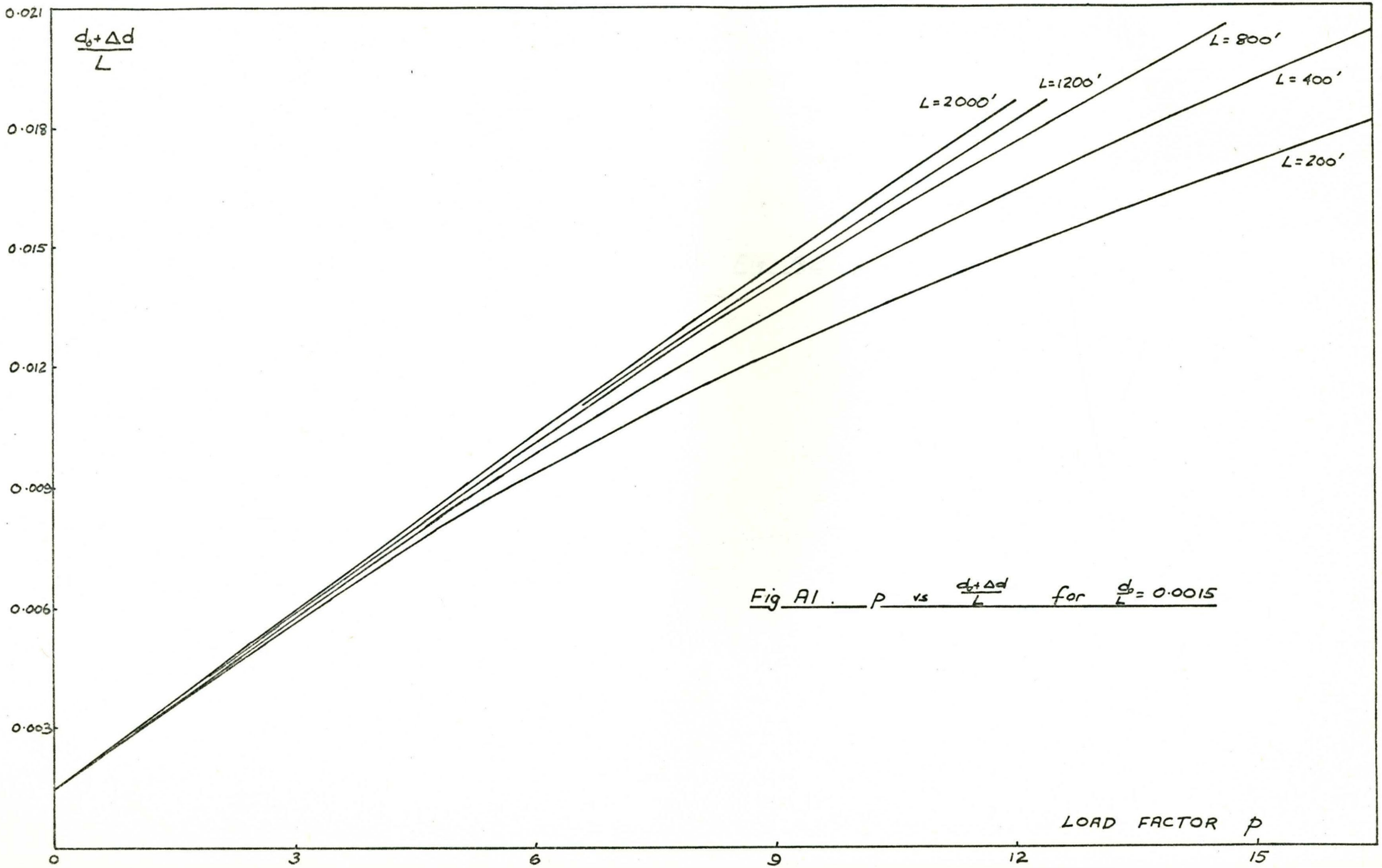

Fig A1. p vs $\frac{d_o+\Delta d}{L}$ for $\frac{d_o}{L}$ = 0.0015

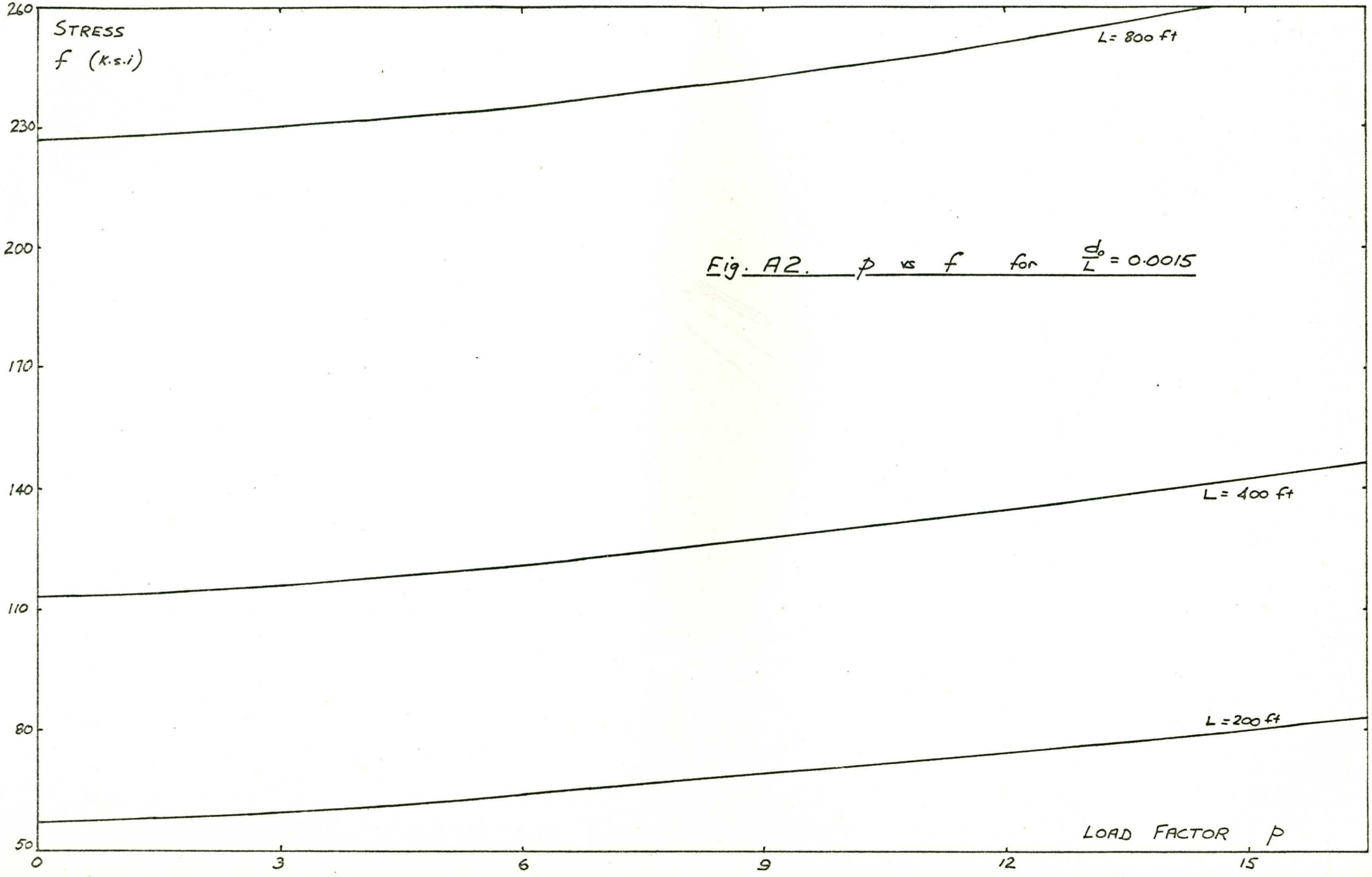

Fig. A2. p vs f for $\frac{d_o}{L} = 0.0015$

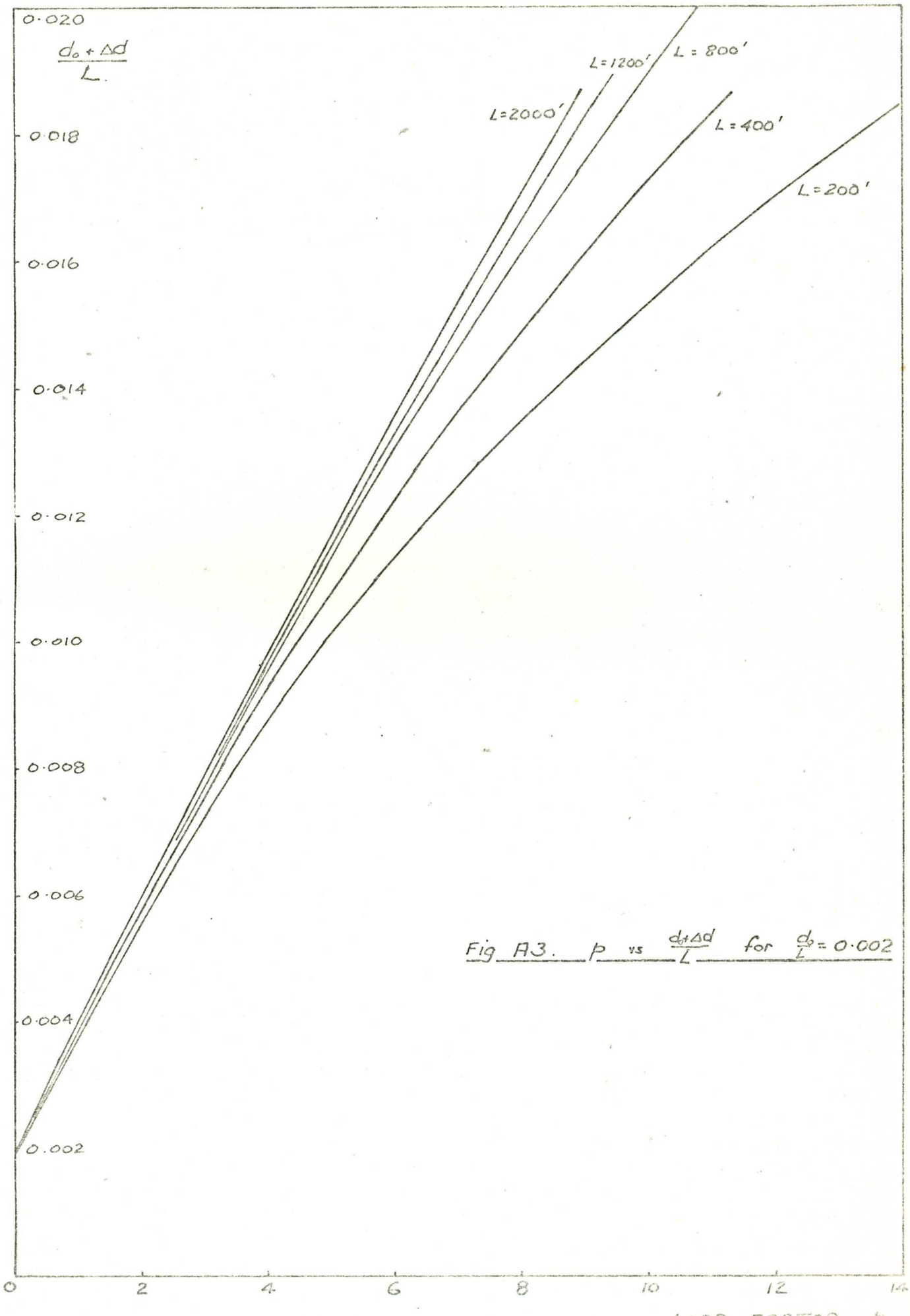

Fig A3. p vs $\frac{d_o+\Delta d}{L}$ for $\frac{d_o}{L} = 0.002$

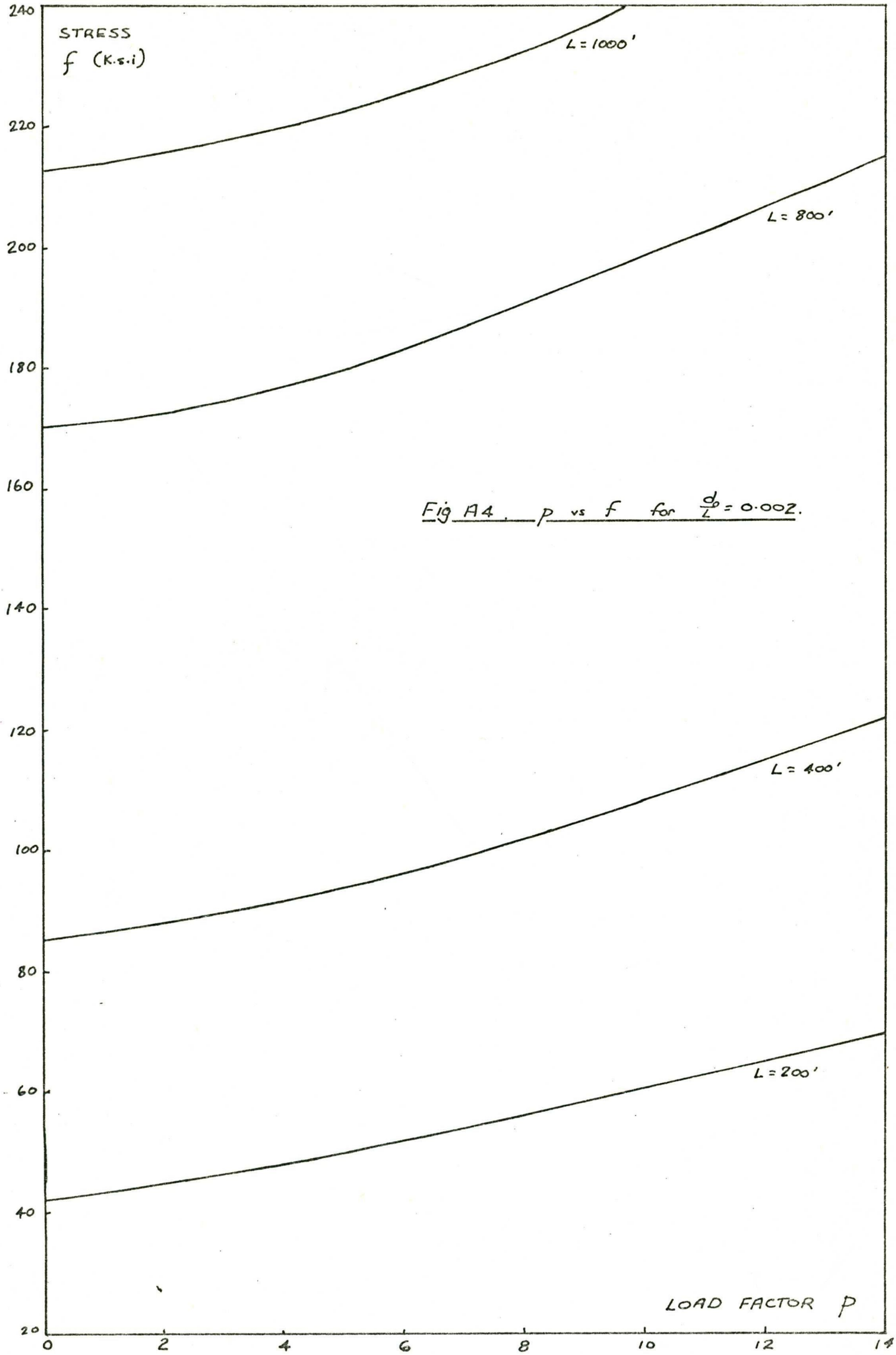

Fig A4. p vs f for $\frac{d}{L} = 0.002$.

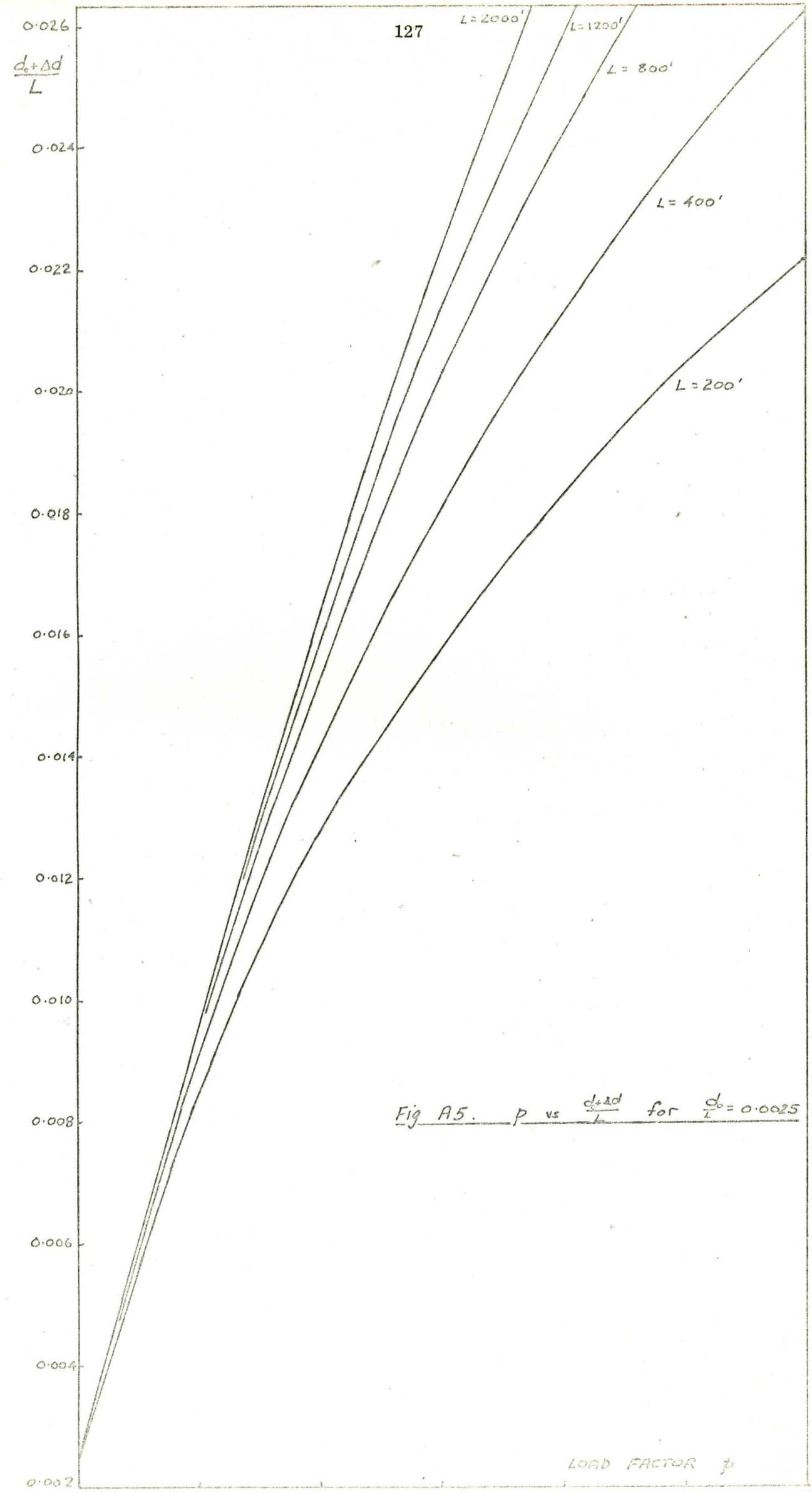

Fig A5. p vs $\frac{d+\Delta d}{L}$ for $\frac{d_o}{L} = 0.0025$

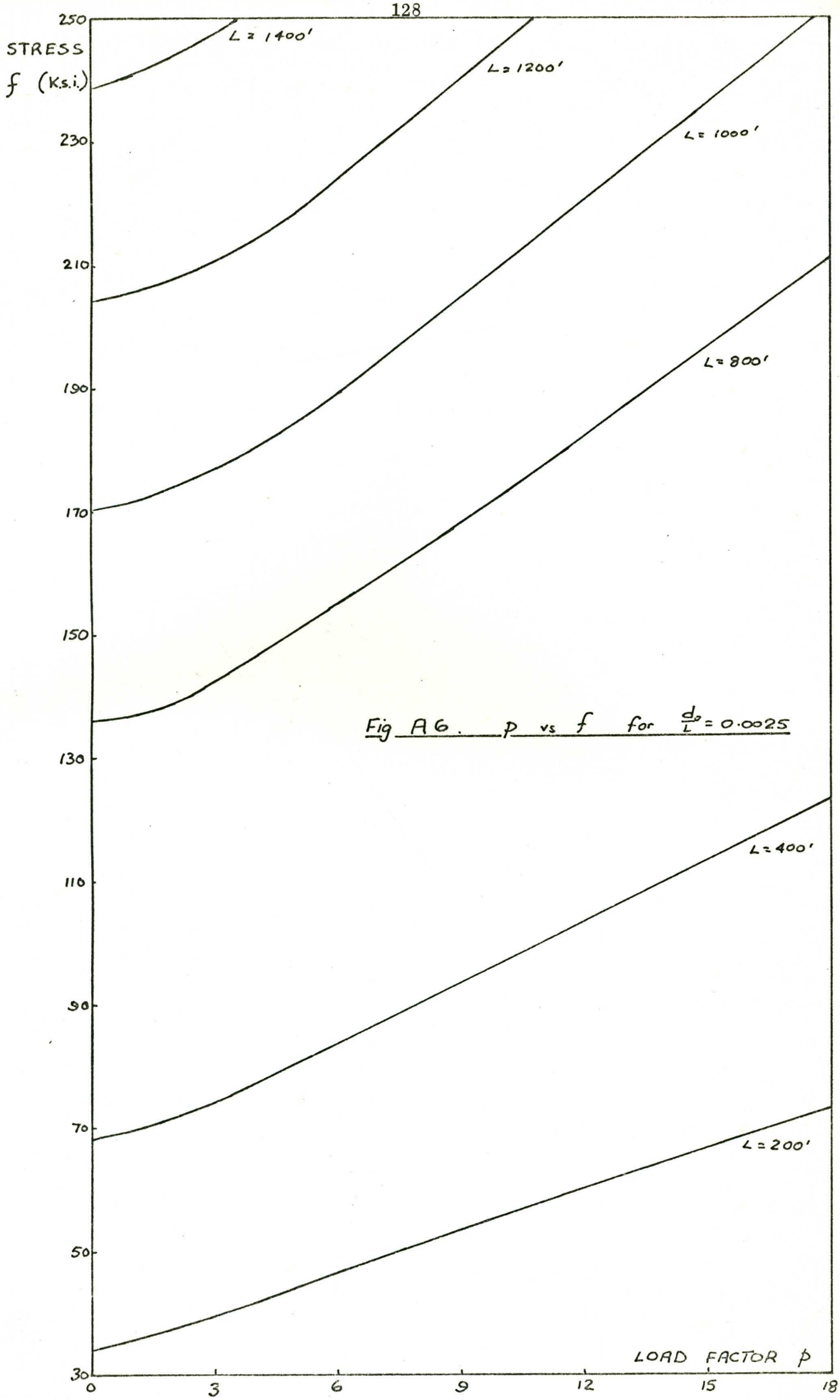

Fig A6. p vs f for $\frac{d_o}{L} = 0.0025$

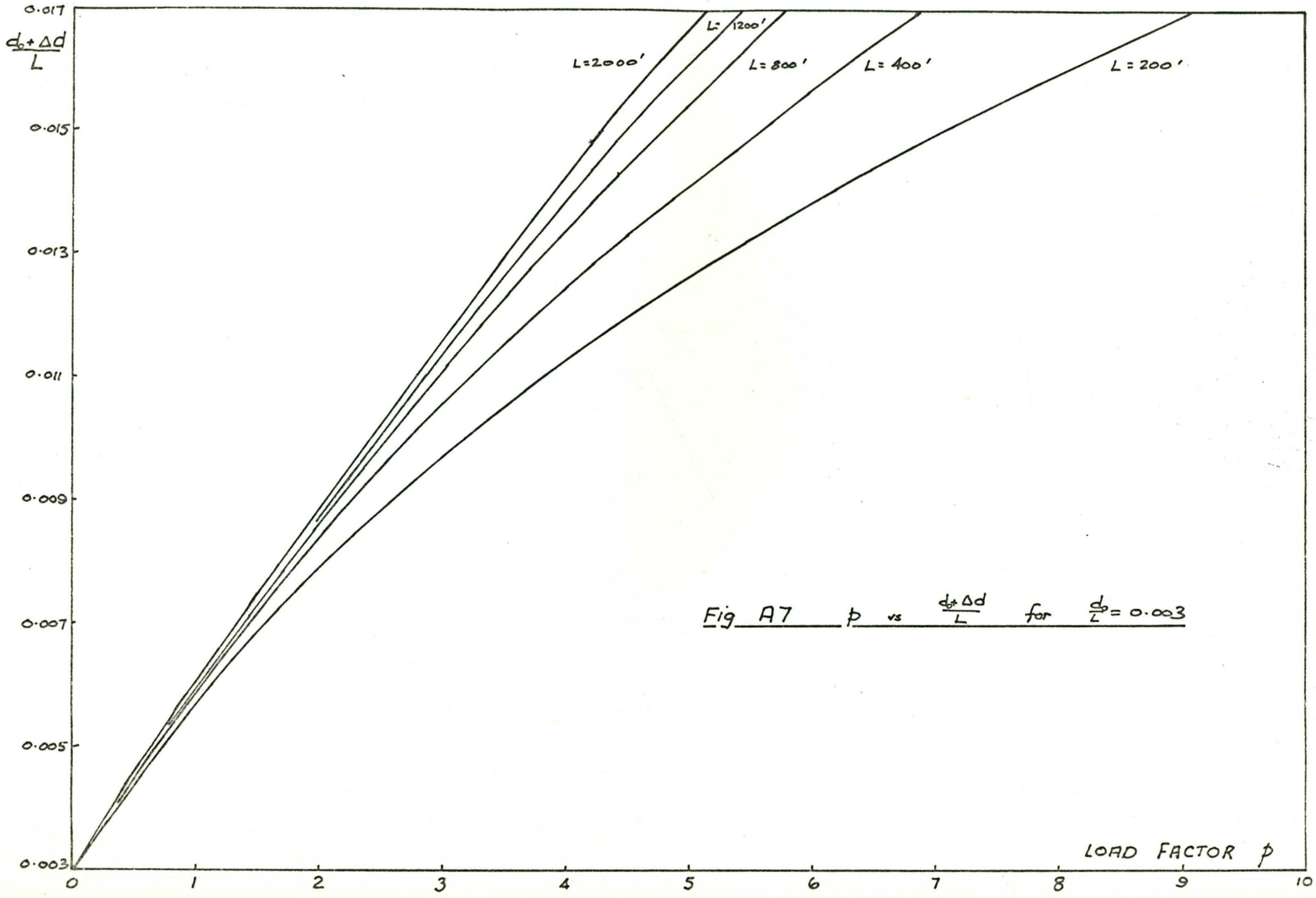

Fig A7 p vs $\frac{d_o+\Delta d}{L}$ for $\frac{d_o}{L}=0.003$

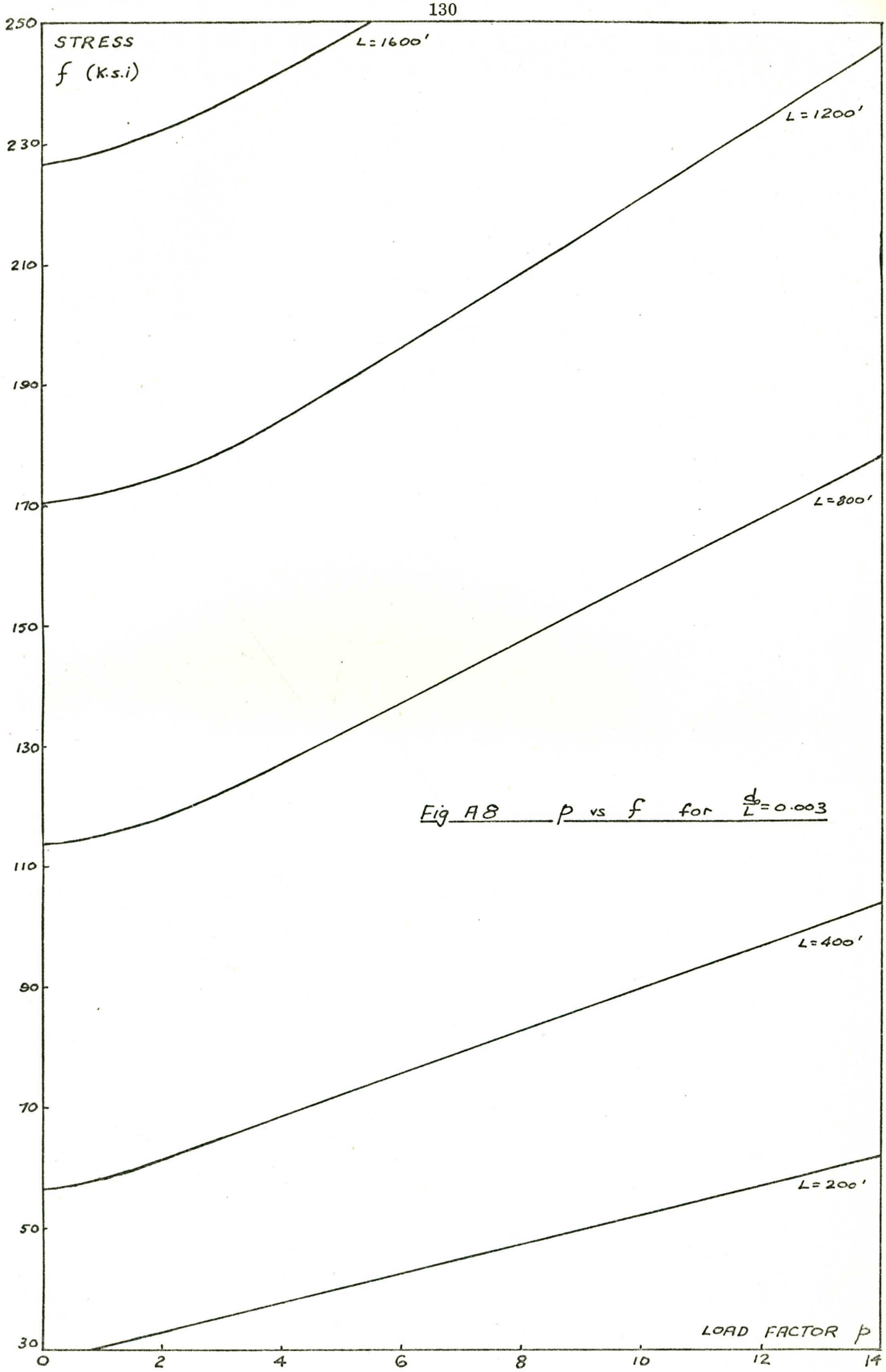

Fig A8 p vs f for $\frac{d_o}{L} = 0.003$

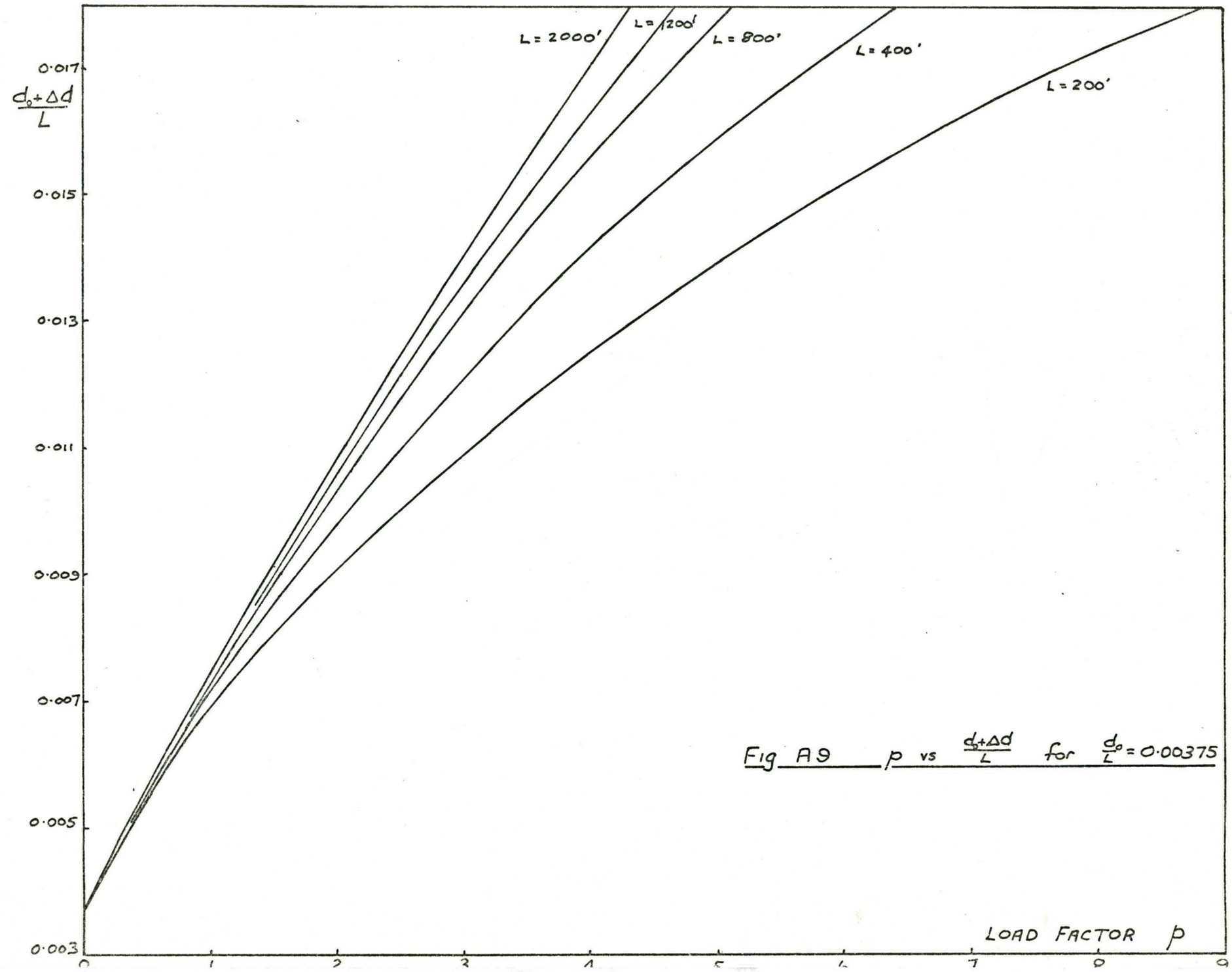

Fig A9 p vs $\frac{d_o+\Delta d}{L}$ for $\frac{d_o}{L}$ = 0·00375

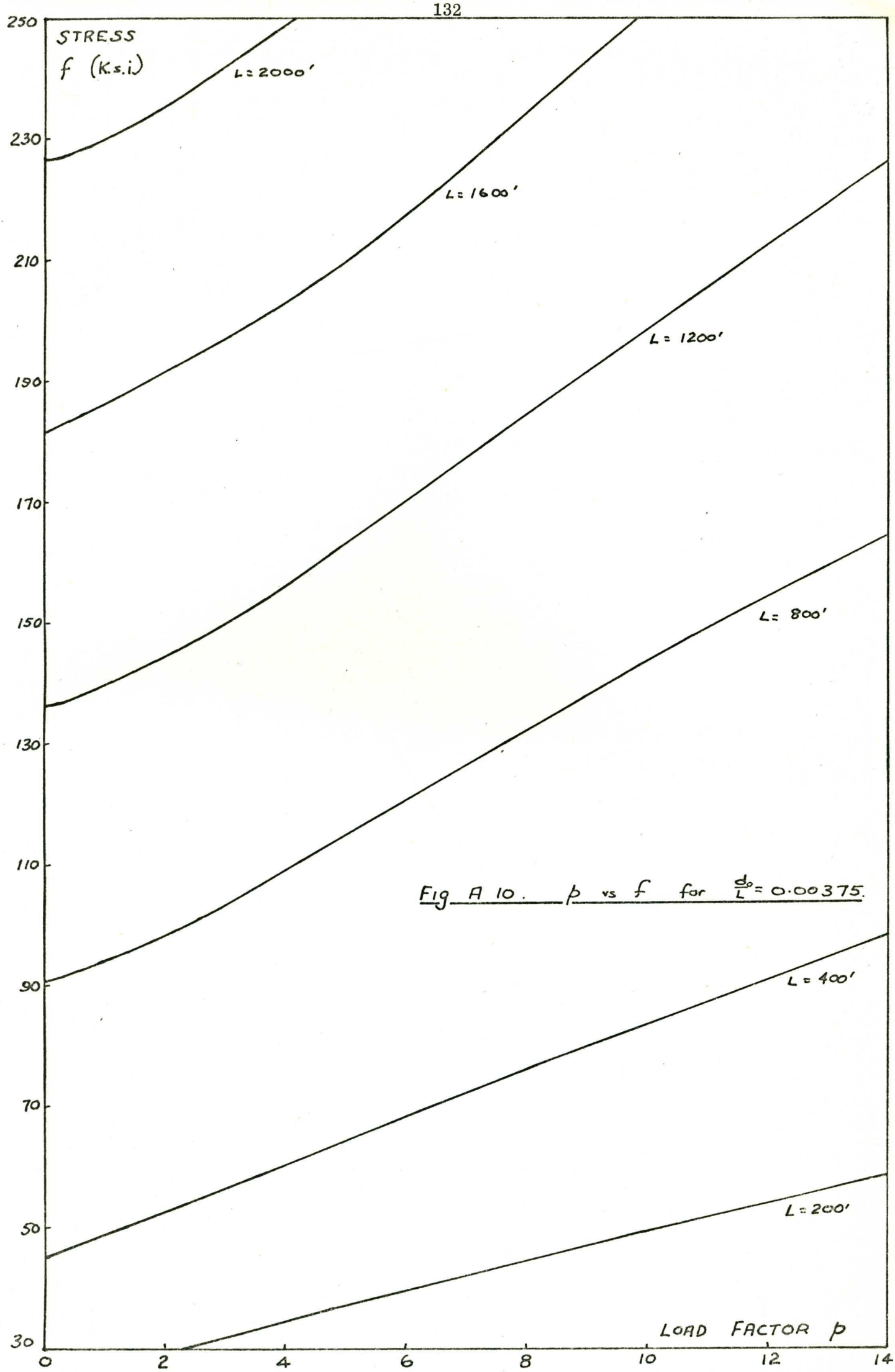

Fig A 10. p vs f for $\frac{d_o}{L} = 0.00375$.

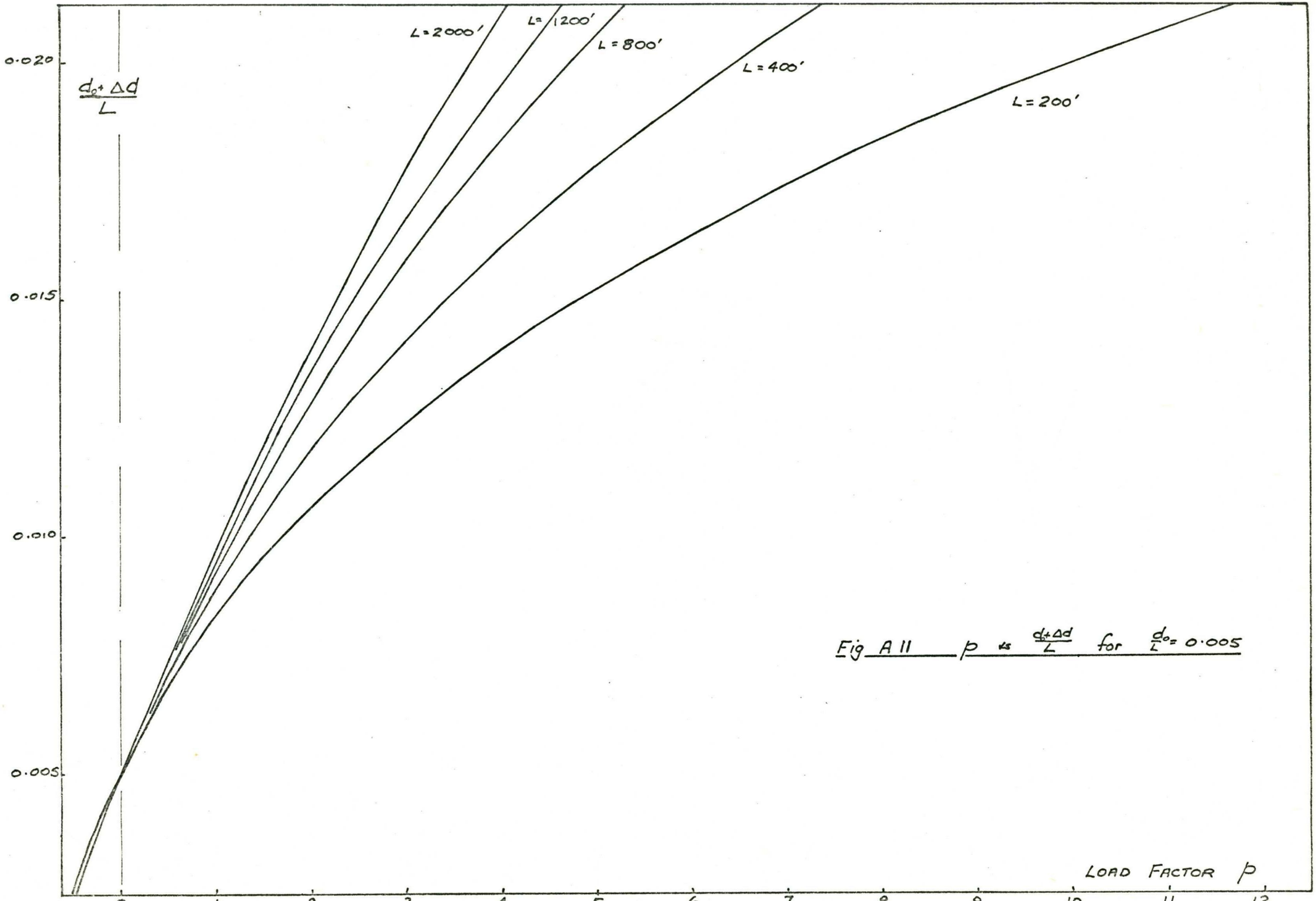

Fig A 11 p vs $\frac{d_o+\Delta d}{L}$ for $\frac{d_o}{L}$ = 0.005

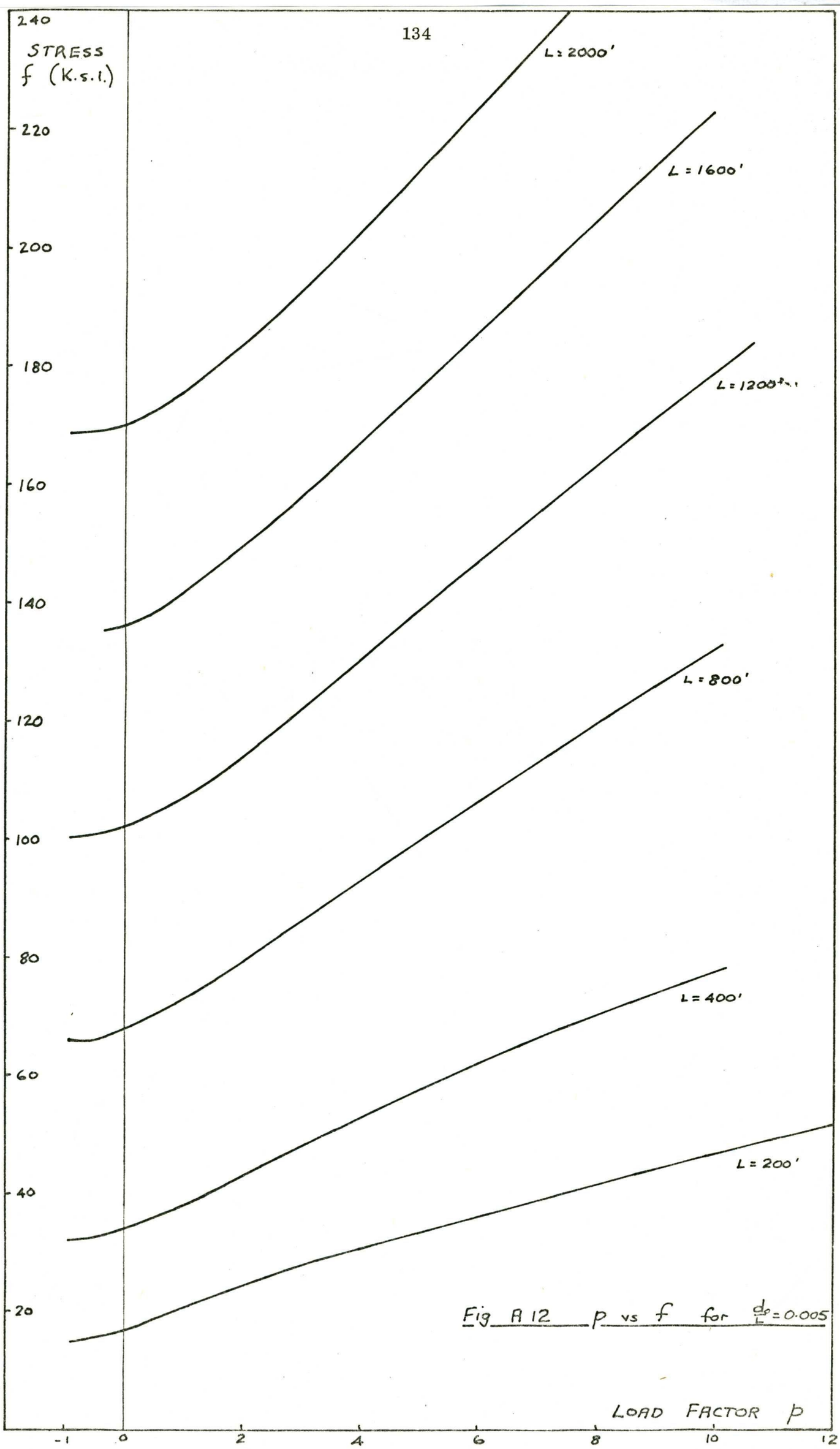

Fig A 12 p vs f for $\frac{d_e}{L} = 0.005$

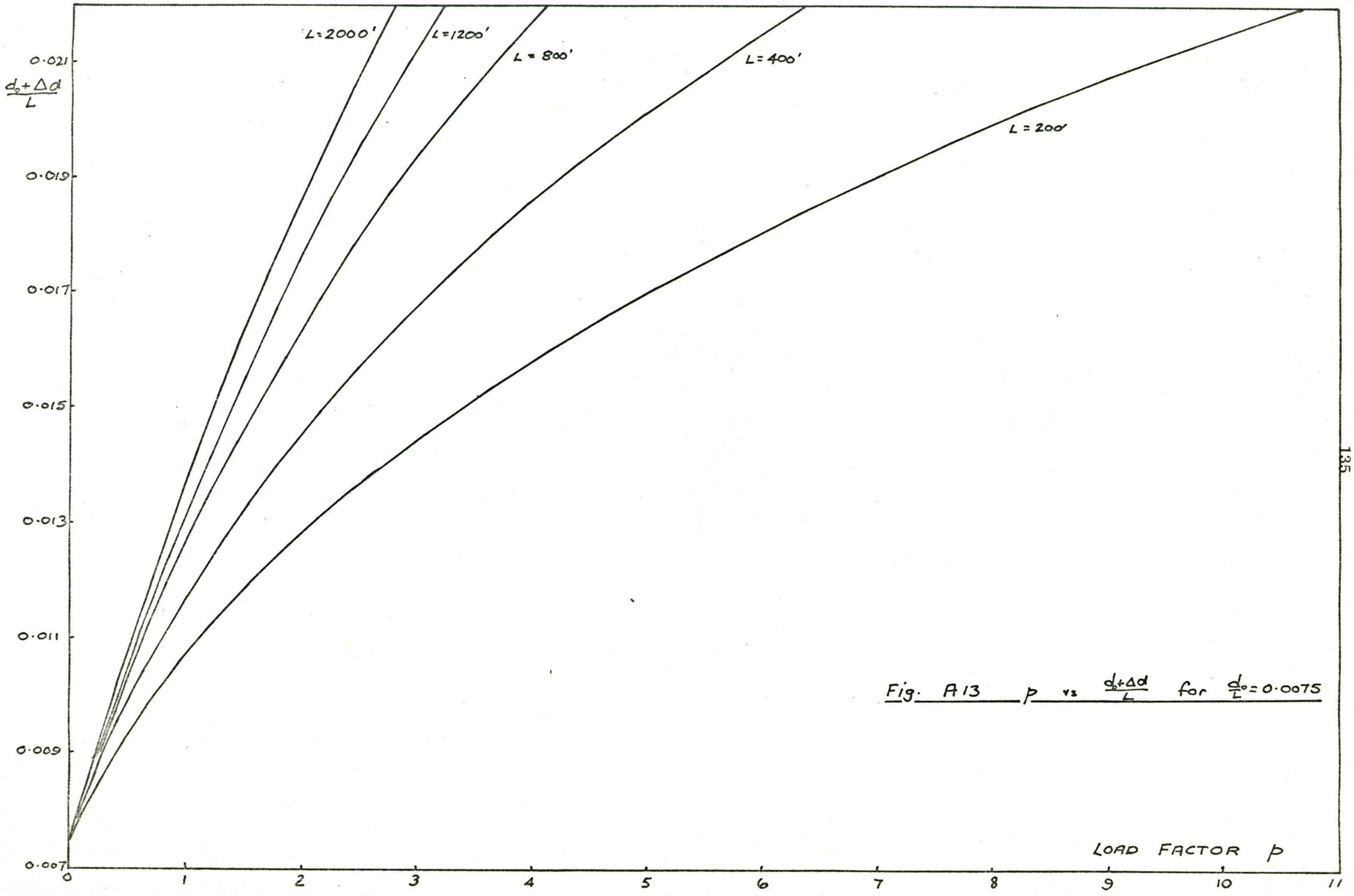

Fig. A13 p vs $\frac{d_o+\Delta d}{L}$ for $\frac{d_o}{L}$ = 0·0075

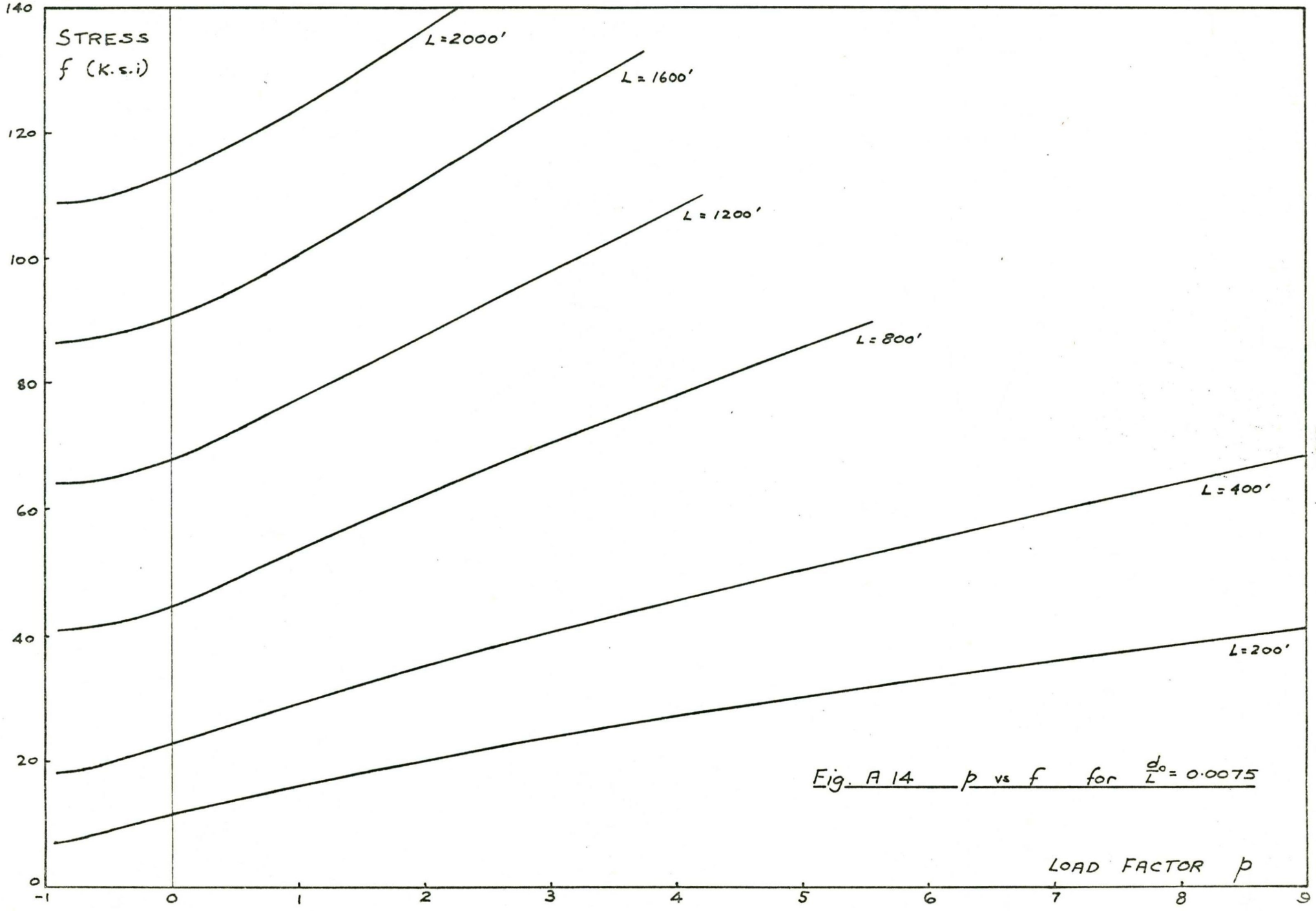

Fig. A 14 p vs f for $\frac{d_o}{L} = 0.0075$

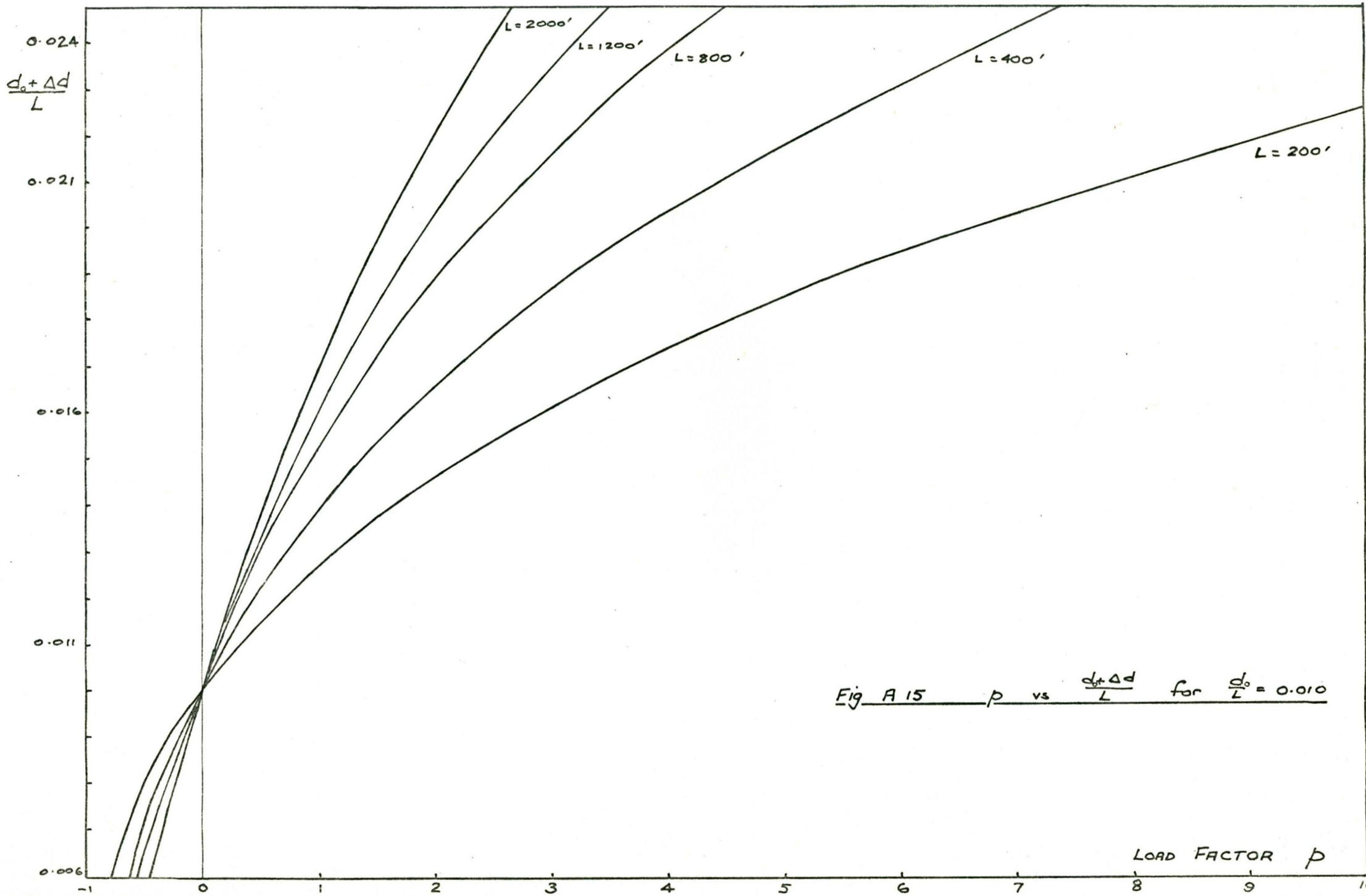

Fig A 15 p vs $\frac{d_o + \Delta d}{L}$ for $\frac{d_o}{L} = 0.010$

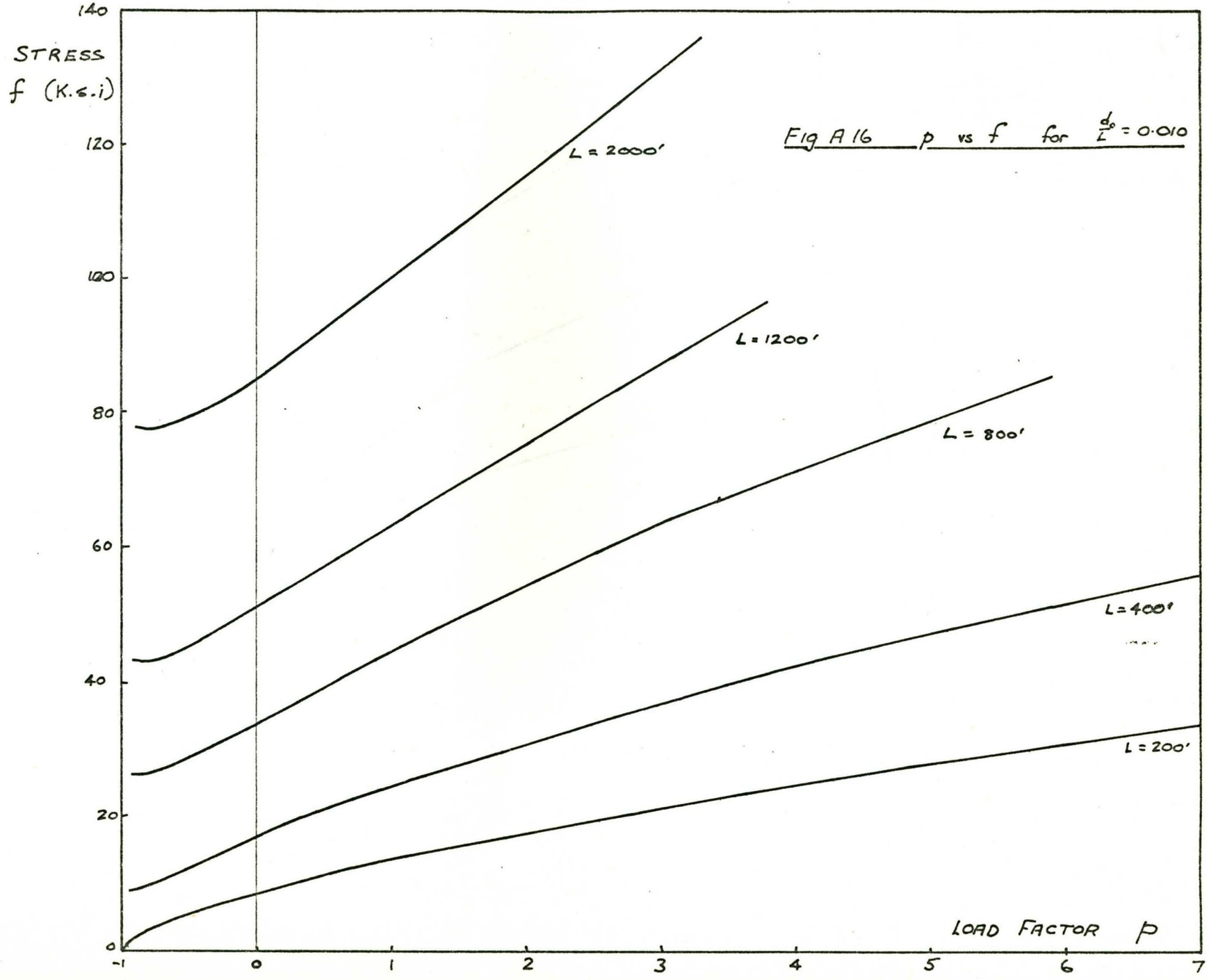

Fig A 16 p vs f for $\frac{d_o}{L} = 0.010$

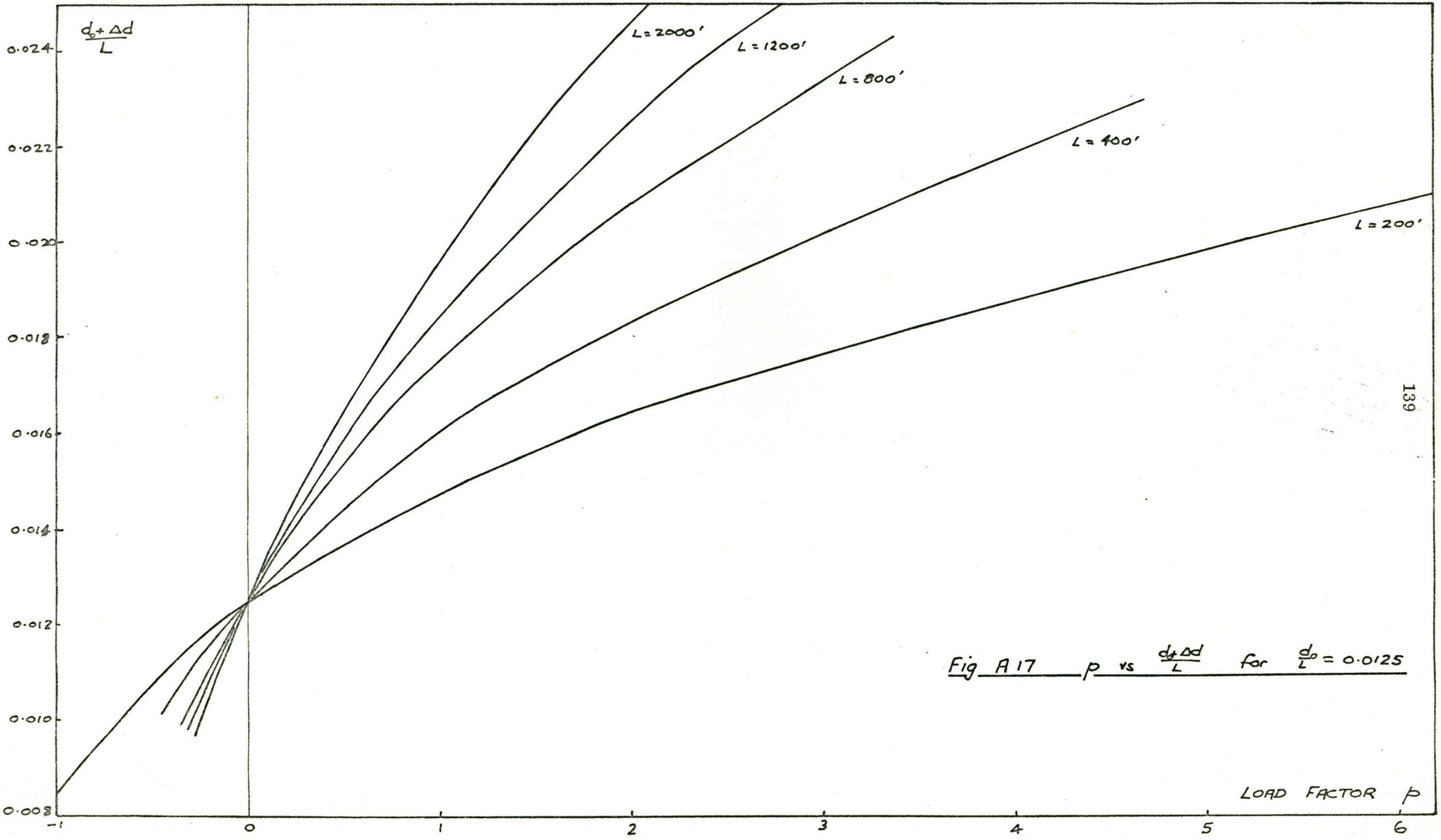

Fig A 17 p vs $\frac{d_o + \Delta d}{L}$ for $\frac{d_o}{L} = 0.0125$

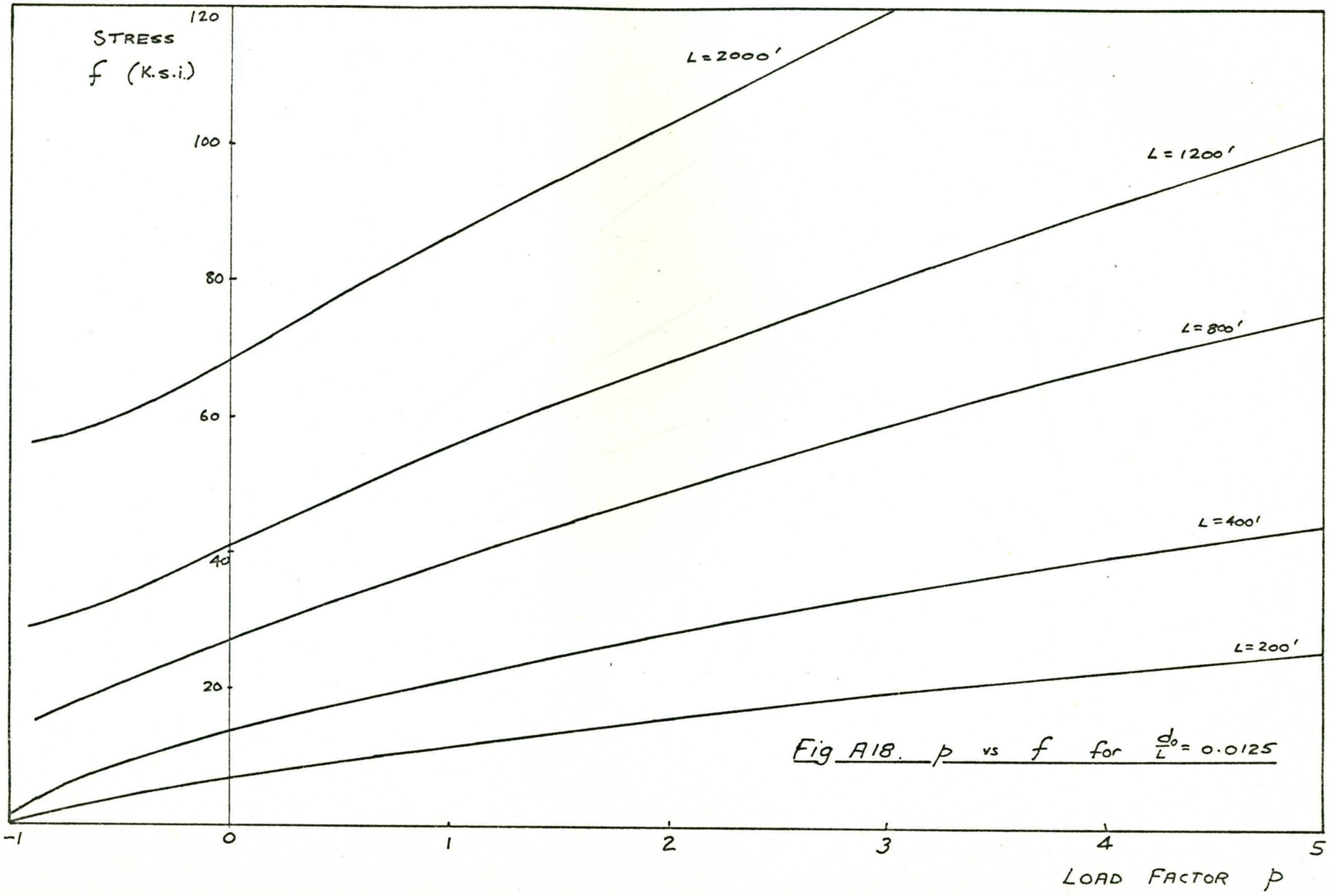

Fig A18. p vs f for $\frac{d_o}{L} = 0.0125$

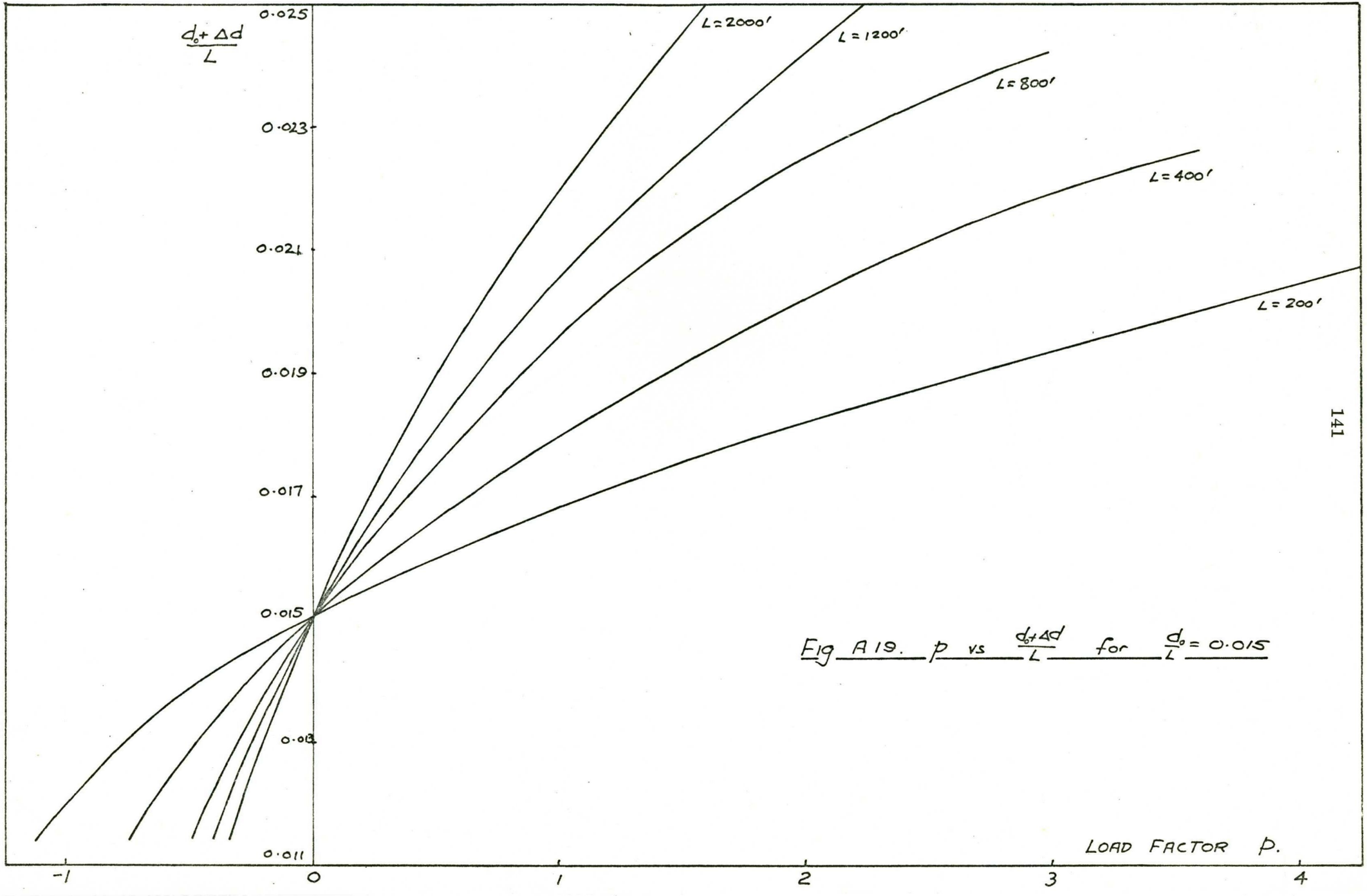

Fig A 19. p vs $\frac{d_o + \Delta d}{L}$ for $\frac{d_o}{L} = 0.015$

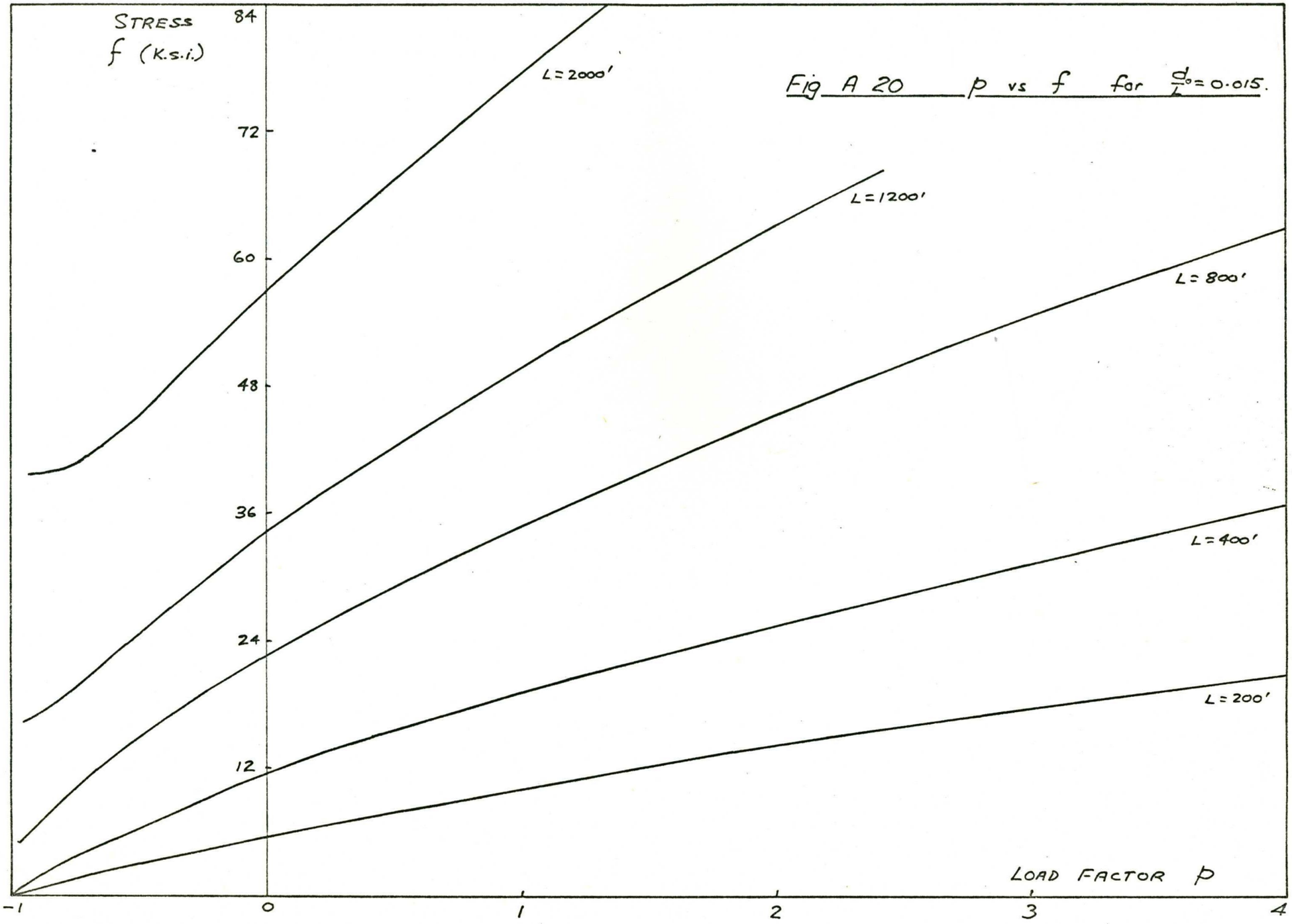

Fig A 20 p vs f for $\frac{d_o}{L} = 0.015$.

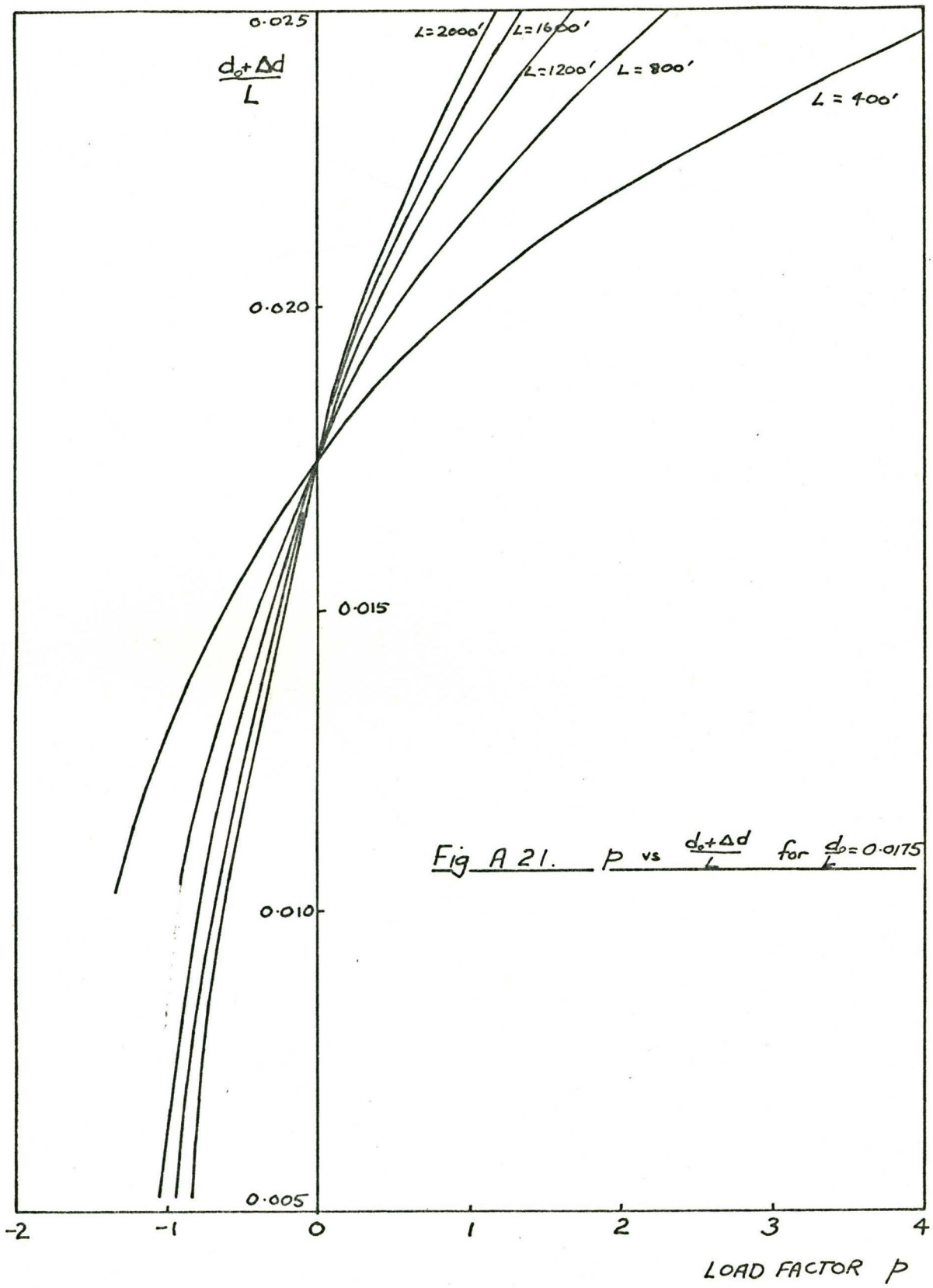

Fig A 21. p vs $\frac{d_o+\Delta d}{L}$ for $\frac{d_o}{L}=0.0175$

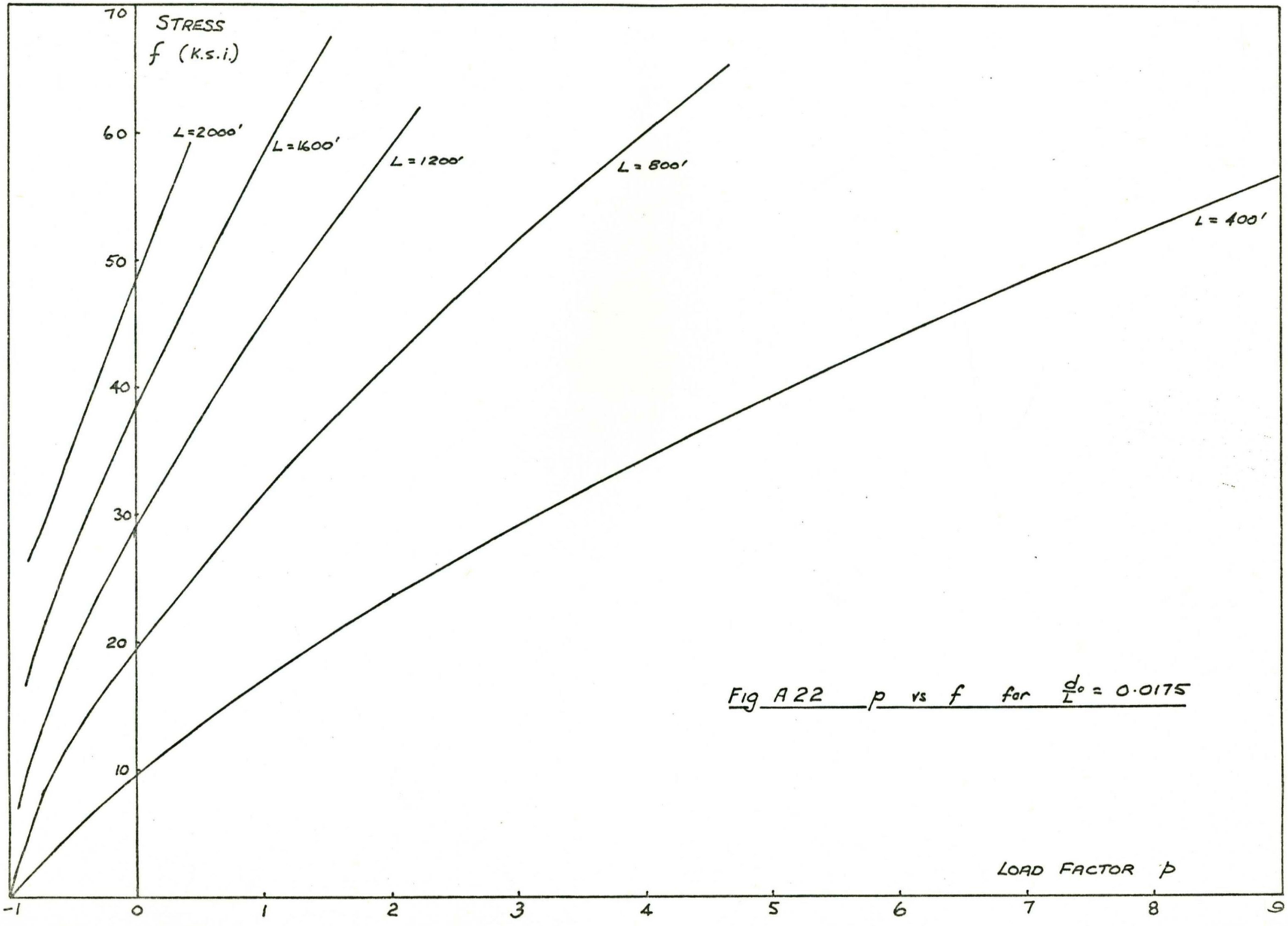

Fig A 22 p vs f for $\frac{d_o}{L} = 0.0175$

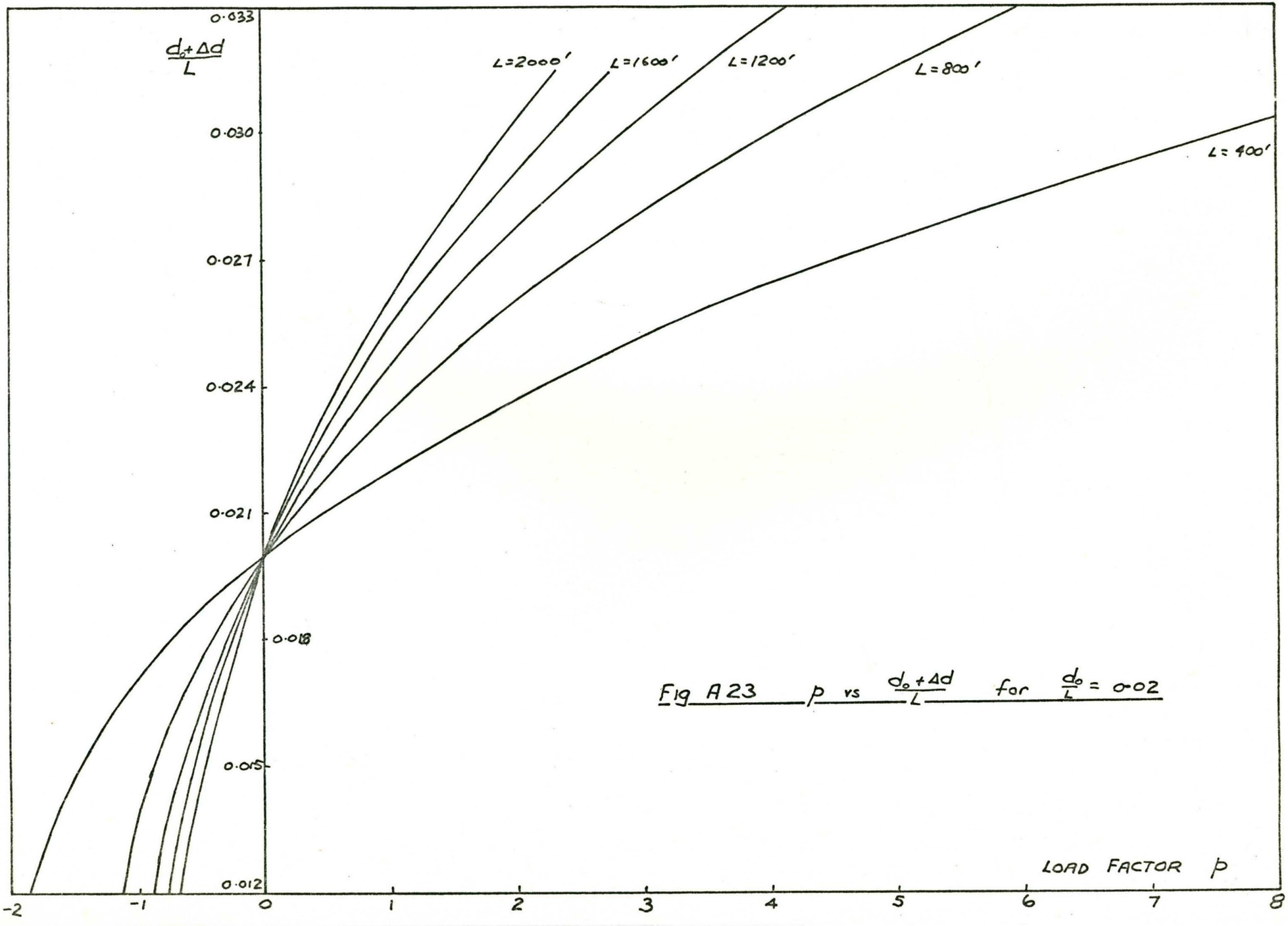

Fig A23 p vs $\frac{d_o+\Delta d}{L}$ for $\frac{d_o}{L}$ = 0·02

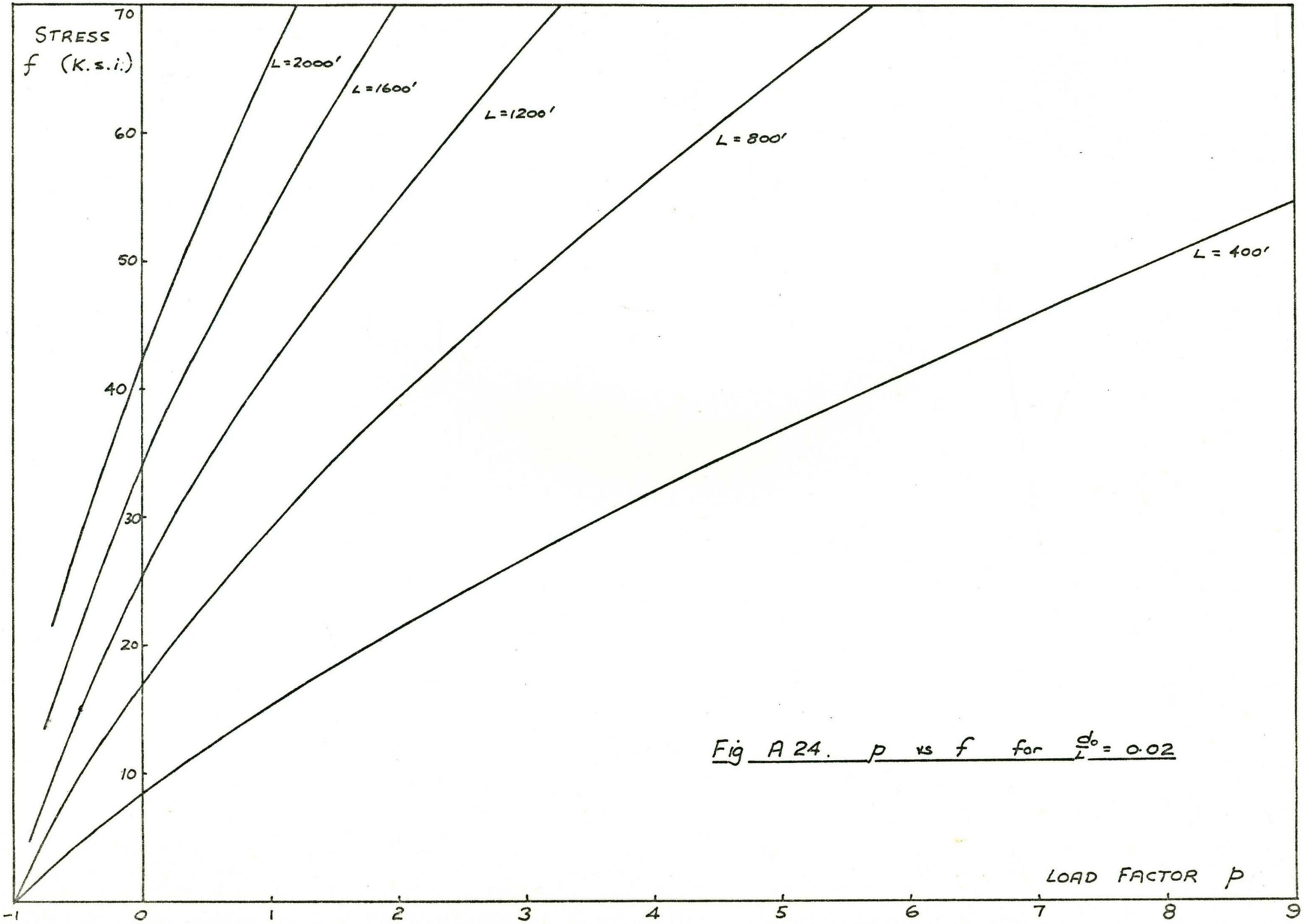

Fig A 24. p vs f for $\frac{d_o}{L} = 0.02$

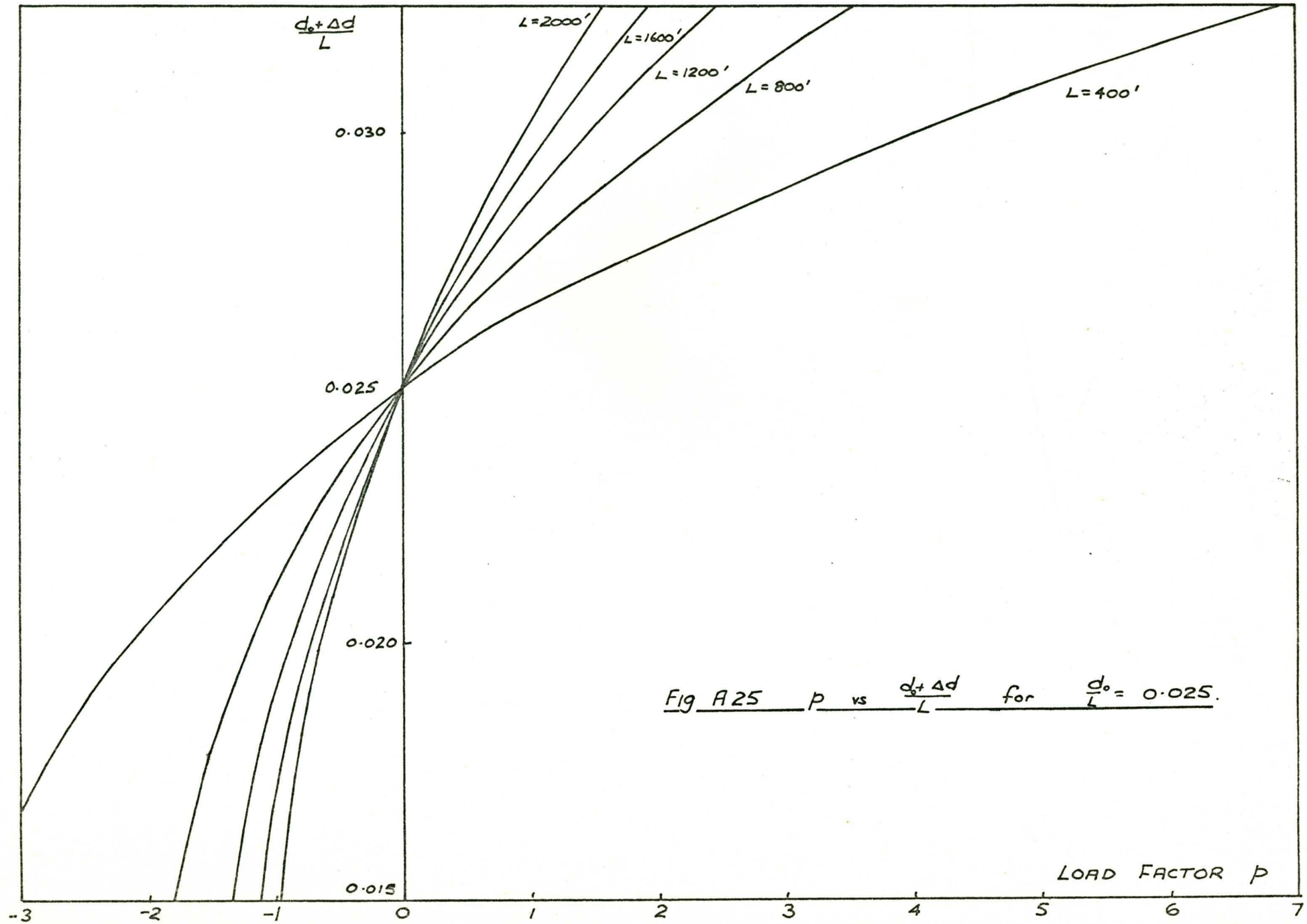

Fig A25 p vs $\frac{d_o+\Delta d}{L}$ for $\frac{d_o}{L}$ = 0.025.

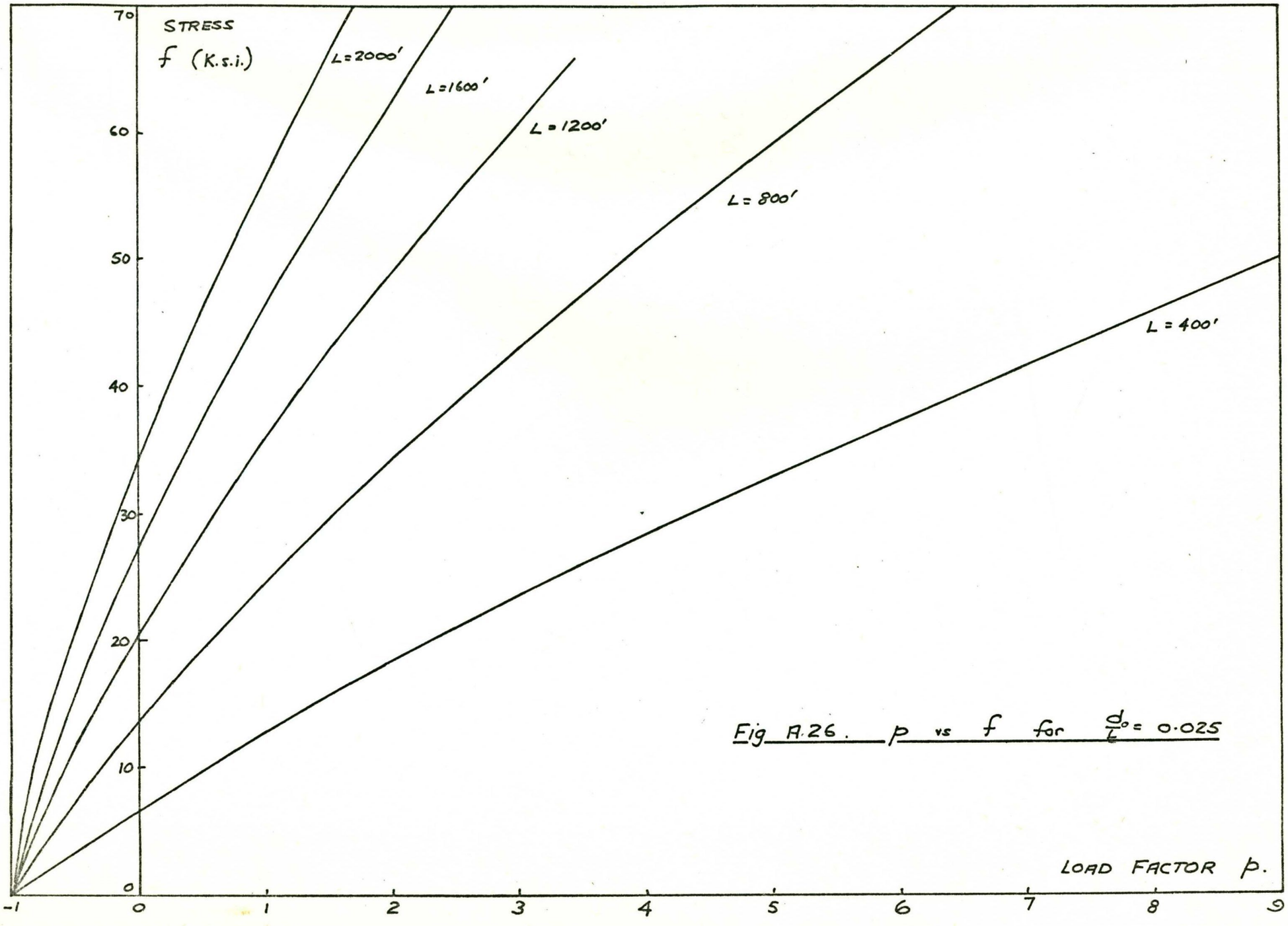

Fig A.26. p vs f for $\frac{d_o}{L} = 0.025$